NAVAL POSTGRADUATE SCHOOL
Monterey, California

THESIS

PASSIVE TARGET TRACKING USING
NONLINEAR ESTIMATION THEORY

by

Marcilio Boavista da Cunha

September 1976

Thesis Advisor: D. E. Kirk

Approved for public release; distribution unlimited.

SECURITY CLASSIFICATION OF THIS PAGE (When Data Entered)

REPORT DOCUMENTATION PAGE

READ INSTRUCTIONS BEFORE COMPLETING FORM

1. REPORT NUMBER

2. GOVT ACCESSION NO.

(9) Doctoral thesis

3. RECIPIENT'S CATALOG NUMBER

4. TITLE (and Subtitle)

(6) Passive Target Tracking Using Nonlinear Estimation Theory

5. TYPE OF REPORT & PERIOD COVERED

Doctor of Philosophy
September 1976

6. PERFORMING ORG. REPORT NUMBER

7. AUTHOR(s)

(10) Marcilio Boavista da Cunha

8. CONTRACT OR GRANT NUMBER(s)

9. PERFORMING ORGANIZATION NAME AND ADDRESS

Naval Postgraduate School
Monterey, California 93940

10. PROGRAM ELEMENT, PROJECT, TASK AREA & WORK UNIT NUMBERS

11. CONTROLLING OFFICE NAME AND ADDRESS

(11) Naval Postgraduate School
Monterey, California 93940

12. REPORT DATE

September 1976

13. NUMBER OF PAGES

205

14. MONITORING AGENCY NAME & ADDRESS (if different from Controlling Office)

(12) 204 p.

15. SECURITY CLASS. (of this report)

Unclassified

15a. DECLASSIFICATION/DOWNGRADING SCHEDULE

16. DISTRIBUTION STATEMENT (of this Report)

Approved for public release; distribution unlimited.

17. DISTRIBUTION STATEMENT (of the abstract entered in Block 20, if different from Report)

18. SUPPLEMENTARY NOTES

19. KEY WORDS (Continue on reverse side if necessary and identify by block number)

20. ABSTRACT (Continue on reverse side if necessary and identify by block number)

The problem of tracking submarine targets with passive sonobuoys is mathematically modelled. A comprehensive study is made of all the information available in the acoustic signals picked up by the sonobuoys and of the usefulness of this information in the estimation process. The presence of nonlinearities in the tracking model leads to the application of nonlinear estimation theory. Bayes formulation concepts are applied to

(cont on p 1473 03)

DD FORM 1 JAN 73 1473 (Page 1) EDITION OF 1 NOV 65 IS OBSOLETE S/N 0102-014-6601

SECURITY CLASSIFICATION OF THIS PAGE (When Data Entered)

20. ABSTRACT (continued) (p. 1473A)

generate approximate solutions and filtering algorithms, and the well known extended Kalman filter equations and higher order filtering algorithms are obtained from this approach.

The concept of partitioning the measurements is presented and shown to bring advantages in computing efficiency and also, for nonlinear measurements, in tracking accuracy. A graphical interpretation of the action of Kalman filters is developed and provides insight into the importance of each variable in the filtering process.

Extensive simulations, designed to test the performance of the algorithms developed, are presented in graphical form and analyzed.

1473B

Passive Target Tracking Using Nonlinear Estimation Theory

by

Marcilio Boavista da Cunha
Lieutenant Commander, Brazilian Navy
B.S., Pontificia Universidade Catolica RJ, 1969
M.S., Naval Postgraduate School, 1974

Submitted in partial fulfillment of the
requirements for the degree of

DOCTOR OF PHILOSOPHY

from the
NAVAL POSTGRADUATE SCHOOL
September 1976

Author Marcilio Boavista da Cunha

Approved by:

D. E. Kirk
Professor of Electrical Engineering. Thesis Advisor

U. R. Kodres
Assoc. Professor of Computer Science

R. Panholzer
Assoc. Professor of Electrical Engineering

V. Michael Powers
Assist. Professor of Computer Science

H. A. Titus
Professor of Electrical Engineering

C. O. Wilde
Professor of Mathematics

Approved by D E Kirk
Chairman, Department of Electrical Engineering

Approved by Jack R Borsting
Academic Dean

ABSTRACT

The problem of tracking submarine targets with passive sonobuoys is mathematically modelled. A comprehensive study is made of all the information available in the acoustic signals picked up by the sonobuoys and of the usefulness of this information in the estimation process. The presence of nonlinearities in the tracking model leads to the application of nonlinear estimation theory. Bayes formulation concepts are applied to generate approximate solutions and filtering algorithms, and the well known extended Kalman filter equations and higher order filtering algorithms are obtained from this approach.

The concept of partitioning the measurements is presented and shown to bring advantages in computing efficiency and also, for nonlinear measurements, in tracking accuracy. A graphical interpretation of the action of Kalman filters is developed and provides insight into the importance of each variable in the filtering process.

Extensive simulations, designed to test the performance of the algorithms developed, are presented in graphical form and analyzed.

CONTENTS

SYMBOLS AND CONVENTIONS FOR TEXT

1 - Underlined small letters represent vectors, thus, $\underline{x}$ denotes the vector x.

2 - Capital letters are used to represent matrices.

3 - A caret indicates an estimated value, e.g., $\hat{x}$ denotes an estimate of x.

- Time points are represented by t_k or, when between parentheses, simply by k, e.g., $\underline{x}(k)$ denotes the value of $\underline{x}$ at time t_k.

5 - Estimates specify the time of estimation and the amount of information used, e.g., $\hat{\underline{x}}(k|j)$ denotes the estimate of $\underline{x}$ at time t_k taking into account all the measurements up to and including t_j. When k = j only one time point is indicated, thus, $\hat{\underline{x}}(k)$ denotes the estimate of $\underline{x}$ at time t_k taking into account all measurements up to and including t_k.

6 - Probability density functions are represented by the small letter p, i.e. $p_{x|y}(x|y)$ denotes the conditional density of x given y. When no confusion is possible, this is simplified to p(x|y).

7 - The expectation operator is represented by E[ ]; the variance by Var[ ].

$\bar{\underline{a}}(k)$ expected value of the estimated state vector at t_k.

$\alpha_s(k)$ random rate of change of target speed.

$\alpha_b(k)$ random rate of change of target heading.

$\alpha_f(k)$ random rate of change of frequency emitted.

$b(k)$ heading of target at time t_k.

$b_i(k)$ bearing measurement by buoy i.

$\underline{b}(k)$ second moment of the state estimate around expected value $\bar{\underline{a}}(k)$.

c average speed of sound.

$d_i(k)$ distance of target to buoy i.

δ_{kj} Kronecker delta; = 1 if $k = j$; = 0 if $k \neq j$.

$\underline{e}(k)$ estimation error vector.

$\bar{\underline{e}}(k)$ expected value of the estimation error.

$f_o(k)$ rest frequency emitted by the target.

$f_i(k)$ frequency measured by buoy i.

$G(k)$ gain matrix.

$H(k)$ observation matrix.

m compression/expansion factor

$P(k)$ estimation error covariance matrix.

$Q(k)$ state excitation covariance matrix.

$R(k)$ measurement noise cavariance matrix.

$s(k)$ speed of target.

$s_i(k)$ relative velocity of target towards buoy i.

$\sigma_s(k)$ standard deviation of $\alpha_s(k)$.

$\sigma_b(k)$ standard deviation of $\alpha_b(k)$.

$\sigma_f(k)$ standard deviation of $\alpha_f(k)$.

τ time delay.

T_{ij} time delay difference between the signals received by buoys i and j.

T_p time spent in prediction.

T_e time spent in estimation.

$\underline{v}(k)$ vector of q random measurement noise signals.

$\underline{w}(k)$ vector of m random forcing inputs.

$\underline{x}(k)$ state vector of dimension n.

$x(k)$ x-position of target.

$x_i(k)$ x-position of buoy i.

$\hat{\underline{x}}(k)$ estimated state vector.

$\underline{y}(k)$ [n(n+3)/2]-dimensional vector containing the state

variables and the distinct components of the matrix P.

$y(k)$ y-position of target.

$y_i(k)$ y-position of buoy i.

$\underline{z}(k)$ vector of q measurements.

Z^k set of all measurements up to and including time t_k, i.e. $[\underline{z}(0), \underline{z}(1), \ldots, \underline{z}(k)]$.

ACKNOWLEDGEMENTS

I am deeply indebted to the United States Navy and the Brazilian Navy for providing me the opportunity to pursue this work.

I wish to express my gratitude to Professor D. E. Kirk, my advisor, and to the members of my Doctoral Committee.

I. INTRODUCTION

This work was oriented to the problem of optimally estimating characteristics and/or parameters of a certain class of nonlinear, dynamic, stochastic systems from observed output sequences which are noise corrupted nonlinear functions of the system states.

In particular, attention was directed to the problem of real-time, short-range optimal localization and tracking of a submarine target by passive acoustical means. The most accurate and reliable estimates of the target's parameters (position, heading, speed) are sought by optimally processing the measurements obtained from the acoustic signals transmitted by the target itself and received by special sonobuoys.

In the unclassified literature there are presently available methods of passive tracking of submarine targets. Reference [1] utilizes doppler-shifted frequency measurements obtained from a group of sensors; [2] uses bearing and doppler-shifted frequency measurements obtained from one or more sonobuoys. These methods provide very good first approximations to the solution of the problem and many of their concepts and notation are used in this work.

As a first step, an attempt was made to produce a comprehensive study of all the information available in the acoustic signals picked up by the sonobuoys and its usefulness in the estimation process.

The estimation algorithms were developed taking into account the advantages of processing information as soon as it becomes available. Flexibility to move, remove and include sensors and measurements at any time was obtained. Constraints were included to account for limitations of practical, inexpensive and presently available sonobuoys and computing equipment.

In Chapter II the problem is described in mathematical terms using state space techniques and the initial assumptions and constraints are given. The model used for the target is similar to the model presented in [2], but with a different set of states. The measurements obtained from the signals received by the sonobuoys are characterized and their functional relationships to the parameters of the target are analyzed.

Chapter III discusses the general theoretical solution for the problem and the difficulties of implementing it. Approximate solutions are then sought and processing equations are developed. The special vectors, matrices and relations characteristic of the tracking problem are prepared for the application of the filtering equations.

In Chapter IV the concept of partitioned measurements is introduced and analyzed. The advantages in accuracy, computing efficiency and filter flexibility are stressed.

Practical and graphical interpretations of the estimation process help in visualizing nonlinear problems and motivate the adoption of iterative techniques. Increased accuracy and possible convergence improvements are shown to result from this approach.

Chapter V introduces the interactive computer program that allowed the application of the ideas described in the previous chapters to the tracking problem. Selected simulations are discussed and presented in graphical form.

This research covers the subject in a much more comprehensive way than earlier works, [1], [2], [3]. The results obtained by using the methods and ideas collected and developed in this study show many ways of improving the tracking accuracy, of increasing computing efficiency, of reducing divergence problems and of obtaining faster convergence.

The importance of having the buoys placed in adequate positions, of having an adequate model for the target, and of having frequent, varied and precise measurements is stressed.

The final chapter summarizes the results of this investigation and presents the conclusions and suggestions for further study.

II. PROBLEM FORMULATION

A. THE ESTIMATION PROBLEM

A general nonlinear, stochastic, dynamic system observed by a set of nonlinear, nonstationary measurements can be represented, for our purposes, in state-space discrete form by the equations

$$\underline{x}(k+1) = \underline{f}(\underline{x}(k), \underline{w}(k), t_k, t_{k+1}) \qquad (2.1)$$

$$\underline{z}(k) = \underline{h}(\underline{x}(k), \underline{v}(k), t_k) \qquad (2.2)$$

where $\underline{x}(k)$ is the state vector of dimension n,

$\underline{w}(k)$ is the vector of the m random forcing inputs,

$\underline{z}(k)$ is the measurement vector of dimension q,

$\underline{v}(k)$ is the vector of p random measurement noises,

$\underline{f}(\ )$ and $h(\ )$ are general vector functions.

The general estimation problem consists of

--- knowing the statistical characteristics of $\underline{w}(k)$ and $\underline{v}(k)$ and having a statistical representation of the initial conditions $\underline{x}(0)$ of the system,

--- processing the observations $\underline{z}(0)$, $\underline{z}(1)$, ..., $\underline{z}(j)$ in a statistically optimal way to obtain the best estimate, in some sense, of the system state $\underline{x}(k)$ at time t_k.

If $k > j$ the processing is called prediction, if $k < j$ it is called smoothing and if $k = j$ it is called filtering.

In this work some departures from the completely general nonlinear case were taken. The first assumption is that the measurement noise is additive and that the system equations are linear with respect to the random input vector $\underline{w}$. Equations (2.1) and (2.2) can then be written as

$$\underline{x}(k+1) = \underline{f}(\underline{x}(k), t_k, t_{k+1}) + \underline{g}(\underline{x}(k), t_k, t_{k+1}).\underline{w}(k) \tag{2.3}$$

$$\underline{z}(k+1) = \underline{h}(\underline{x}(k), t_k) + \underline{v}(k) \tag{2.4}$$

where $\underline{f}(\ )$ and $\underline{h}(\ )$ represent general vector functions and $\underline{g}(\ )$ a general matrix of functions.

Secondly, the measurement noise and random forcing input are assumed to be uncorrelated in time, zero mean, discrete Gaussian sequences, independent of one another and independent of the initial condition of the state of the system, i.e.,

$$E[\underline{w}(k)] = \underline{0} \qquad E[\underline{v}(k)] = \underline{0} \tag{2.5}$$

$$E[\underline{w}(k)\underline{w}^T(j)] = Q(k).\,\delta_{kj} \qquad E[\underline{v}(k)\underline{v}^T(j)] = R(k).\,\delta_{kj}$$

$$E[\underline{w}(k)\underline{v}^T(j)] = 0 \qquad E[\underline{x}(0)\underline{w}^T(k)] = 0 \qquad E[\underline{v}(k)\underline{x}^T(0)] = 0$$

$$\delta_{kj} = \begin{cases} 1 & \text{if } k = j \\ 0 & \text{if } k \neq j \end{cases}$$

B. THE PASSIVE TRACKING PROBLEM

Many practical situations can be formulated as estimation problems and characterized by the equations described above. The situation that motivated this study assumes a submarine target following (most of the time) an approximately constant speed and constant heading path in a field of passive sonobuoys.

The target unintentionally emits acoustic signals which are picked up by hydrophones. The transduced signals are sent up by wire to the buoys and then frequency-modulate VHF carriers which are transmitted by the buoys and received at a nearby ship or aircraft. After the recovery of the signal, data processing equipment generates measurement values which contain numerical information about the target parameters.

The first step in the analysis of the signals collected by the sonobuoys is the attempt to detect the presence of a real target.

After a target is detected, frequency spectrum information is added to intelligence data in an attempt to classify it. Other measurements and information from any other source are also used to obtain a first approximation to the target's parameters (position, heading, speed), generally through the use of least mean square techniques [1],[3].

The third phase of the process, if a wartime condition doesn't exist, is the tracking of the target. That is, the

determination of its path while reducing, if possible, the initial uncertainties about its parameters, in real-time, through the optimal processing of the sparse information provided by the sonobuoys. The passive characteristic causes severe limitations but is necessary to avoid revealing to the target the fact that it is being observed.

This investigation was devoted to the tracking phase and it was assumed that the main characteristics of the buoys as well as their positions are known.

C. THE MODEL OF THE TARGET

The problem is, of course, three-dimensional. Nevertheless the measurements are not a direct function of the target's depth but of the difference in depth between the target and the hydrophones. Anticipating the accuracy of the measurements and the precision of the data processing equipment and algorithms, it is justifiable to consider only two dimensions initially, adding depth as the third dimension whenever necessary and with no conceptual difficulty.

The target's path is frequently one with nearly constant speed and heading, disturbed by currents and random thrust and control variations. Intentional maneuvers which have no evasive purposes are normally simple and smooth.

A basic plant having as states two position coordinates (x and y), heading (b) and speed (s) of the target, describing a constant velocity path, as shown in Fig 1, seems

adequate.

Random forcing inputs should be considered to account for noise processes and imperfections of the model, such as target maneuvers.

As suggested by [2] these random forcing functions can be approximately represented by two independent zero-mean, piecewise-constant random rates of change, α_s and α_b, acting on the speed and heading of the target.

The formulation of this basic plant in discrete state-space form, similar to Equation (2.3), can be obtained in the following way

$$s(k+1) - s(k) = \int_{t_k}^{t_{k+1}} \alpha_s(t)\, dt \tilde{=} (t_{k+1} - t_k)\cdot\alpha_s(k)$$

$$b(k+1) - b(k) = \int_{t_k}^{t_{k+1}} \alpha_b(t)\, dt \tilde{=} (t_{k+1} - t_k)\cdot\alpha_b(k)$$

$$x(k+1) - x(k) = \int_{t_k}^{t_{k+1}} s(t)\cos b(t)\, dt \tilde{=}$$

$$= \int_{t_k}^{t_{k+1}} [s(k) + (t - t_k)\alpha_s(k)]\cos[b(k) +$$

$$+ (t - t_k)\alpha_b(k)]\, dt =$$

$$= \int_{t_k}^{t_{k+1}} s(k)\cos b(k)\, dt +$$

$$+ \int_{t_k}^{t_{k+1}} (t - t_k)\alpha_s(k)\cos b(k)\, dt -$$

$$- \int_{t_k}^{t_{k+1}} (t - t_k)\alpha_b(k)\, s(k)\sin b(k)\, dt + \ldots =$$

$$= (t_{k+1} - t_k)\, s(k)\cos b(k) +$$

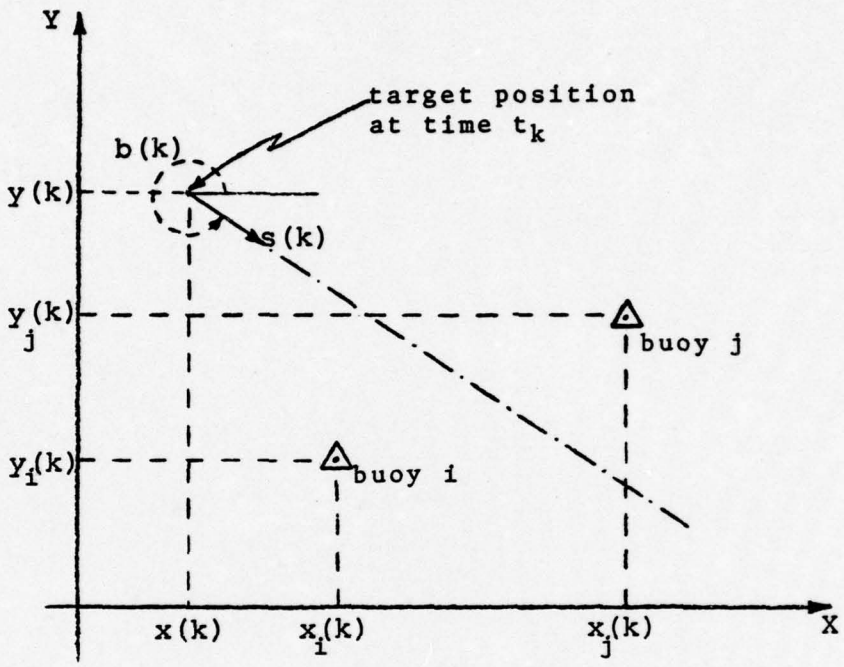

Figure 1 : Geometry of target and sensors.

$$+ \frac{1}{2} (t_{k+1} - t_k)^2 [\alpha_s(k) \cos b(k) -$$

$$- \alpha_b(k)\, s(k) \sin b(k)] + HOT \qquad (2.6)$$

where HOT represents Higher-Order Terms.

In the same way,

$$y(k+1) - y(k) = \int_{t_k}^{t_{k+1}} s(t) \sin b(t)\, dt \cong$$

$$= (t_{k+1} - t_k)\, s(k) \sin b(k) +$$

$$+ \frac{1}{2} (t_{k+1} - t_k)^2 [\alpha_s(k) \sin b(k) +$$

$$+ \alpha_b(k)\, s(k) \cos b(k)] + HOT \qquad (2.7)$$

If $(t_{k+1} - t_k)\alpha_s(k)$ and $(t_{k+1} - t_k)\alpha_b(k)$ are sufficiently small so that the higher order terms in Equations (2.6) and (2.7) can be neglected, one has, in vector form

$$\underline{x}(k+1) = \underline{f}(\underline{x}(k), t_k, t_{k+1}) + \underline{g}(\underline{x}(k), t_k, t_{k+1}) \cdot \underline{w}(k)$$

where

$$\underline{x}(k) = \begin{bmatrix} x(k) \\ y(k) \\ s(k) \\ b(k) \end{bmatrix} \qquad (2.8)$$

$$w(k) = \begin{bmatrix} \alpha_s(k) \\ \\ \alpha_b(k) \end{bmatrix} \qquad (2.9)$$

$$\underline{f}(\underline{x}(k), t_{k+1}, t_k) = \tag{2.10}$$

$$\begin{bmatrix} x(k) + (t_{k+1} - t_k)\, s(k) \cos b(k) \\ y(k) + (t_{k+1} - t_k)\, s(k) \sin b(k) \\ s(k) \\ b(k) \end{bmatrix}$$

and

$$\underline{g}(\underline{x}(k), t_{k+1}, t_k) = \tag{2.11}$$

$$\begin{bmatrix} \frac{1}{2}(t_{k+1} - t_k)^2 \cos b(k) & - \frac{1}{2}(t_{k+1} - t_k)^2 s(k) \sin b(k) \\ \frac{1}{2}(t_{k+1} - t_k)^2 \sin b(k) & \frac{1}{2}(t_{k+1} - t_k)^2 s(k) \cos b(k) \\ (t_{k+1} - t_k) & 0 \\ 0 & (t_{k+1} - t_k) \end{bmatrix}$$

When frequency measurements are to be processed directly, as shown in Section II,D,1,b, an additional state variable must be included --- the rest frequency f_o emitted by the target.

This frequency is assumed to be approximately constant with a small random disturbance α_f that is assumed to be zero-mean, piecewise-constant, and independent of α_s and α_b.

The expanded state variable formulation is given by

$$\underline{x}^e(k) = \begin{bmatrix} \underline{x}(k) \\ \hline f_o(k) \end{bmatrix} \tag{2.12}$$

$$\underline{w}^e(k) = \begin{bmatrix} \underline{w}(k) \\ \hline \alpha_f(k) \end{bmatrix} \qquad (2.13)$$

$$\underline{x}^e(k+1) = \underline{f}^e(\underline{x}^e(k), t_{k+1}, t_k) + \underline{g}^e(\underline{x}^e(k), t_{k+1}, t_k) \cdot \underline{w}^e(k) \qquad (2.14)$$

where

$$\underline{f}^e(\underline{x}^e(k), t_{k+1}, t_k) = \begin{bmatrix} \underline{f}(\underline{x}(k), t_{k+1}, t_k) \\ \hline f_o(k) \end{bmatrix} \qquad (2.15)$$

$$\underline{g}^e(\underline{x}^e(k), t_{k+1}, t_k) = \left[\begin{array}{cc|c} \multicolumn{2}{c|}{\underline{g}(\underline{x}(k), t_{k+1}, t_k)} & \begin{matrix} 0 \\ 0 \end{matrix} \\ \hline 0 & 0 & (t_{k+1} - t_k) \end{array}\right] \qquad (2.16)$$

D. MEASUREMENTS

The sonobuoys can perform one or both of the following tasks:

--- pick up underwater sound signals

--- indicate the approximate direction of the vectorial sum of the received acoustic signals.

The target emits a signal r(t) which is distorted and modulated by the propagation medium between the source and the hydrophone, and by extraneous sound sources present in the ocean.

When all of these disturbances are of relatively mild strength, the signal received by a stationary buoy i will be approximately an attenuated and delayed version of the previously emitted signal, i.e.,

$$r_i(t) \tilde{=} a_i(t).r(t - \tau_i(t)) \qquad (2.17)$$

where $a_i(t)$ is an attenuation factor and $\tau_i(t)$ is the time delay given by

$$\tau_i(t) = d_i(t - \tau_i(t)) / c \qquad (2.18)$$

that is, the distance d_i between the target and the buoy at the time of emission divided by the average velocity of sound in the medium.

Since the target velocity is much smaller than the sound velocity, for small distances and delays one has

$$d_i(t - \tau_i(t)) \tilde{=} d_i(t) + s_i(t).\tau_i(t) \qquad (2.19)$$

where $s_i(t)$ is the relative speed of the target toward buoy i as shown in Fig 2.

Thus, from Equations (2.18) and (2.19) one has

$$\tau_i(t) \tilde{=} d_i(t) / (c - s_i(t)) \qquad (2.20)$$

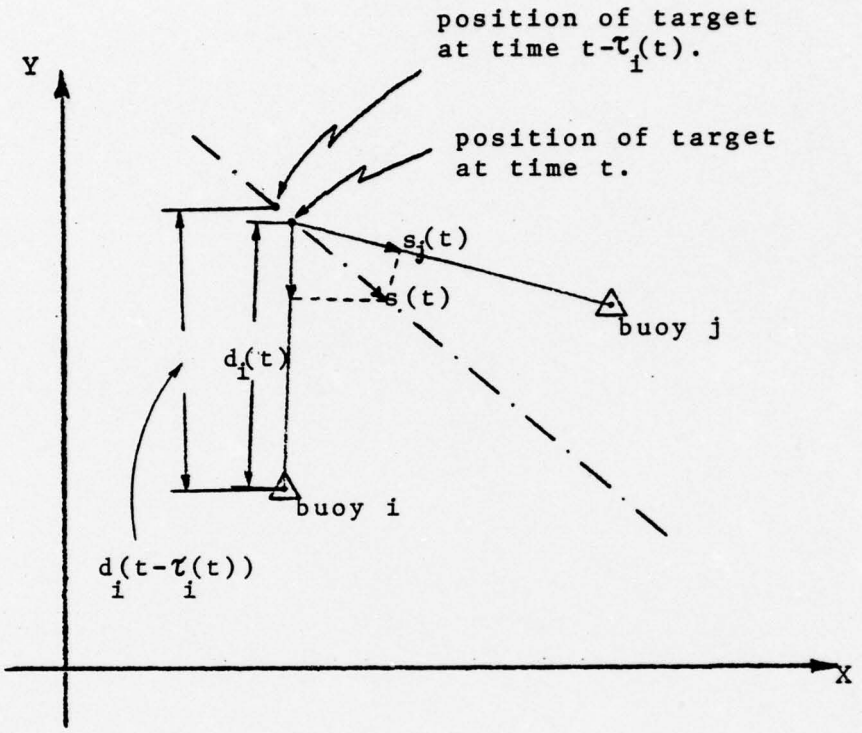

Figure 2 : Target-sensors geometry - distances and relative velocities.

and the received signal is given by

$$r_i(t) \tilde{=} a_i(t).r[t - d_i(t)/(c - s_i(t))] \qquad (2.21)$$

If this signal is recorded from $t = t_o$ to $t = t_o + T$, one has recorded

$$r_i(t_o + t') \tilde{=} a_i(t_o + t').r[t_o + t' - d_i(t_o + t')/(c - s_i(t_o + t'))]$$

$$0 \leq t' \leq T$$

If during this period T the relative target speed towards buoy i doesn't change significantly,

$$s_i(t_o + t') \tilde{=} s_i(t_o)$$

$$d_i(t_o + t') \tilde{=} d_i(t_o) - t'.s_i(t_o)$$

and hence

$$r_i(t_o + t') \tilde{=} a_i(t_o + t').r\left[t_o - d_i(t_o)/(c - s_i(t_o)) + t'.[1 + s_i(t_o)/(c - s_i(t_o))]\right]$$

or

$$r_i(t_o + t') \tilde{=} a_i(t_o + t').r[t_o - d_i(t_o)/(c - s_i(t_o)) + c.t'/(c - s_i(t_o))] \qquad (2.22)$$

In Equation (2.22), the second term inside the brackets is a fixed time delay. The third term is a variable time delay and can be seen as a compression/expansion term, show-

ing the different value of the variable time for the original and the received signals.

If the emitted signal had a single frequency component w_o one would have

$$r_i(t_o + t') \tilde{=} a_i(t_o + t').\cos(w_i(t_o + t'))$$

where

$$\cos(w_i(t_o + t')) = \cos(\phi_{io} + w_i.t') \tilde{=}$$

$$= \cos[w_o.t_o - w_o.d_i(t_o)/(c - s_i(t_o)) +$$

$$+ w_o.c.t'/(c - s_i(t_o))] =$$

$$= \cos[\phi_{io} + w_o.c.t'/(c - s_i(t_o))]$$

and the received frequency would be

$$w_i = w_o.c \;/\; (c - s_i)$$

$$f_i = f_o.c \;/\; (c - s_i) \qquad (2.23)$$

The signals collected by various sonobuoys are sent to a ship or aircraft normally equipped with equipment and skills to extract the information described below.

1. Isolated Buoys

By processing the signals collected by each buoy alone, one can obtain the following noisy measurements:

a. Bearing Indication

Bearing is given directly by the buoys or preprocessed (filtered) to reduce noise effects.

Since the bearing is obtained from a vectorial sum, it can be reasonably accurate only when the acoustic noise is approximately omnidirectional or much weaker than the target signal. For some sensors this vectorial sum can be limited to a selectable frequency band, thereby easing the noise problem.

The relationships between a bearing indication obtained by a buoy i and the states of the target is shown in Fig 3 and given by

$$b_i(k) = \arctan\left[[y(k) - y_i(k)]/[x(k) - x_i(k)]\right] + v(k) \qquad (2.24)$$

where v(k) must account for all the noise disturbing this measurement, including acoustic noise, transducer inaccuracies, preprocessing noise and errors due to the finite speed of the sound in the water. This last factor is caused by the time delay between the emission of a sound by the target and reception at the hydrophone. At the end of this period the target and the hydrophone have slightly different relative positions.

According to [2] typical accuracies of $\pm$ 5 degrees are common for strong signals and inexpensive DIFAR buoys, and as cited by [3] inaccuracies down to $\pm$ 1 degree

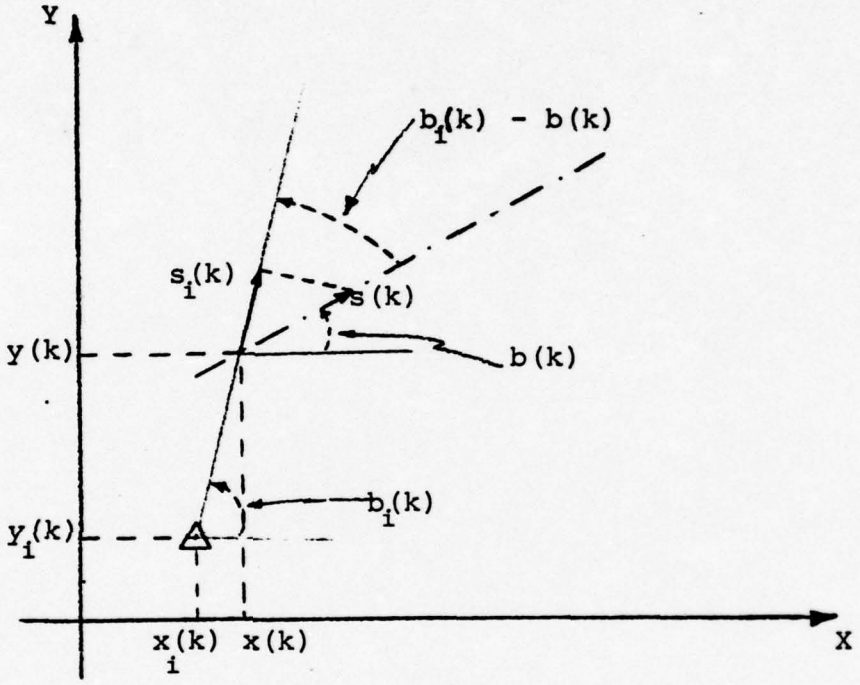

Figure 3 : Bearing measurement.

or less can be obtained with arrays of hydrophones and proper preprocessing.

b. Frequency Indication

By analyzing records of length T seconds of the acoustic signals picked up by the sonobuoys with Fast Fourier Transform algorithms, one can obtain approximate frequency spectrum descriptions with a resolution of 1/T Hertz.

By detecting, measuring and possibly tracking [4] some of the strongest frequencies contained in the signal, very useful data about the target parameters is obtained since the received frequencies are functions of the originally emitted frequencies, the speed, the heading and the position of the target, as shown in the relationship

$$f_i(k) = f_o(k).c \;/\; (c - s_i(k)) \;+\; v(k) \qquad (2.25)$$

where

$$s_i(k) = -s(k).\cos[b(k) - b_i(k)] \qquad (2.26)$$

is the relative velocity toward buoy i, as shown in Fig 3.

The term v(k) now has to account also for the errors introduced in the various paths of the signal from the target to the ship or aircraft, and for variations in target-sensor geometries during the record time T.

As suggested in [1],[2] and [3], inaccuracies ranging between 0.5 and 0.01 Hertz can be obtained in most situations for values of f_o of the order of hundreds of Hertz.

c. Signal Strength Indication

The strength of the signals varies not only with the strength of the originally emitted sound but also with the distance between the target and the buoy. The signal strength also depends on the random aspects and the directivities of the target, the hydrophones, and of the transmitting and receiving VHF antennas. Random absorption and scattering in the various media from the target to the processing equipments may also have a significant influence on the signal presented to the processors.

A mathematical formulation of all these effects would be extremely difficult task and would obscure the desired distance information. For this reason the information contained in the strength of the collected signals, which can be used by an experienced and skilled audio operator, was not incorporated in this study.

Attenuation factors are thrown away by setting the strength of the received signals at a good working level.

2. Two or More Buoys

Considering the signals received by two or more buoys, indications can be obtained which may be used in addition to, or instead of, the measurements available from a single buoy.

a. Frequency Difference Indication

To process frequency measurements obtained from one buoy requires inclusion of the rest frequency as one of the states. This is the case because this measurement is very sensitive to errors in the assumed rest frequency, i.e.,

$$f_i = f_o \cdot c \; / \; (c - s_i)$$

$$\Delta f_i = \Delta f_o \cdot c \; / \; (c - s_i) \tilde{=} \Delta f_o$$

Having the frequencies received by two buoys and taking their difference one gets

$$f_i - f_j = f_o \cdot c/(c - s_i) - f_o \cdot c/(c - s_j) =$$

$$= f_o \cdot c \cdot (s_i - s_j) \; / \; [(c - s_i) \cdot (c - s_j)] =$$

$$\tilde{=} f_o \cdot (s_i - s_j)/c \qquad (2.27)$$

The sensitivity of this difference to errors in the assumption of the rest frequency is given by

$$\Delta(f_i - f_j) \tilde{=} \Delta f_o \cdot (s_i - s_j)/c$$

or is reduced by a very large factor since c is of the order of 1500 m/s and $(s_i - s_j)$ is normally very small.

This way, if one has a reasonable approximation for f_o, instead of processing two measurements in a five-state plant one can process only one frequency-difference measurement in a four-state plant with greatly reduced computing time and hopefully not a detectable reduction in accuracy.

The variance of the errors in each measurement must be added to give the variance of the error in the frequency difference measurement.

b. Frequency Ratio Indication

If one divides the frequencies measured at two sonobuoys, a new relationship is obtained that retains the information on position, heading and speed of the target, but is independent of the rest frequency emitted

$$f_i / f_j = [f_o.c/(c - s_i)].[(c - s_j)/(f_o.c)] =$$

$$= (c - s_j) / (c - s_i) \qquad (2.28)$$

or

$$f_i / f_j = 1 + (s_i - s_j)/c \cdot [1 + s_i/c + (s_i/c)^2 + \ldots] =$$

$$\simeq 1 + (s_i - s_j) / c \qquad (2.29)$$

As with the frequency difference indication, this measurement can be used in a four-state plant instead of using two frequency measurements in a five-state plant.

If this ratio is generated by the division of the frequencies obtained from the analysis of each of the signals, the characteristics of the frequency-ratio measurement noise is complicated and state dependent. If however this relation is obtained as described in the following discussion, this uncomfortable situation can be avoided.

c. Time Delay Indication

As shown at the beginning of this section on measurements, the signal collected by a sonobuoy is a noisy, delayed, attenuated and compressed/expanded reproduction of the original signal emitted by the target. The delay is due to the finite time the signal takes to reach the buoy and the compression/expansion is caused by the variation of this delay with time (doppler effect).

The signals received by two sonobuoys have different noise contributions and different delay and compression/expansion factors even after their strengths are equalized.

Supoose one recorded the signals received by buoys i and j from $t = t_o$ to $t = t_o + T$. The signals are related to the original signal as shown in Equation (2.22), i.e.,

$$r_i(t_o + t') \tilde{=} a_i(t_o + t').r[t_o - d_i(t_o)/(c - s_i(t_o)) + \\ + c.t'/(c - s_i(t_o))] \qquad (2.30)$$

$$r_j(t_o + t') \tilde{=} a_j(t_o + t').r[t_o - d_j(t_o)/(c - s_j(t_o)) + \\ + c.t'/(c - s_j(t_o))] \qquad (2.31)$$

If one now amplifies these two signals to a good working level, correlate them by evaluating

$$\rho(\tau) = \int_o^T r_i(t_o + t').r_j(t_o + t' + \tau).dt' \qquad (2.32)$$

and look for the value of τ that maximizes $\rho(\tau)$ one finds that:

(1) if $s_i(t_o) \tilde{=} s_j(t_o)$ and, consequently, the frequency shifts are about the same in both signals, then $r_i(t_o + t')$ will be simply an approximate delayed or advanced replica of $r_j(t_o + t')$, as can be seen from the above equations.

In this case the maximum of $\rho(\tau)$ is easy to find and corresponds to the value τ_{max} at which

$$t_o - d_i(t_o)/(c - s_i(t_o)) + c.(t' + \tau_{max})/(c - s_i(t_o)) = \\ = t_o - d_j(t_o)/(c - s_j(t_o)) + c.t'/(c - s_j(t_o))$$

solving for τ_{max} yields

$$\tau_{max} = [d_i(t_o) - d_j(t_o)] / c \qquad (2.33)$$

(2) if $s_i(t_o) \neq s_j(t_o)$, $\rho(\tau)$ does not have a simply-determined maximum value because the two signals have frequency components whose phases are shifted by different amounts.

If ones now change the time scale of one of the signals, say $r_j(t_o + t')$, one has

$$r'_j(t') = r_j(t_o + m.t') =$$

$$\tilde{=} a_j.r\left[[t_o - d_j(t_o)/(c - s_j(t_o))] + \right.$$

$$\left. + c.m.t'/(c - s_j(t_o))\right] \qquad (2.34)$$

Comparing this equation with Equation (2.30) one sees that if m can be found such that

$$m.c/(c - s_j(t_o)) = c/(c - s_i(t_o))$$

or

$$m = [c - s_j(t_o)] \; / \; [c - s_i(t_o)] \qquad (2.35)$$

one again has case (1) and the correlation function will give a maximum at approximately

$$\tau_{max} \tilde{=} [d_i(t_o) - d_j(t_o)] \; / \; c \qquad (2.36)$$

It is interesting to note that Equation (2.35) is the same as Equation (2.28). The compression/expansion factor is thus the ratio between the frequencies received by buoys i and j.

The $\rho(\tau,m)$ function, if the two recorded signals were broadband, of long duration and with high S/N ratios, would appear as shown in Fig 4.

Low signal to noise ratios could hide the real maximum and create false ones; narrowband or coherent signals would present ambiguities with the creation of many close maxima.

By considering the availability of equipments and techniques to obtain the proper elimination of the difference in frequency shifts in the recorded signals , this study assumed the possibility of having time delay measurements available to provide information about the target position according to the relationship

$$T_{ij}(k) = [d_i(k) - d_j(k)] / c + v(k) \qquad (2.37)$$

where v(k) must account for the errors caused by the different noise contributions in each signal, for the accuracy and precision of the cross-correlation algorithm or device, and for variations in target-sensors geometry during the recording of the signals.

Inaccuracies anywhere from 0.5 sec down to a few milliseconds seem very reasonable to expect in many cases.

d. Signal Strength Difference

For the same reasons already explained in II,D,1,c the information contained in the difference of

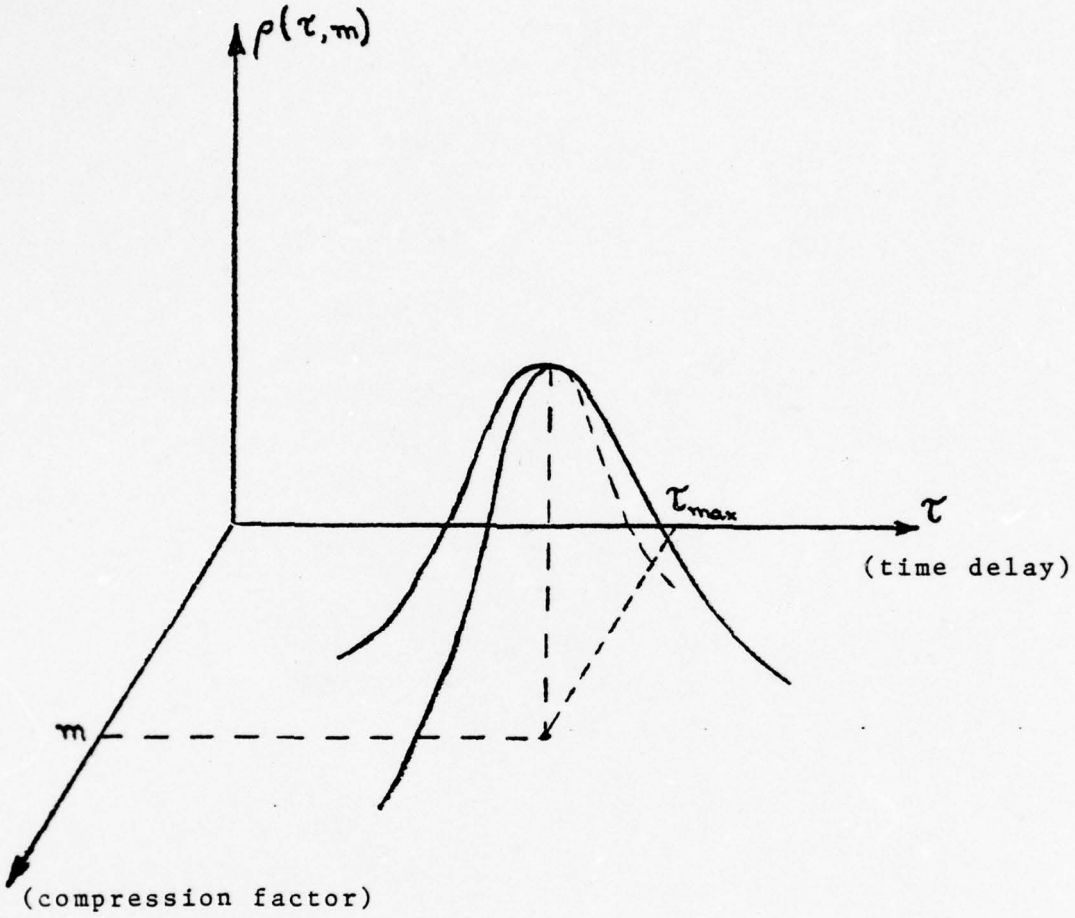

Figure 4 : Correlation function.

strength of the collected signals, while of great use for an experienced and skilled audio operator, was not incorporated in this study.

III. THEORETICAL SOLUTION

A. RECURSIVE BAYES FORMULATION

The maximum amount of information at time t_k, in a probabilistic sense, is concentrated in the conditional density function of the states given all the observations up to this time, $p(\underline{x}(k)|Z^k)$, where Z^k represents the set $\{\underline{z}(k), \underline{z}(k-1), \ldots, \underline{z}(0)\}$.

By specifying a cost function one determines how this information is used to obtain the best estimate [5]. For example, the minimum variance estimate is the mean of the conditional density.

From the assumptions made in Section II,A, the random processes $\underline{x}(k)$ and $\{\underline{x}(k),\underline{z}(k)\}$ are Markov and the conditional density can be written in recursive form using Bayes' Law, as is shown in [5], [6], [7], [8].

$$p(\underline{x}(k)|Z^k) = c(k).p(\underline{x}(k)|Z^{k-1}).p(\underline{z}(k)|\underline{x}(k)) \qquad (3.1)$$

where

$$p(\underline{x}(k)|Z^{k-1}) = \int p(\underline{x}(k-1)|Z^{k-1}).p(\underline{x}(k)|\underline{x}(k-1)).d\underline{x}(k-1) \qquad (3.1a)$$

and

$$1 / c(k) = p(\underline{z}(k) | Z^{k-1}) =$$

$$= \int p(\underline{x}(k) | Z^{k-1}) . p(\underline{z}(k) | \underline{x}(k)) . d\underline{x}(k) \qquad (3.1b)$$

Given the initial condition $p(\underline{x}(0) | Z^{-1}) = p(\underline{x}(0))$ and the probability law of the system random input and measurement noise, $p(\underline{w}(k))$ and $p(\underline{v}(k))$, one can proceed to evaluate these equations and the filtering problem can be regarded as having been solved when $p(\underline{x}(k) | Z^k)$ can be determined for all k.

For any situation different from the one where the system and measurement equations are linear and the apriori distributions are Gaussian, the density $p(\underline{x}(k) | Z^k)$ is not Gaussian and generally cannot be determined in closed form.

In the problem studied here, the conditional densities in Equation (3.1) are nonlinear functions of the states and the measurements. Linearizations, Taylor expansions and Gaussian approximations will be used, however, as an engineering compromise, in order to avoid complex numerical integrations in n dimensions. This approach was chosen taking into account the limitations on processing equipment available for the practical solution of the addressed tracking problem.

B. ONE-STEP PREDICTION

Let us assume that at time t_{k-1}, during a filtering process, an approximately Gaussian density $p(\underline{x}(k-1)|Z^{k-1})$ has been obtained with mean value $\underline{\mu}(k-1)$ and covariance matrix $M(k-1)$.

If one chooses the mean of this conditional density as the estimate at time t_{k-1},

$$\underline{\hat{x}}(k-1) = E[\underline{x}(k-1)|Z^{k-1}] = \underline{\mu}(k-1)$$

the estimation error at time k-1 has the same probability density as $p(\underline{x}(k-1)|Z^{k-1})$ but with zero mean, i.e.,

$$E[\underline{e}(k-1)] = E[(\underline{\hat{x}}(k-1) - \underline{x}(k-1))|Z^{k-1}] = 0 \qquad (3.2)$$

$$E[\underline{e}(k-1)\underline{e}^T(k-1)] = P(k-1) = M(k-1) \qquad (3.3)$$

At time t_k a new set of measurements arrives and a prediction at that time must first be obtained based on the measurements up to t_{k-1}.

The dynamics of the system are described by Equation (2.5) and it can be seen that, even if $p(\underline{x}(k-1)|Z^{k-1})$ were really Gaussian, the density $p(\underline{x}(k)|Z^{k-1})$ would not normally be because of the nonlinearities involved. Nevertheless it will be assumed that a reasonably close approximation to a Gaussian density exists and proceed to find approximate values for the first two moments of the conditional one-step pre-diction density $p(\underline{x}(k)|Z^{k-1})$.

The first step is to expand Equation (2.3) in a Taylor series about the estimate $\hat{\underline{x}}(k-1)$. The dependence on t_k and t_{k-1} is dropped for simplicity. Note that Z^{k-1} is known and was used in determining $\hat{\underline{x}}(k-1)$.

$$\underline{x}(k) = \underline{f}(\underline{x}(k-1)) + \underline{g}(\underline{x}(k-1)).\underline{w}(k-1) =$$

$$= \underline{f}(\hat{\underline{x}}(k-1)) + \left.\frac{\partial \underline{f}}{\partial \underline{x}}\right|_{\hat{\underline{x}}(k-1)} .[\underline{x}(k-1) - \hat{\underline{x}}(k-1)] + \ldots +$$

$$+ \underline{g}(\hat{\underline{x}}(k-1)).\underline{w}(k-1) + \ldots =$$

$$= \underline{f}(\hat{\underline{x}}(k-1)) - \sum_{i=1}^{n} \left[\left.\frac{\partial \underline{f}}{\partial x_i}\right|_{\hat{\underline{x}}(k-1)} .e_i(k-1) \right] +$$

$$+ \sum_{i=1}^{n} \sum_{j=1}^{n} \left[\left.\frac{\partial f}{\partial x_i \partial x_j}\right|_{\hat{\underline{x}}(k-1)} .e_i(k-1).e_j(k-1) \right] + \ldots +$$

$$+ \underline{g}(\hat{\underline{x}}(k-1)).\underline{w}(k-1) -$$

$$- \sum_{i=1}^{n} \left[\left.\frac{\partial \underline{g}_i}{\partial \underline{x}}\right|_{\hat{\underline{x}}(k-1)} .w_i(k-1) \right] .\underline{e}(k-1) + \ldots \qquad (3.4)$$

where x_i and e_i are individual components of $\hat{\underline{x}}$ and $(\underline{x} - \underline{x})$; $\underline{g}_i$ is a column vector of $\underline{g}$; and w_i is a component of $\underline{w}$.

1. Linear Approximation

In this case only the terms in the expansion which are linear in $\underline{e}(k-1)$ and $\underline{w}(k-1)$ are considered, i.e.,

$$\underline{x}(k) \cong \underline{f}(\hat{\underline{x}}(k-1)) - \phi(k-1).\underline{e}(k-1) +$$

$$+ \underline{g}(\hat{\underline{x}}(k-1)).\underline{w}(k-1) \qquad (3.5)$$

where

$$\phi(k-1) = \frac{\partial}{\partial \underline{x}} \underline{f}(\hat{\underline{x}}(k-1), t_k, t_{k-1}) \qquad (3.6)$$

From Equation (3.5) the mean value of $p(\underline{x}(k)|Z^{k-1})$, which is chosen as our predicted value, is

$$\hat{\underline{x}}(k|k-1) = E[\underline{x}(k)|Z^{k-1}] = \underline{f}(\hat{\underline{x}}(k-1)) -$$

$$- \phi(k-1).E[\underline{e}(k-1)] + \underline{g}(\hat{\underline{x}}(k-1)).E[\underline{w}(k-1)]$$

But $\underline{e}(k-1)$ and $\underline{w}(k-1)$ have zero means, therefore,

$$\hat{\underline{x}}(k|k-1) = \underline{f}(\hat{\underline{x}}(k-1), t_k, t_{k-1}) \qquad (3.7)$$

Thus the one-step prediction error has the mean

$$E[\underline{e}(k|k-1)] = E[(\hat{\underline{x}}(k|k-1) - \underline{x}(k))|Z^{k-1}] =$$

$$= E[\phi(k-1).\underline{e}(k-1) - \underline{g}(\hat{\underline{x}}(k-1)).\underline{w}(k-1)] = 0$$

The prediction error covariance matrix, which is also the covariance matrix of $p(\underline{x}(k)|Z^{k-1})$, is, using simplified notation,

$$P(k|k-1) = E[\underline{e}(k|k-1)\underline{e}^T(k|k-1)] \tilde{=}$$

$$= E\left[[\phi(k-1).\underline{e}(k-1) - \underline{g}(\hat{\underline{x}}(k-1)).\underline{w}(k-1)][\ldots]^T\right] =$$

$$= E[\phi.\underline{e}.\underline{e}^T.\phi^T - \phi.\underline{e}.\underline{w}^T.\underline{g}^T - \underline{g}.\underline{w}.\underline{e}^T.\phi^T + \underline{g}.\underline{w}.\underline{w}^T.\underline{g}^T]$$

From the assumptions about the independence and discrete white noise characteristics of w, the terms

$$\phi(k-1).E[\underline{e}(k-1).\underline{w}^T(k-1)].\underline{g}^T(\hat{\underline{x}}(k-1)) = 0$$

$$\underline{g}(\hat{\underline{x}}(k-1)).E[\underline{w}(k-1).\underline{e}^T(k-1)].\phi^T(k-1) = 0$$

and

$$P(k|k-1) = \phi(k-1).P(k-1).\phi^T(k-1) +$$

$$+ \underline{g}(\hat{\underline{x}}(k-1)).Q(k-1).\underline{g}^T(\hat{\underline{x}}(k-1)) \qquad (3.8)$$

2. First Order Approximation

In this development one retains all terms in Equation (3.4) up to first order partial derivatives, i.e.,

$$\underline{x}(k) \cong \underline{f}(\underline{x}(k-1)) - \phi(k-1).\underline{e}(k-1) +$$

$$+ \underline{g}(\hat{\underline{x}}(k-1)).\underline{w}(k-1) -$$

$$- \sum_{i=1}^{m} A_i(k-1).w_i(k-1) \cdot \underline{e}(k-1) \qquad (3.9)$$

where

$$A_i(k-1) = \frac{\partial}{\partial \underline{x}} \; \underline{a}_i(\hat{\underline{x}}(k-1), t_k, t_{k-1}) \qquad (3.10)$$

As in the last section, the predicted value is

$$\hat{\underline{x}}(k|k-1) = \underline{f}(\hat{\underline{x}}(k-1)) - \phi(k-1).E[\underline{e}(k-1)] +$$

$$+ \underline{g}(\hat{\underline{x}}(k-1)).E[\underline{w}(k-1)] - \sum_{i=1}^{m} A_i.E[w_i(k-1).\underline{e}(k-1)]$$

From the assumptions about $\underline{w}(k-1)$ and $\underline{e}(k-1)$, the prediction is

$$\hat{\underline{x}}(k|k-1) = \underline{f}(\hat{\underline{x}}(k-1)),$$

the same as in Equation (3.7).

The one-step prediction error has zero mean and covariance matrix given by, in simplified notation,

$$P(k|k-1) = E\left[[\phi(k-1).\underline{e}(k-1) - \underline{g}(\hat{\underline{x}}(k-1)).\underline{w}(k-1) + \right.$$
$$\left. + \sum_{i=1}^{m} A_i(k-1).w_i(k-1).\underline{e}(k-1)]\,[\ldots]^T\right] =$$
$$= E[\phi.\underline{e}.\underline{e}^T.\phi^T - \phi.\underline{e}.\underline{w}^T.\underline{g}^T + \sum_{i=1}^{m} \phi.\underline{e}.\underline{e}^T.A_i^T.w_i -$$
$$- \underline{g}.\underline{w}.\underline{e}^T.\phi^T + \underline{g}.\underline{w}.\underline{w}^T.\underline{g}^T - \sum_{i=1}^{m} \underline{g}.\underline{w}.\underline{e}^T.A_i^T.w_i +$$
$$+ \sum_{i=1}^{m} A_i.\underline{e}.\underline{e}^T.\phi^T.w_i - \sum_{i=1}^{m} A_i.\underline{e}.\underline{w}^T.\underline{g}^T.w_i +$$
$$+ \sum_{i=1}^{m}\sum_{j=1}^{m} A_i.\underline{e}.\underline{e}^T.A_j^T.w_i.w_j]$$

From the assumptions about $\underline{w}$, one has that

$$E[\underline{e}(k-1).\underline{w}^T(k-1)] = 0$$

$$E[\underline{e}(k-1).\underline{e}^T(k-1).w_i(k-1)] = E[\underline{e}(k-1).\underline{e}^T(k-1)].$$
$$E[w_i(k-1)] = 0$$

$$E[\underline{w}(k-1).\underline{e}^T(k-1).w_i(k-1)] = E[\underline{w}(k-1).w_i(k-1)].$$
$$E[\underline{e}^T(k-1)] = 0$$

$$E[\underline{e}(k-1).\underline{e}^T(k-1).w_i(k-1).w_j(k-1)] =$$

$$= E[\underline{e}(k-1).\underline{e}^T(k-1)].E[w_i(k-1).w_j(k-1)] =$$

$$= P(k-1) \; . \; q_{ji}(k-1)$$

where $q_{ji}(k-1)$ is the j,ith term of $Q(k-1)$.

Thus,

$$P(k|k-1) = \phi(k-1).P(k-1).\phi^T(k-1) +$$

$$+ \underline{g}(\hat{\underline{x}}(k-1)).Q(k-1).\underline{g}^T(\hat{\underline{x}}(k-1)) +$$

$$+ \sum_{=1}^{m} \sum_{j=1}^{m} A \; .P(k-1).A_j^T.q_{ji}(k-1) \qquad (3.11)$$

If the Q matrix is diagonal, $q_{ji} = 0$ for $j \neq 1$ and

$$P(k|k-1) = \phi(k-1).P(k-1).\phi^T(k-1) +$$

$$+ \underline{g}(\hat{\underline{x}}(k-1)).Q(k-1).\underline{g}^T(\hat{\underline{x}}(k-1)) +$$

$$+ \sum_{i=1}^{m} A_i.P(k-1).A_i^T.q_{ii}(k-1) \qquad (3.12)$$

3. Other Approximations

Depending on how many terms of Equation (3.4) are considered, other different prediction values and prediction error covariance matrices are obtained. Higher moments of the conditional densities would be required with increased complexity and computational burden.

C. UP-DATING THE ESTIMATE

Let us assume that we have an approximately Gaussian density $p(\underline{x}(k)|Z^{k-1})$ whose mean value is the prediction $\hat{\underline{x}}(k|k-1)$ and whose second central moment is the prediction error covariance matrix $P(k|k-1)$.

A new set of measurements is given, consisting of non-linear noisy observations of the states, represented by the relationship

$$\underline{z}(k) = \underline{h}(\underline{x}(k), t_k) + \underline{v}(k)$$

It is now necessary to process $\underline{z}(k)$ and extract the information it brings. A new approximate Gaussian density $p(\underline{x}(k)|Z^k)$ is assumed to be generated whose moments are the new estimate $\hat{\underline{x}}(k)$ and the estimation error covariance matrix $P(k)$.

This new density is given by Equation (3.1) or by

$$p(\underline{x}(k)|Z^k) = p(\underline{z}(k)|\underline{x}(k)).p(\underline{x}(k)|Z^{k-1}) \;/\; p(\underline{z}(k)|Z^{k-1}) \tag{3.13}$$

$p(\underline{x}(k)|Z^{k-1})$ is assumed to be approximately Gaussian with moments $\hat{\underline{x}}(k|k-1)$ and $P(k|k-1)$.

Expanding the measurement equation around $\hat{\underline{x}}(k|k-1)$ one has

$$\underline{z}(k) = \underline{h}(\hat{\underline{x}}(k|k-1)) + \left.\frac{\partial \underline{h}}{\partial \underline{x}}\right|_{\hat{\underline{x}}(k|k-1)} .[\underline{x}(k) - \hat{\underline{x}}(k|k-1)] + \ldots + \underline{v}(k)$$

Retaining only the linear terms, one has

$$\underline{z}(k) = \underline{h}(\hat{\underline{x}}(k|k-1) + H(k).[\underline{x}(k) - \hat{\underline{x}}(k|k-1)] + \underline{v}(k) \tag{3.14}$$

where

$$H(k) = \frac{\partial}{\partial \underline{x}} \underline{h}(\hat{\underline{x}}(k|k-1), t_k) \tag{3.15}$$

From Equation (3.14) one obtains

$$E[\underline{z}(k)|Z^{k-1}] = \underline{h}(\hat{\underline{x}}(k|k-1))$$

and it is easily shown that

$$Var[\underline{z}(k)|Z^{k-1}] = H(k).P(k|k-1).H^T(k) + R(k)$$

Also from Equation (3.14),

$$E[\underline{z}(k)|\underline{x}(k)] = \underline{h}(\hat{\underline{x}}(k|k-1)) + H(k).[\underline{x}(k) - \hat{\underline{x}}(k|k-1)]$$

$$Var[\underline{z}(k)|\underline{x}(k)] = R(k)$$

If one now assumes that $p(\underline{z}(k)|Z^{k-1})$ and $p(\underline{z}(k)|\underline{x}(k))$ are approximately Gaussian densities with the moments given above, then Equation (3.13) becomes

$$p(\underline{x}(k)|Z^K) \cong |H(k).P(k|k-1).H^T(k) + R(k)|^{1/2} /$$

$$/ [(2\pi)^{n/2}.|P(k|k-1)|^{1/2}.|R(k)|^{1/2}] . \exp[B]$$

where

$$\exp[B] = \exp\left\{-\frac{1}{2}\left[\left[\left[\underline{x}(k) - \underline{\hat{x}}(k|k-1)\right]^T . P^{-1}(k|k-1) . [\ldots]\right] + \right.\right.$$

$$+ \left[\left[\underline{z}(k) - \underline{h}(\underline{\hat{x}}(k|k-1)) - H(k).[\underline{x}(k) - \underline{\hat{x}}(k|k-1)]\right]^T . \right.$$

$$R^{-1}(k).[\ldots]\Big] -$$

$$\left. - \left[\left[\underline{z}(k) - \underline{h}(\underline{\hat{x}}(k|k-1))\right]^T . \right.\right.$$

$$\left.\left.\left.[H(k).P(k|k-1).H^T(k) + R(k)]^{-1}.[\ldots]\right]\right]\right\}$$

(3.16)

Simplifying the notation, this exponent can be rearranged in the following way

$$(x - \hat{x})^T . P^{-1} . (x - \hat{x}) + [z - h(\hat{x}) - H.(x - \hat{x})]^T . R^{-1} . [\ldots] -$$

$$- [z - h(\hat{x})]^T . [H.P.H^T + R]^{-1} . [z - h(\hat{x})] =$$

$$= (x - \hat{x})^T P^{-1}(x - \hat{x}) + (x - \hat{x})^T H^T R^{-1} H(x - \hat{x}) -$$

$$- [z - h(\hat{x})]^T R^{-1} H(x - \hat{x}) - (x - \hat{x})^T H^T R^{-1}[z - h(\hat{x})] +$$

$$+ [z - h(\hat{x})]^T R^{-1}[z - h(\hat{x})] -$$

$$- [z - h(\hat{x})]^T [HPH^T + R]^{-1}[z - h(\hat{x})] =$$

$$= (x - \hat{x})^T (P^{-1} + H^T R^{-1} H)(x - \hat{x}) -$$

$$- (x - \hat{x})^T H^T R^{-1}[z - h(\hat{x})] -$$

$$- [z - h(\hat{x})]^T R^{-1} H(x - \hat{x}) -$$

$$- [z - h(\hat{x})]^T [R^{-1} - (HPH^T + R)^{-1}][z - h(\hat{x})]$$

Using the matrix inversion lemma [9],

$$R^{-1} - (HPH^T + R)^{-1} = R\,H(P^{-1} + H^T R^{-1} H)^{-1} H^T R^{-1}$$

Since R and P are symmetric matrices,

$$R^{-1} H (P^{-1} + H^T R^{-1} H)^{-1} H^T R^{-1} = A^T [P^{-1} + H^T R^{-1} H] A$$

where

$$A = (P^{-1} + H^T R^{-1} H)^{-1} H^T R^{-1}$$

and the exponent of Equation (3.16) becomes

$$(x - \hat{x})^T (P^{-1} + H^T R^{-1} H)(x - \hat{x}) -$$

$$- (x - \hat{x})^T H^T R^{-1} [z - h(\hat{x})] -$$

$$- [z - h(\hat{x})]\, R^{-1} H (x - \hat{x}) -$$

$$- [(P^{-1} + H^T R^{-1} H)^{-1} H^T R^{-1} (z - h(\hat{x}))]^T [P^{-1} + H^T R^{-1} H] [\ldots]$$

which is a quadratic form that can be expressed as

$$\left[x - \hat{x} - [P^{-1} + H^T R^{-1} H]^{-1} H^T R^{-1} [z - h(\hat{x})]\right] . [P^{-1} + H^T R^{-1} H] . \left[\ldots\right]$$

And finally the conditional density of Equation (3.16) can be put in the form

$$p(\underline{x}(k) | Z^k) = a(k) . \exp\left[-\frac{1}{2} [\underline{x}(k) - \underline{\hat{x}}(k)]^T . P^{-1}(k) . [\ldots]\right]$$

where, by definition,

$$\underline{\hat{x}}(k) = \underline{\hat{x}}(k|k-1) + P(k).H^T(k).R^{-1}(k).[\underline{z}(k) - \underline{h}(\underline{\hat{x}}(k|k-1),t_k)]$$

(3.17)

and

$$P^{-1}(k) = P^{-1}(k|k-1) + H^T(k)R^{-1}(k)H(k)$$

or, using the matrix inversion lemma again,

$$P(k) = P(k|k-1) - P(k|k-1)H^T(k).[H(k)P(k|k-1)H^T(k) + R(k)]^{-1}.H(k)P(k|k-1)$$

or

$$P(k) = [I - G(k)H(k)].P(k|k-1) \qquad (3.18)$$

where

$$G(k) = P(k|k-1).H^T(k).[H(k).P(k|k-1).H^T(k) + R(k)]$$

(3.19)

From Equation (3.19) one obtains

$$G(k) = P(k|k-1).H^T(k).R^{-1}(k).[H(k).P(k|k-1).H^T(k).R^{-1}(k) + I]^{-1}$$

Premultiplying by $P(k)P^{-1}(k)$, and using the expression found earlier for $P^{-1}(k)$ gives

$$G(k) = P(k).[I + H^TR^{-1}HP(k|k-1)]H^TR^{-1}.[HP(k|k-1)H^TR^{-1} + I]^{-1} =$$

$$= P(k).[H^T R^{-1} + H^T R^{-1} H P(k|k-1) H^T R^{-1}] .$$

$$[I + H P(k|k-1) H^T R^{-1}]^{-1}$$

and finally,

$$G(k) = P(k).H^T(k).R^{-1}(k) \qquad (3.20)$$

Applying this result to Equation (3.17) gives

$$\hat{\underline{x}}(k) = \hat{\underline{x}}(k|k-1) + G(k).[\underline{z}(k) - \underline{h}(\hat{\underline{x}}(k|k-1), t_k)] \qquad (3.21)$$

If more terms were taken in the expansion of $\underline{h}(\underline{x}(k), t_k)$ than the ones considered in Equation (3.14), different estimates and covariance matrices would be obtained. Higher moments of the conditional densities would then be required.

We are now in position to restart the one-step prediction of Section III,B and process a measurement ocurring at time t_{k+1}.

The initial step in the whole process is at t_o where it is assumed that an approximate Gaussian distribution exists for the initial value of the states, $\underline{x}(0)$. Choosing the initial estimate as the mean value of this distribution, one has

$$\hat{\underline{x}}(0) = E[\underline{x}(0)]$$

$$E[\underline{e}(0)] = E[\hat{\underline{x}}(0) - \underline{x}(0)] = \underline{0}$$

$$P(0) = E[\underline{e}(0)\underline{e}^T(0)] = Var[\underline{x}(0)]$$

The set of Equations (3.7), (3.8), (3.18), (3.19) and (3.21) is generally known as the Extended Kalmam Filter equations.

D. PARAMETERS FOR THE TRACKING PROBLEM

In order to apply the above relations to the passive tracking problem, a series of vectors and matrices first must be determined.

1. System Dynamics

Applying definition (3.6) to Equation (2.10) yields

$$\phi(k) = \tag{3.22}$$

$$\begin{bmatrix} 1 & 0 & \Delta t.\cos \hat{b}(k) & -\Delta t.\hat{s}(k).\sin \hat{b}(k) \\ 0 & 1 & \Delta t.\sin \hat{b}(k) & \Delta t.\hat{s}(k).\cos \hat{b}(k) \\ 0 & 0 & 1 & 0 \\ 0 & 0 & 0 & 1 \end{bmatrix}$$

where $\Delta t = (t_{k+1} - t_k)$

Breaking up Equation (2.11) into its column vectors gives

$$\underline{g}_1(\hat{\underline{x}}(k), t_{k+1}, t_k) = \begin{bmatrix} \frac{1}{2}\Delta t^2 . \cos \hat{b}(k) \\ \frac{1}{2}\Delta t^2 . \sin \hat{b}(k) \\ \Delta t \\ 0 \end{bmatrix} \qquad (3.23)$$

$$\underline{g}_2(\hat{\underline{x}}(k), t_{k+1}, t_k) = \begin{bmatrix} -\frac{1}{2}\Delta t^2 . \hat{s}(k) . \sin \hat{b}(k) \\ \frac{1}{2}\Delta t^2 . \hat{s}(k) . \cos \hat{b}(k) \\ 0 \\ \Delta t \end{bmatrix} \qquad (3.24)$$

Definition (3.10) requires

$$A_1(k) = \qquad (3.25)$$

$$\begin{bmatrix} 0 & 0 & 0 & -\frac{1}{2}\Delta t^2 . \sin \hat{b}(k) \\ 0 & 0 & 0 & \frac{1}{2}\Delta t^2 . \cos \hat{b}(k) \\ 0 & 0 & 0 & 0 \\ 0 & 0 & 0 & 0 \end{bmatrix}$$

$$A_2(k) = \tag{3.26}$$

$$\begin{bmatrix} 0 & 0 & -\frac{1}{2}\Delta t^2 . \sin \hat{b}(k) & -\frac{1}{2}\Delta t^2 . \hat{s}(k) . \cos \hat{b}(k) \\ 0 & 0 & \frac{1}{2}\Delta t . \cos \hat{b}(k) & -\frac{1}{2}\Delta t^2 . \hat{s}(k) . \sin \hat{b}(k) \\ 0 & 0 & 0 & 0 \\ 0 & 0 & 0 & 0 \end{bmatrix}$$

Assuming independent random forcing inputs yields

$$Q(k) = E[\underline{w}(k)\underline{w}^T(k)] = \begin{bmatrix} \sigma_s^2(k) & 0 \\ 0 & \sigma_b^2(k) \end{bmatrix} \tag{3.27}$$

Equations (3.8) and (3.11) require the product

$$\underline{g}(\hat{\underline{x}}(k), t_{k+1}, t_k) . Q(k) . \underline{g}^T(\hat{\underline{x}}(k), t_{k+1}, t_k) =$$

$$= \Delta t^2 . \begin{bmatrix} a & b & d & e \\ b & c & i & j \\ d & i & \sigma_s^2(k) & 0 \\ e & j & 0 & \sigma_b^2(k) \end{bmatrix} \tag{3.28}$$

where

$$a = \frac{1}{4}\Delta t^2 . [\cos^2 \hat{b}(k) . \sigma_s^2(k) + \hat{s}^2(k) . \sin^2 \hat{b}(k) . \sigma_b^2(k)]$$

$$b = \frac{1}{4}\Delta t^2 . \sin \hat{b}(k) . \cos \hat{b}(k) . [\sigma_s^2(k) - \hat{s}^2(k) . \sigma_b^2(k)]$$

$$c = \frac{1}{4}\Delta t^2 . [\sin^2 \hat{b}(k) . \sigma_s^2(k) + \hat{s}^2(k) . \cos^2 \hat{b}(k) . \sigma_b^2(k)]$$

and

$$d = \frac{1}{2}\Delta t . \cos \hat{b}(k) . \sigma_s^2(k)$$

$$e = -\frac{1}{2}\Delta t . \hat{s}(k) . \sin \hat{b}(k) . \sigma_b^2(k)$$

$$i = \frac{1}{2}\Delta t . \sin \hat{b}(k) . \sigma_s^2(k)$$

$$j = \frac{1}{2}\Delta t . \hat{s}(k) . \cos \hat{b}(k) . \sigma_b^2(k)$$

If the expanded state variable formulation is used, the matrices given below are needed

$$Q^e(k) = E[\underline{w}^e(k)\underline{w}^{eT}(k)] = \begin{bmatrix} Q(k) & 0 \\ & 0 \\ 0 \quad 0 & \sigma_f^2 \end{bmatrix} \qquad (3.29)$$

$$\underline{g}^e . Q . \underline{g}^{eT} = \begin{bmatrix} \underline{g} . Q . \underline{g}^T & 0 \\ 0 & \Delta t^2 . \sigma_f^2 \end{bmatrix} \qquad (3.30)$$

$$\phi^e = \begin{bmatrix} \phi & 0 \\ 0 & 1 \end{bmatrix} \qquad (3.31)$$

2. Measurements

In the following development Equation (3.15) is applied to each of the measurements described in Section II,D to yield the appropriate linearized observation matrix.

a. Bearing Measurement

From Equation (2.24) one has

$$\frac{\partial}{\partial \xi} b_i = (x - x_i)^2 / [(x - x_i)^2 + (y - y_i)^2] \cdot \frac{\partial}{\partial \xi} [(y - y_i)/(x - x_i)]$$

and then

$$H_{bi}(k) = \frac{\partial}{\partial \underline{x}} b_i(\hat{\underline{x}}(k|k-1), t_k) =$$

$$= \left[-[\hat{y}(k|k-1) - y_i(k)]/\alpha \quad [\hat{x}(k|k-1) - x_i(k)]/\alpha \right] \quad 0 \quad 0 \tag{3.32}$$

where

$$\alpha = \hat{d}_i^2(k) = [\hat{x}(k|k-1) - x_i(k)]^2 + [\hat{y}(k|k-1) - y_i(k)]^2 \tag{3.33}$$

and $\hat{d}_i(k)$ is the predicted distance of the target from buoy i.

b. Frequency Measurement

From Equation (2.25),

$$\frac{\partial}{\partial \xi} f_i = [c/(c - s_i)] \cdot \frac{\partial}{\partial \xi} f_o + [f_o \cdot c/(c - s_i)^2] \cdot \frac{\partial}{\partial \xi} s_i =$$

$$= f_i/f_o \cdot \frac{\partial}{\partial \xi} f_o + f_i^2/(f_o \cdot c) \cdot \frac{\partial}{\partial \xi} s_i$$

where s_i is given in Equation (2.26) and

$$\frac{\partial}{\partial \xi} s_i = - \cos(b - b_i) \cdot \frac{\partial}{\partial \xi} s +$$

$$+ s \cdot \sin(b - b_i) \cdot \frac{\partial}{\partial \xi} b -$$

$$- s \cdot \sin(b - b_i) \cdot \frac{\partial}{\partial \xi} b_i \qquad (3.34)$$

and then,

$$H_{fi}(k) = \frac{\partial}{\partial \underline{x}} f_i(\hat{\underline{x}}(k|k-1), t_k) =$$

$$= \left[[\hat{y}(k|k-1) - y_i(k)]/\xi \quad -[\hat{x}(k|k-1) - x_i(k)]/\xi \quad \beta \quad \gamma \quad \hat{f}_i/f_o \right] \qquad (3.35)$$

where

$$\hat{f}_i = f_i(\hat{\underline{x}}(k|k-1), t_k) = \hat{f}_o(k|k-1) \cdot c \; / \; [c +$$

$$+ \hat{s}(k|k-1) \cdot \cos(\hat{b}(k|k-1) - \hat{b}_i(k))]$$

$$\hat{b}_i(k) = \arctan\left[[\hat{y}(k|k-1) - y_i(k)] / [\hat{x}(k|k-1) - x_i(k)] \right] \qquad (3.36)$$

$$\gamma = \hat{f}_i^2 \cdot \hat{s}(k|k-1) \cdot \sin(\hat{b}(k|k-1) - \hat{b}_i(k)) \; /$$

$$[\hat{f}_o(k|k-1).c]$$

$$\beta = -\hat{f}_i^2.\cos(\hat{b}(k|k-1) - \hat{b}_i(k)) \;/\; [\hat{f}_o(k|k-1).c]$$

$\delta = \alpha/\gamma$, α as in (3.33).

c. Frequency Difference Measurement

From Equation (2.26),

$$\frac{\partial}{\partial \xi}(f_i - f_j) \tilde{=} f_o/c \cdot \frac{\partial}{\partial \xi}(s_i - s_j)$$

where $\frac{\partial}{\partial \xi} s_i$ is given in Equation (3.34). Then,

$$H_{di}(k) = \frac{\partial}{\partial \underline{x}}(f_i - f_j)\Big|_{\underline{x}(k|k-1)} = f_o/c \cdot [h_1 \quad h_2 \quad h_3 \quad h_4] \quad (3.37)$$

where

$$h_1 = a_i.[\hat{y}(k|k-1) - y_i(k)] - a_j.[\hat{y}(k|k-1) - y_j(k)]$$

$$h_2 = a_j.[\hat{x}(k|k-1) - x_j(k)] - a_i.[\hat{x}(k|k-1) - x_i(k)]$$

$$h_3 = \cos(\hat{b}(k|k-1) - \hat{b}_j(k)) - \cos(\hat{b}(k|k-1) - \hat{b}_i(k))$$

$$h_4 = \hat{s}(k|k-1).[\sin(\hat{b}(k|k-1) - \hat{b}_i(k)) - \sin(\hat{b}(k|k-1) - \hat{b}_j(k))]$$

$$a_i = \hat{s}(k|k-1).\sin(\hat{b}(k|k-1) - \hat{b}_i(k)) \;/\alpha$$

$\hat{b}_i(k)$ as in (3.36) and α as in (3.33).

d. Frequency Ratio Measurement

From Equation (2.28),

$$\frac{\partial}{\mu\xi}(f_i/f_j) \tilde{=} 1/c \cdot \frac{\partial}{\partial\xi}(s_i - s_j)$$

Comparing with the frequency difference measurement, one has

$$H_{ri}(k) = \frac{\partial}{\partial \underline{x}}(f_i/f_j)\Big|_{\hat{\underline{x}}(k|k-1)} \tilde{=} 1/f_o \cdot H_{di}(k) \qquad (3.38)$$

e. Time Delay Measurement

From Equation (2.36),

$$\frac{\partial}{\partial\xi} T_{ij} = 1/c \cdot \frac{\partial}{\partial\xi}(d_i - d_j)$$

where

$$d_i^2 = (x - x_i)^2 + (y - y_i)^2$$

and then,

$$H_{Tij}(k) = \frac{\partial}{\partial \underline{x}} T_{ij}\Big|_{\hat{\underline{x}}(k|k-1)} = 1/c \cdot [h_1 \quad h_2 \quad 0 \quad 0] \qquad (3.39)$$

where

$$h_1 = [\hat{x}(k|k-1) - x_i(k)] / \hat{d}_i(k) - [\hat{x}(k|k-1) - x_j(k)] / \hat{d}_j(k)$$

$$h_2 = [\hat{y}(k|k-1) - y_i(k)] / \hat{d}_i(k) -$$

$$[\hat{y}(k|k-1) - y_j(k)] / \hat{d}_j(k)$$

and $\hat{d}_i$ is given in Equation (3.33).

IV. SPECIAL CHARACTERISTICS OF KALMAN FILTERS

Equations (3.7) and (3.8) characterize the one-step prediction of an Extended Kalman Filter; Equations (3.18), (3.19) and (3.21) represent the estimation update.

When implemented in a computing device, the timing of these steps is shown in Fig. 5. The actual state is represented by a broken line and the output of the filter by the solid line. In general, one is dealing with vector processes so Figure 5 is representative of only one component. Nevertheless, this representation is helpful in visualizing the steps involved in the estimation process.

In a general problem the times of occurrence of measurements are not equally separated and are not known in advance. At a time t_{k-1}, when a new set of α measurements becomes available, the output of the filter is still the last estimate made close to t_{k-2}, unless predictions are made at regular time intervals independent of the spacing between measurements.

A time period T_p is spent in a prediction phase to evaluate Equations (3.7) and (3.8), after which the best information about the state of the plant is the predicted value $\hat{\underline{x}}(k-1|k-2)$.

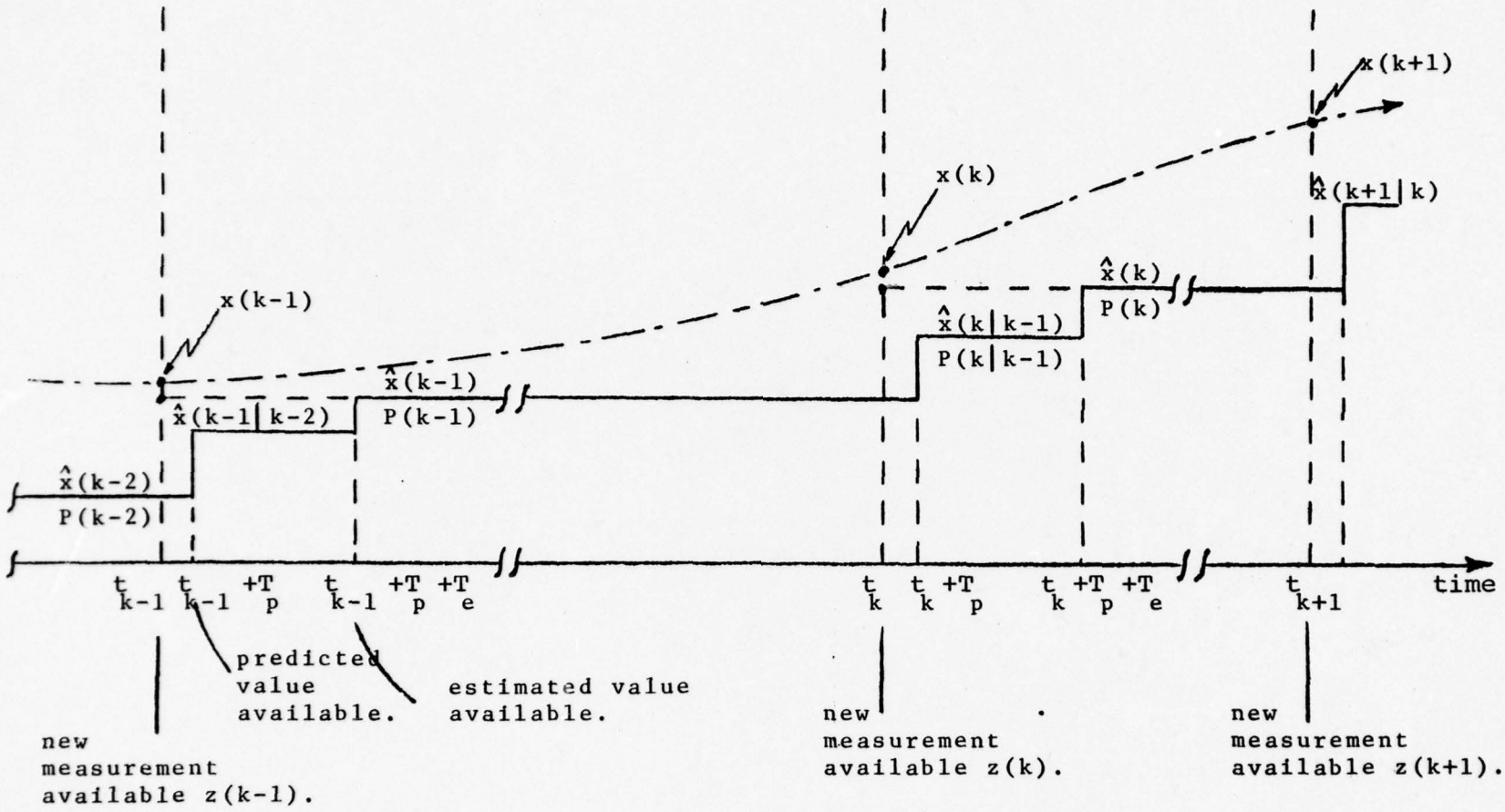

Figure 5 : Timing in a Kalman Filtering Process.

If the times of occurrence of measurements were known in advance, the predictions could be made any time the system was idle waiting for the new measurements and T_p could be made zero.

Next, the q measurements are processed using Equations (3.18), (3.19) and (3.21) and a time T_e is spent which is relatively large mainly because of a matrix inversion of dimension (q x q), in the gain equation, (3.19). Only after this time has passed is the new estimate $\underline{\hat{x}}(k-1)$ available. This estimate will be the output of the filter until t_k when the process is repeated.

Some important points in this estimation process must be stressed:

--- the new estimates are only available $T_p + T_e$ seconds after the arrival of new measurements.

--- a major part of the time period of duration T_e is spent in the gain equation due to the required matrix inversion.

--- from the end of the computation of an estimate until the arrival of a new set of measurements the computing equipment is idle and thus free to execute other chores.

--- the one-step prediction is based on a linearization of the plant dynamics over an extended period, for example, from t_{k-1} to t_k.

--- the measurement equations are based on a linearization about the predicted values.

A. PARTITIONING OF MEASUREMENTS

When some of the measurements come from statistically independent sources, steps can be taken to alleviate problems which arise. Considering the special case when all the measurement noise components are independent, the covariance matrix R(k) is diagonal and the following development applies.

1. The Linear Case

Assume a dynamic system with linear observations of the form

$$\underline{z}(k) = H(k).\underline{x}(k) + \underline{v}(k) \tag{4.1}$$

where H(k) is not a function of the states.

The estimation equations of Chapter III become the standard Kalman Filter equations

$$G(k) = P(k|k-1)H^T(k)[H(k)P(k|k-1)H^T(k) + R(k)]^{-1} \tag{4.2}$$

$$\underline{\hat{x}}(k) = \underline{\hat{x}}(k|k-1) + G(k)[\underline{z}(k) - H(k).\underline{\hat{x}}(k|k-1)] \tag{4.3}$$

$$P(k) = [I - G(k)H(k)]P(k|k-1) \tag{4.4}$$

The measurements are assumed to occur simultaneously and, as shown for the first time in [9], for this linear case, the results obtained by processing all q measurements

at once using these equations are the same as the final results obtained by processing one measurement at a time.

In the latter approach, the result of processing one measurement component is used in the following computation to process the next measurement component.

A general way to show that the two approaches yield the same estimate after all measurement components have been processed is given in the following paragraphs.

In short it is to be proved that the estimates $\underline{\hat{x}}(k)$ and $P(k)$ obtained by the use of Equations (4.2), (4.3) and (4.4), when all measurements are grouped in a vector $\underline{z}$, are the same as those obtained by the use of the following iterative equations q times, once for each component:

$$G_i = P_{i-1} . H_i^T / [H_i P_{i-1} H_i^T + R_i] \tag{4.5}$$

$$\underline{x}_i = \underline{x}_{i-1} + G_i [\underline{z}_i - H_i \underline{x}_{i-1}] =$$

$$= [I - G_i H_i] \underline{x}_{i-1} + G_i \underline{z}_i \tag{4.6}$$

$$P_i = [I - G_i H_i] . P_{i-1} \tag{4.7}$$

$i = 1, 2, \ldots, q$

where

$$P_o = P(k|k-1), \qquad \underline{x}_o = \underline{\hat{x}}(k|k-1)$$

$$P_q = P(k), \qquad \underline{x}_q = \hat{\underline{x}}(k)$$

$$\underline{z}(k) = \begin{bmatrix} z_1 \\ z_2 \\ \cdot \\ \cdot \\ z_q \end{bmatrix} = \begin{bmatrix} H_1 \\ H_2 \\ \cdot \\ \cdot \\ H_q \end{bmatrix} x(k) + \begin{bmatrix} v_1 \\ v_2 \\ \cdot \\ \cdot \\ v_q \end{bmatrix}$$

and $E[v_i^2] = R_i$

If Equation (4.6) is applied q times, the following relationship between $\hat{\underline{x}}(k)$ (or $\underline{x}_q$) and $\hat{\underline{x}}(k|k-1)$ (or $\underline{x}_o$) results

$$\hat{\underline{x}}(k) = [I - G_q H_q][I - G_{q-1} H_{q-1}] \ldots [I - G_1 H_1]\hat{\underline{x}}(k|k-1) +$$
$$+ G_q z_q + [I - G_q H_q] G_{q-1} z_{q-1} + \ldots +$$
$$+ [I - G_q H_q][I - G_{q-1} H_{q-1}] \ldots [I - G_2 H_2] G_1 z_1 \qquad (4.8)$$

and recursive use of Equation (4.7) gives

$$P(k) = [I - G_q H_q][I - G_{q-1} H_{q-1}] \ldots [I - G_1 H_1] P(k|k-1) \qquad (4.9)$$

Comparing (4.8) to (4.3) and (4.9) to (4.4) one sees that the assertion can be proved by showing the validity of the relations

$$[I - G(k)H(k)] = [I - G_q H_q][I - G_{q-1} H_{q-1}] \ldots [I - G_1 H_1] \tag{4.10}$$

$$G(k) = \left[\begin{array}{c|c|c} \underset{(n \times 1)}{[I - G_q H_q] \ldots [I - G_2 H_2] G_1} & \ldots & \underset{(n \times 1)}{[I - G_q H_q] G_{q-1}} \;\; \underset{(n \times 1)}{G_q} \end{array}\right] \tag{4.11}$$

or, in a compressed way,

$$G(k) = \left[\begin{array}{c|c} \underset{(n \times (q-1))}{[I - G_q H_q] G^*} & \underset{(n \times 1)}{G_q} \end{array}\right] \tag{4.12}$$

and

$$[I - G(k)H(k)] = [I - G_q H_q][I - G^* H^*] \tag{4.13}$$

where G^* is the gain obtained from Equation (3.19) if one has a $q-1$ dimensional measurement vector, and H^* and R^* are equivalent matrices, as shown below

$$H(k) = \left[\begin{array}{c} H^* \\ - - - \\ H_q \end{array}\right] \tag{4.14}$$

$$R(k) = \left[\begin{array}{c|c} R^* & 0 \\ - - - & - - - \\ 0 & R_q \end{array}\right] \tag{4.15}$$

$$G^* = P(k|k-1)H^{*T}\,[H^*P(k|k-1)H^{*T} + R^*]^{-1} \qquad (4.16)$$

Let us expand Equation (4.2) and try to manipulate it into the form of Equations (4.10) - (4.13). We have

$$[HPH^T + R] = \left[\begin{array}{c|c|c|c} H_1PH_1^T + R_1 & H_1PH_2^T & \cdots & H_1PH_q^T \\ \hline H_2PH_1^T & H_2PH_2^T + R_2 & \cdots & H_2PH_q \\ \hline \cdots & \cdots & \cdots & \cdots \\ \hline H_qPH_1^T & \cdots & \cdots & H_qPH_q^T + R_q \end{array}\right]$$

or

$$[HPH^T + R] = \left[\begin{array}{c|c} A_1 & \underline{a}_2 \\ \hline \underline{a}_3^T & a_4 \end{array}\right] \qquad (4.17)$$

where

$$A_1 = H^*PH^{*T} + R^*$$

$$\underline{a}_2 = H^*PH_q^T$$

$$\underline{a}_3^T = H_qPH^{*T} = \underline{a}_2^T$$

$$a_4 = H_qPH_q^T + R_q$$

Next define the scalar c as

$$c = a_4 - \underline{a}_3^T \underline{A}_1^{-1} \underline{a}_2$$

Thus,

$$c = H_q P H_q^T + R_q - H_q P H^{*T} [H^* P H^{*T} + R^*]^{-1} H^* P H_q^T$$

Using the definition of G^* in Equation (4.16) gives

$$c = H_q P H_q^T + R_q - H_q G^* H^* P H_q^T =$$

$$= H_q [I - G^* H^*] P H_q^T + R_q \qquad (4.18)$$

It is shown in [10] that

$$\left[\begin{array}{c|c} A_1 & \underline{a}_2 \\ \hline \underline{a}_3^T & a_4 \end{array}\right]^{-1} = \left[\begin{array}{c|c} B_1 & \underline{b}_2 \\ \hline \underline{b}_3^T & b_4 \end{array}\right]$$

where

$$B_1 = A_1^{-1} + A_1^{-1} \underline{a}_2 \underline{a}_3^T A_1^{-1} c^{-1} \qquad (4.19a)$$

$$\underline{b}_2 = - A_1^{-1} \underline{a}_2 c^{-1} \qquad (4.19b)$$

$$\underline{b}_3^T = - \underline{a}_3^T A_1^{-1} c^{-1} \qquad (4.19c)$$

$$b_4 = c^{-1} \qquad (4.19d)$$

Using these relationships,

$$G = P H^T [H P H^T + R]^{-1} =$$

$$= [P H^{*T} \; ; \; P H_q^T] \left[\begin{array}{c|c} B_1 & \underline{b}_2 \\ \hline \underline{b}_3^T & b_4 \end{array}\right] =$$

$$= [PH^{*T}B_1 + PH_q^T b_3^T \;;\; PH^{*T}\underline{b}_2 + PH_q^T b_4] =$$

$$= [C \;;\; D] \qquad (4.20)$$

Applying Equations (4.19a) - (4.19d) to (4.20),

$$D = - PH^{*T}[H^*PH^{*T} + R^*]^{-1}H^*PH_q^Tc^{-1} + PH_q^Tc^{-1} =$$

$$= - G^*H^*PH_q^Tc^{-1} + PH_q^Tc^{-1} = [I - G^*H^*]PH_q^Tc^{-1} =$$

$$= [I - G^*H^*]PH_q^T[H_q(I - G^*H^*)PH_q^T + R_q]^{-1}$$

Let $P^* = [I - G^*H^*]P$ be the estimation error covariance matrix after the processing of q-1 measurement components, as seen from Equation (3.18). Then,

$$D = P^*H_q^T[H_qP^*H_q^T + R_q]^{-1} = G_q \qquad (4.21)$$

is the gain when processing the qth measurement.

We also have

$$C = PH^{*T}[H^*PH^{*T} + R^*]^{-1} + PH^{*T}[H^*PH^{*T} + R^*]^{-1}H^*PH_q^TH_qPH^{*T}$$

$$[H^*PH^{*T} + R^*]^{-1}c^{-1} - PH_q^TH_qPH^{*T}[H^*PH^{*T} + R^*]^{-1}c^{-1} =$$

$$= G^* + G^*H^*PH_q^TH_qG^*c^{-1} - PH_q^TH_qG^*c^{-1}$$

Since c is a scalar, one can write

$$C = G^* - [I - G^*H^*]PH_q^Tc^{-1}H_qG^* = G^* - DH_qG^*$$

and, therefore,

$$C = [I - G_q H_q]G^* \tag{4.22}$$

and from (4.15),

$$G = \left[[I - G_q H_q]G^* \;\middle|\; G_q \right] \tag{4.23}$$

It is also the case that

$$GH = \left[[I - G_q H_q]G^* \quad G_q \right] \begin{bmatrix} H^* \\ - - \\ H_q \end{bmatrix} =$$

$$= [I - G_q H_q]G^* H^* + G_q H_q$$

so

$$I - GH = I - G_q H_q - [I - G_q H_q]G^* H^*$$

and, thus

$$I - GH = [I - G_q H_q][I - G^* H^*] \tag{4.24}$$

Equations (4.23) and (4.24) are the same as Equations (4.12) and (4.13), proving the initial proposition.

Computationally, one can replace a (qxq) matrix inversion and a (nxq) x (qxq) matrix multiplication by only q scalar divisions. For an indication of how much computing time can be saved, consider that a matrix multiplication requires approximately nq^2 scalar multiplications and additions, and that a matrix inversion requires at least q^3 multiplications and additions, not counting logic and indexing

time nor considering storage requirements.

The partitioning of the measurements then corresponds to trading at least $q^2(n + q)$ multiplications and additions for q divisions. For a machine with average multiplication time of 10 microseconds, addition time of 2 microseconds and division time of 12 microseconds, if n and q are equal to 4 a saving of about 1.5 ms is obtained; if n and q are of the order of 20, this saving could be of the order of 200 ms at each measurement time.

Besides this computing time saving, the processing of one measurement at a time provides partial estimates that can be used as improvements over the predicted values, as shown in Figure 6. Also, the final estimate is obtained sooner, although with the same accuracy as when the measurements are all processed simultaneously.

2. The Nonlinear Case

We assume the same system as before but with nonlinear observations of the form

$$\underline{z}(k) = \underline{h}(\underline{x}(k), t_k) + \underline{v}(k)$$

By linearizing this equation as shown in Chapter III, using the definition

$$H(k) = \frac{\partial}{\partial \underline{x}} \underline{h}(\hat{\underline{x}}(k|k-1), t_k) ,$$

the proof of the last section is still valid for the

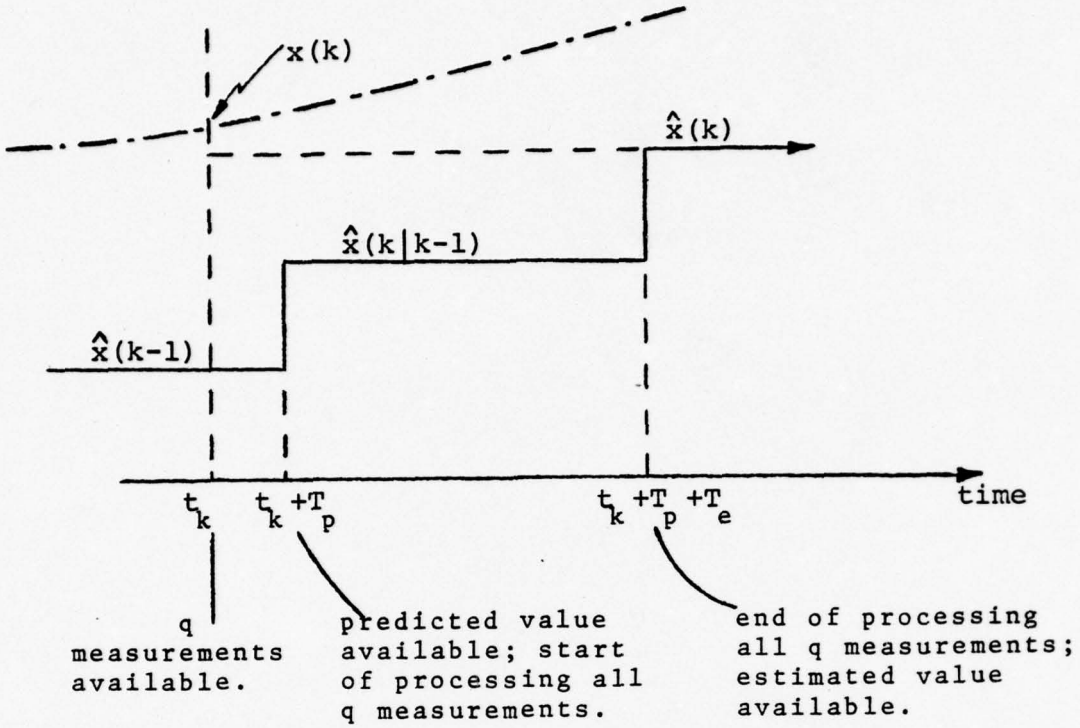

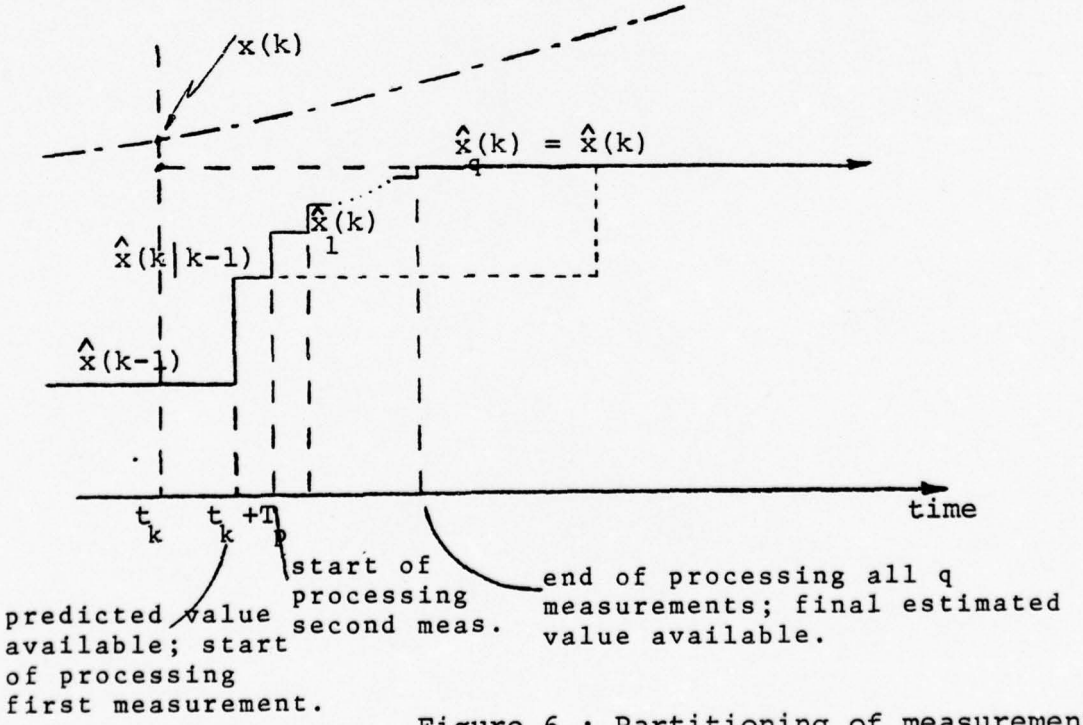

Figure 6 : Partitioning of measurements - Linear case.

linearized equations.

If, however, the partial estimates obtained by processing one measurement (hopefully a better approximation to $\underline{x}(k)$ than $\hat{\underline{x}}(k|k-1)$ results) are used to calculate the H_i vector for the processing of the next measurement, better accuracy should be expected than when all H_i vectors are obtained using the relatively crude predicted value. This effect should be particularly significant when the time between each group of measurements is relatively large.

Thus, partitioning the measurements in an Extended Kalman Filter should provide improvement in estimation accuracy in addition to the advantages pointed out in the previous section. This improvement can be visualized as shown in Figure 7.

The expected improvement in the estimation process, brought by partitioning the measurements in Extended Kalman Filters, can be explained in terms of the conditional densities.

Consider two independent simultaneous measurements,

$$\underline{z}(k) = \begin{bmatrix} z_1(k) \\ \\ z_2(k) \end{bmatrix} = \begin{bmatrix} h_1(\underline{x}(k)) + v_1(k) \\ \\ h_2(\underline{x}(k)) + v_2(k) \end{bmatrix}$$

The conditional density after processing the two measurements is, from Equation (3.1),

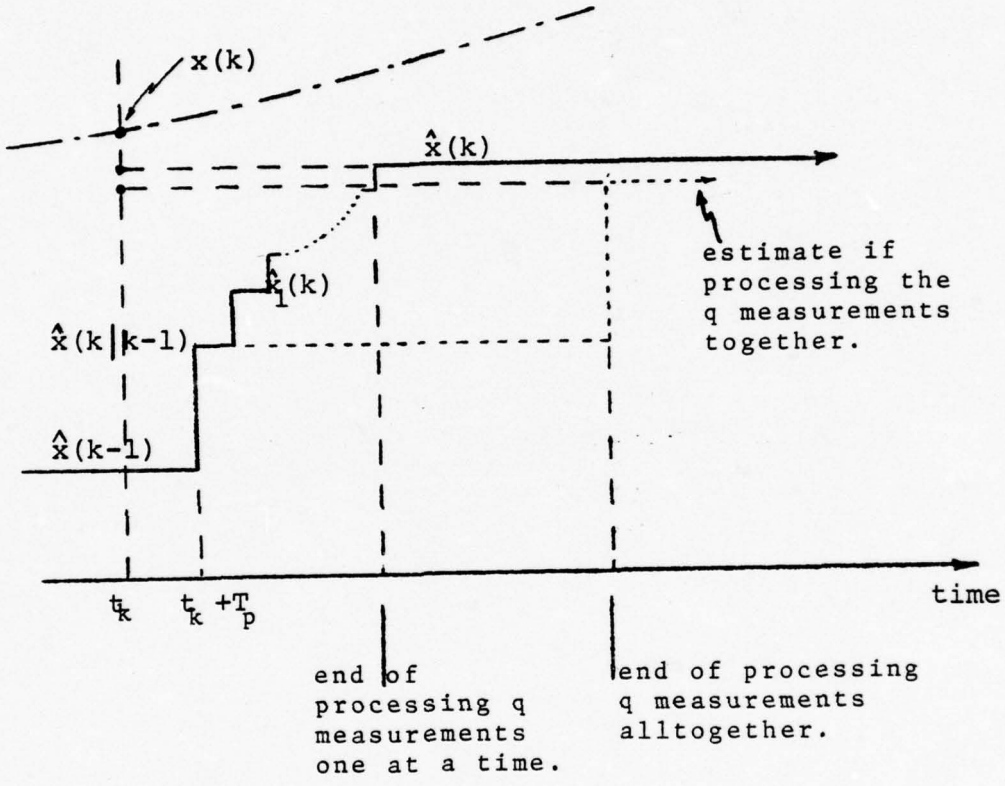

Figure 7 : Partitioning of measurements - Nonlinear case.

$$p(\underline{x}(k)|Z^k) = p(\underline{x}(k)|z_1(k), z_2(k), Z^{k-1}) =$$

$$= p(z_1(k), z_2(k)|\underline{x}(k)).p(\underline{x}(k)|Z^{k-1})/p(z_1(k), z_2(k)|Z^{k-1}) =$$

$$= [p(z_2(k)|z_1(k), \underline{x}(k)) \; / \; p(z_2(k)|z_1(k), Z^{k-1})].$$

$$[p(z_1(k)|\underline{x}(k)).p(\underline{x}(k)|Z^{k-1})/p(z_1(k)|Z^{k-1})]$$

But, from (3.1)

$$p(\underline{x}(k)|z_1(k), Z^{k-1}) = p(z_1(k)|\underline{x}(k)).p(\underline{x}(k)|Z^{k-1}) \; /$$

$$p(z_1(k)|Z^{k-1})$$

also,

$$p(z_2(k)|z_1(k), \underline{x}(k)) = p(z_2(k)|\underline{x}(k))$$

because of the independence assumption.

And so,

$$p(\underline{x}(k)|Z^k) = [p(z_2(k)|\underline{x}(k)) \; / \; p(z_2(k)|z_1(k), Z^{k-1})].$$

$$p(\underline{x}(k)|z_1(k), Z^{k-1}) \qquad (4.25)$$

The terms on the right hand side of (4.25) are:

$p(\underline{x}(k)|z_1(k), Z^{k-1})$ --- has all the information about the states from processing up to the first measurement component $z_1(k)$.

$p(z_2(k)|\underline{x}(k))$ --- is obtained directly from the

measurement equation and doesn't depend on the first measurement.

$p(z_2(k)|z_1(k),Z^{k-1})$ --- is obtained from the measurement equation but using all the results given by the processing of the first measurement component.

This last term indicates that information is lost if, in a Extended Kalman Filter, the linearization for processing a measurement is based on the predicted value instead of on the value estimated after processing the preceding measurement component.

3. The Tracking Problem

In the tracking problem here addressed, the measurements naturally occur at different times. Bearing indications are basically continuous or, if preprocessed, successive measurements are available within short intervals of time. Frequency indications must be obtained from digital processing of records of considerable time length. Time delay indications are also obtained from digital processing but with longer time intervals.

In earlier work, [1], [2] and [3], these measurements are forced to occur simultaneously and are processed together.

In the previous sections of this chapter it was shown that, if the measurements are all available at the

same time, they should be processed separately for better computing efficiency and, with nonlinear measurements, for possibly better estimation accuracy.

Since one is now free from having to process the measurements together, and encouraged to do so, why not use the idle time of the computing equipment and process the measurements at different times?

If one does this the decrease in computation time obtained previously will be diminished because of the extra computation time required to do many predictions, one for each time a measurement is to be processed. Nevertheless, the advantages are potentially of great value, that is,

--- a measurement can be processed as soon as it is available, with no waiting for other measurements.

--- measurements that occur more often can be processed more times than measurements ocurring less frequently.

--- the output of the filter is updated frequently.

--- the one-step prediction is based on linearizations through much smaller time-steps than before, hopefully with improved accuracy and fewer divergence problems.

Figure 8 gives an idea of the improvement one expects to obtain by (1) processing simultaneous measurements separately and (2) processing the measurements as they

naturally occur, when a Extended Kalman Filter is being used.

B. GRAPHICAL INTERPRETATION

General understanding of the actions taken by a Kalman Filter during the processing of a measurement can be obtained through the graphical interpretation and visualization of these actions in a two-dimensional problem.

From the conclusions of Section IV,A, it is advantageous to process any group of measurements with statistically independent noise components separately. In this section, thus, the processing of only one measurement at a time is considered.

1. The Linear Measurement Case

We will consider a dynamic system with two state variables, and a linear measurement of the form

$$z(k) = H(k).\underline{x}(k) + v(k) =$$

$$= h_1(k).x_1(k) + h_2(k).x_2(k) + v(k)$$

with $v(k)$ a zero-mean, discrete white Gaussian noise process with $E[v^2(k)] = r^2(k)$.

At time t_k a prediction is made from previous estimates and knowledge of the plant and system noise characteristics. Equations (4.3) and (4.4) are used for a linear

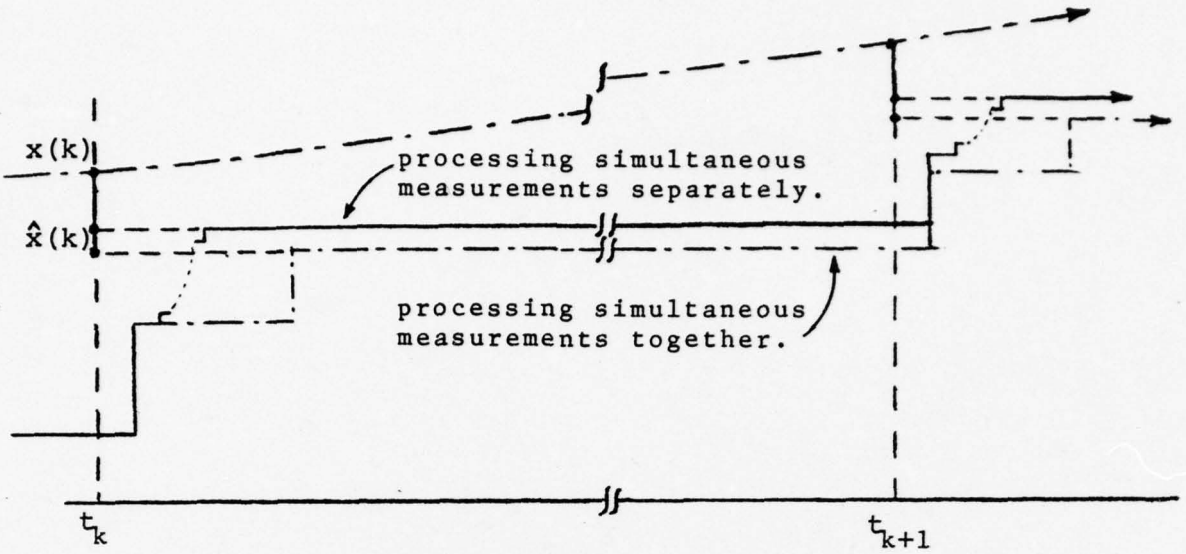

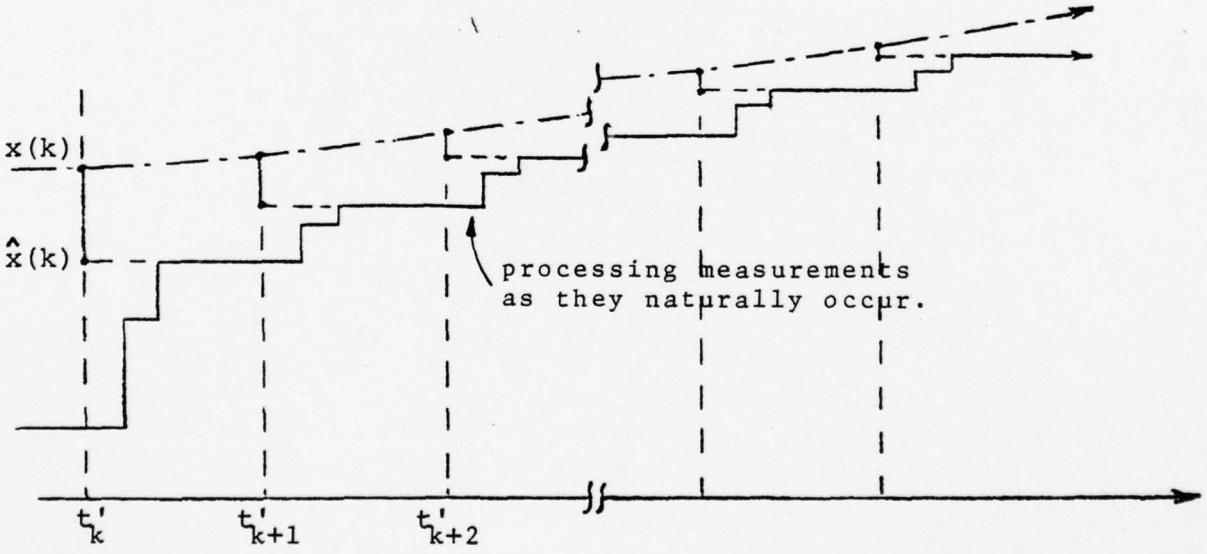

Figure 8 : Comparision of processing policies.

system, (3.7) and (3.8) for a general nonlinear system.

The Kalman equations (4.5), (4.6) and (4.7) are now applied to correct the predicted value according to the new measurement.

Let's represent the quantities and relations involved as shown in Figures 9 and 10, where $\underline{e}_1$ and $\underline{e}_2$ are a pair of orthonormal basis vectors and a general vector is represented by

$$\underline{x} = x_1 \underline{e}_1 + x_2 \underline{e}_2$$

The following conventions and simplifications apply

$$\underline{x}^* = \underline{x}(k) = \begin{bmatrix} x_1(k) \\ \\ x_2(k) \end{bmatrix} = \begin{bmatrix} x_1^* \\ \\ x_2^* \end{bmatrix}$$

$$\hat{\underline{x}} = \hat{\underline{x}}(k) = \begin{bmatrix} \hat{x}_1 \\ \\ \hat{x}_2 \end{bmatrix}$$

$$\underline{x}' = \hat{\underline{x}}(k|k-1) = \begin{bmatrix} x_1' \\ \\ x_2' \end{bmatrix}$$

$$\underline{h} = \begin{bmatrix} \underline{h}_1(k) \\ \\ h_2(k) \end{bmatrix} = \begin{bmatrix} h_1 \\ \\ h_2 \end{bmatrix}$$

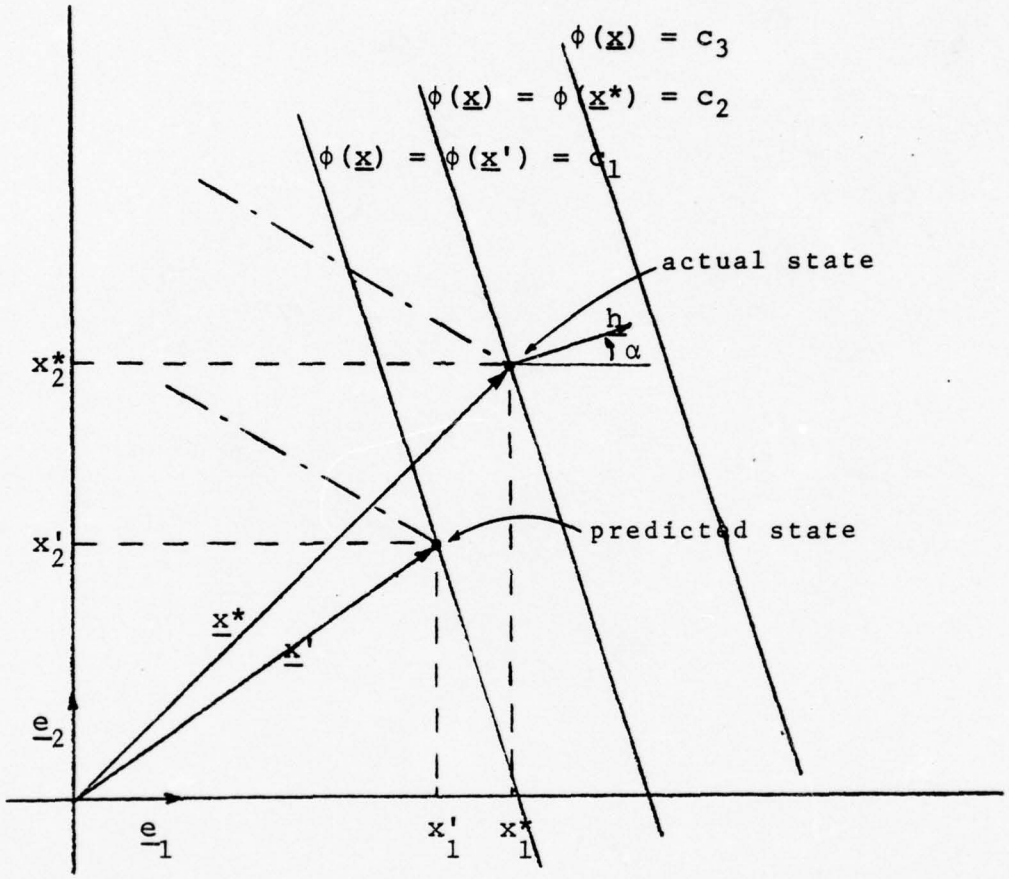

Figure 9 : Graphical interpretation - Measurement lines and gradient.

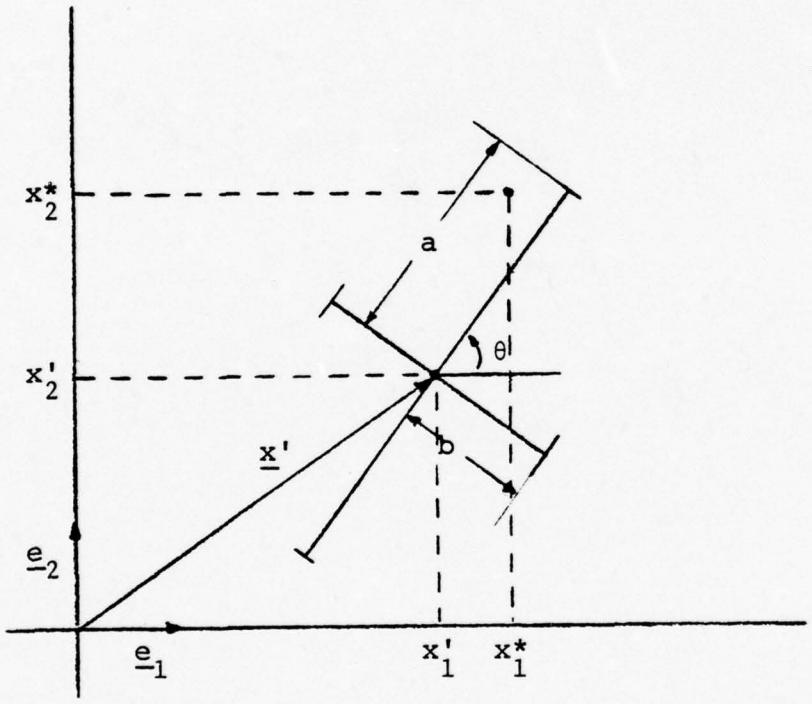

Figure 10 : Graphical interpretation - Error ellipse.

$$\underline{g} = G(k) = \begin{bmatrix} g_1(k) \\ \\ g_2(k) \end{bmatrix} = \begin{bmatrix} g_1 \\ \\ g_2 \end{bmatrix}$$

$$|h| = [\underline{h}^T \underline{h}]^{1/2} = [h_1^2 + h_2^2]^{1/2}$$

$$|g| = [g_1^2 + g_2^2]^{1/2}$$

$$\alpha = \arctan [h_2/h_1]$$

$$\beta = \arctan [g_2/g_1]$$

Let's define the function

$$\phi(\underline{x}) = h_1 x_1 + h_2 x_2 \qquad (4.26)$$

and call "measurement line" the locus of points where ϕ is constant. Some of these lines are shown in Fig 9.

Using this definition one sees that the previously defined $\underline{h}$ is the gradient of ϕ with respect to $\underline{x}$, or $\frac{\partial \phi}{\partial \underline{x}}$, which in this linear measurement case is not a function of the states.

The prediction error covariance matrix,

$$P(k|k-1) = P' = \begin{bmatrix} p'_{11} & p'_{12} \\ \\ p'_{12} & p'_{22} \end{bmatrix}$$

is represented by an error ellipse whose direction (θ) and axis dimensions (a - major axis; b - minor) are given by,

[2]

$$\tan 2\theta = 2p'_{12} / (p'_{11} - p'_{22}) \quad \ldots -\pi < 2\theta \leq \pi \tag{4.27}$$

$$a = (p'_{11} + p'_{22})/2 + p'_{12} / \sin 2\theta \tag{4.28}$$

$$b = (p'_{11} + p'_{22})/2 - p'_{12} / \sin 2\theta \tag{4.29}$$

a. The State Estimate

Equation (4.6) can be represented in the form

$$\hat{\underline{x}} = \underline{x}' + \underline{g}.[\text{residual}] \tag{4.30}$$

where

$$[\text{residual}] = z(k) - H(k).\hat{\underline{x}}(k|k-1) =$$

$$= \phi(\underline{x}^*) - \phi(\underline{x}') + v(k) \tag{4.31}$$

and (4.30) means that a vector correction of magnitude $|g|.|\text{residual}|$ is made to the predicted state in the direction of the vector $\underline{g}$ which has an angle β as shown in Figure 11.

Equation (4.5) gives, as shown in Appendix A,

$$\underline{g} = \begin{bmatrix} g_1 \\ g_2 \end{bmatrix} = \begin{bmatrix} \dfrac{p'_{11} h_1 + p'_{12} h_2}{p'_{11} h_1^2 + 2p'_{12} h_1 h_2 + p'_{22} h_2^2 + r^2} \\ \dfrac{p'_{12} h_1 + p'_{22} h_2}{p'_{11} h_1^2 + 2p'_{12} h_1 h_2 + p'_{22} h_2^2 + r^2} \end{bmatrix} \tag{4.32}$$

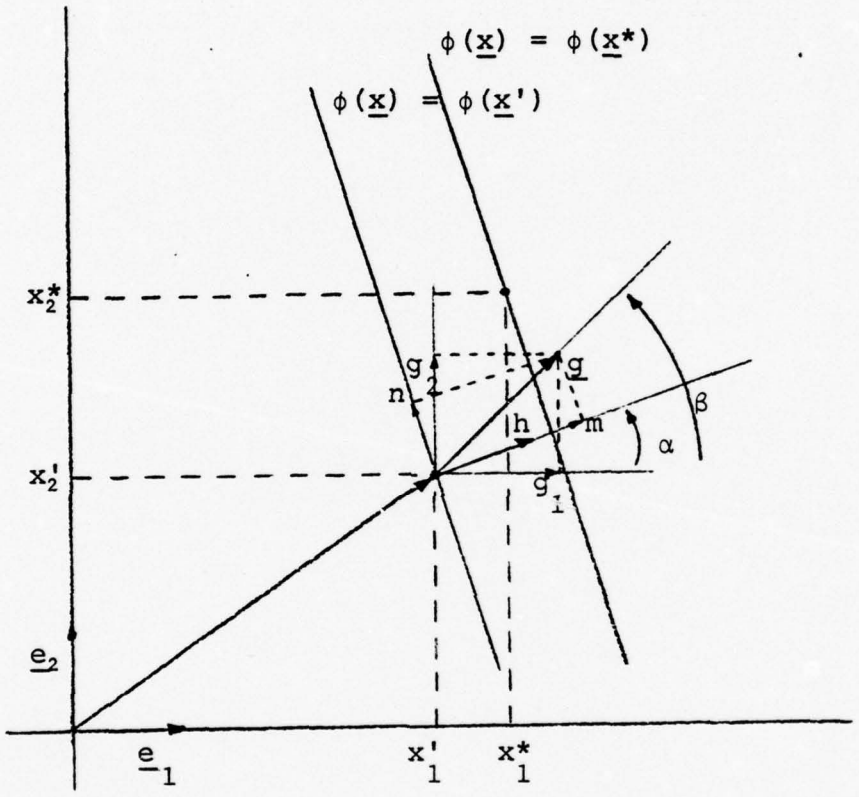

Figure 11 : Graphical interpretation - Gain vector.

(1) The Direction of Correction

The direction of $\underline{g}$ is seen to be independent of the measurement noise, or, given $\underline{h}$ and $P(k|k-1)$ the direction of correction is already determined by

$$\beta = \arctan [(p'_{12} h_1 + p'_{22} h_2) / (p'_{11} h_1 + p'_{12} h_2)] \tag{4.33}$$

From Equations (4.27) - (4.29) one obtains

$$p'_{12} = \frac{1}{2} (a - b).\sin 2\theta \tag{4.34}$$

$$p'_{11} = \frac{1}{2} [(a + b) + (a - b).\cos 2\theta] \tag{4.35}$$

$$p'_{22} = \frac{1}{2} [(a + b) - (a - b).\cos 2\theta] \tag{4.36}$$

Applying these equations and the definition of α to (4.33) gives,

$$\tan \beta = \frac{(a/b - 1).\sin 2\theta + [(a/b + 1) - (a/b - 1).\cos 2\theta].\tan \alpha}{(a/b + 1) + (a/b - 1).\cos 2\theta + (a/b - 1).\sin 2\theta.\tan \alpha} \tag{4.37}$$

which can be reduced to

$$\tan \beta = \frac{(a/b).\tan\theta.[\tan\theta.\tan\alpha + 1] + [\tan\alpha - \tan\theta]}{(a/b).[\tan\theta.\tan\alpha + 1] - \tan\theta.[\tan\alpha - \tan\theta]} \tag{4.38}$$

This equation shows that the direction of the correction generated by the Kalman Filter, in this two-state problem, is a function only of the direction (α) of the gradient ($\underline{h}$) and of the alignment (θ) and the ratio (a/b) of the prediction error ellipse.

Three special cases of interest occur when (i) a/b = 1, (ii) b = 0, and (iii) $\theta = \alpha$.

Case (i) - If a/b = 1 the error "ellipse" is actually a circle meaning that the prediction has the same uncertainty in any direction. No preferable direction pre-exists and the correction is in the direction of the gradient of the measurement function, as can be seen from (4.37)

$$\tan \beta = (0 + 2.\tan\alpha) / (2 + 0) = \tan\alpha$$

or

$$\beta = \alpha + n\pi$$

Case (ii) - If b = 0 the error ellipse is a line meaning that the prediction is exact along the minor axis and that only corrections along the major axis are necessary. As can be anticipated, the direction of correction will be the direction of the major axis, as can be seen by taking the limit as $b \to 0$ of Eq. (4.30), which yields

$$\tan \beta = \tan \theta$$

or

$$\beta = \theta + n\pi$$

For any other intermediate value of a/b between 1 and ∞, the value of β will be between α and θ $(+ n\pi)$.

Case (iii) - When $\theta = \alpha$ the gradient is colinear with the major axis of the prediction error ellipse and, from (4.38),

$$\tan\beta = [(a/b).\tan\theta.(\tan^2\theta + 1) + 0] \;/\; [(a/b).(\tan^2\theta + 1) - 0]$$

or

$$\tan\beta = \tan\theta \qquad \text{and} \qquad \beta = \theta + n\pi = \alpha + n\pi$$

Thus the direction of the correction is along the major axis of the ellipse which is colinear with the gradient of the measurement function.

(2) The Amount of Correction

The magnitude of the correction ($|\text{residual}|.|g|$) can be better seen if one decomposes g into components m and n, along the gradient and the tangent to the measurement function, as shown in Fig. 11.

$$m = g_1.\cos\alpha + g .\sin\alpha \qquad (4.39)$$

and from the definition of α,

$$\cos\alpha = h_1/|\underline{h}| \ , \qquad \sin\alpha = h_2/|\underline{h}| \tag{4.40}$$

Using Equations (4.32), (4.39) and (4.40),

$$m = \frac{p'_{11}h_1^2 + p'_{12}h_1h_2 + p'_{12}h_1h_2 + p'_{22}h_2^2}{p'_{11}h_1^2 + 2p'_{12}h_1h_2 + p'_{22}h_2^2 + r^2} \cdot \frac{1}{|\underline{h}|} =$$

$$= \frac{1}{1+\gamma^2} \cdot \frac{1}{|\underline{h}|} \tag{4.41}$$

where

$$\gamma^2 = r^2 \ / \ (p'_{11}h_1^2 + 2p'_{12}h_1h_2 + p'_{22}h_2^2) \tag{4.42}$$

Consider some special cases. How would the new estimate be computed if a noise-free measurement were obtained and the Kalman filter were aware of this fact, i.e., r = 0?

Note from Equations (4.41) and (4.42) that when the measurement is noise-free, r = 0, γ = 0 and

$m = 1 \ / \ |\underline{h}|$, a constant.

No matter what P(k|k-1) is, the projection of the correction into the gradient is a constant if r = 0, or, the tip of the correction vector follows a line normal to the gradient when P(k|k-1) is varied.

Figure 12 shows the correction made to the predicted state when b = 0. In Appendix C it is shown that

for the present case of a linear measurement function the vector OA, in the direction of $\underline{h}$ and length [residual]/$|h|$ has its end point A on the line

$$\phi(\underline{x}) = \phi(\underline{x}') + \text{residual} = \phi(\underline{x}') + \phi(\underline{x}^*) + v - \phi(\underline{x}')$$

or

$$\phi(\underline{x}) = \phi(\underline{x}^*) + v = z$$

which, for r = 0 (i.e. v = 0) passes through the point $\underline{x} = \underline{x}^*$.

Since the correction has the direction of the prediction error ellipse (line) and has OA as its projection into the vector $\underline{h}$, it can be seen from Figure 12 that in this case of b = 0 and r = 0 the estimate will coincide with the true state.

Figure 13 shows the correction for a general error ellipse but still with r = 0. It is seen that the projection into h is the same as before. The direction of correction β is somewhere between α and θ.

A general correction for a noisy measurement is shown in Figure 14, with different scaling than the previous figures. The direction of correction β is first determined and suppose it is as shown. The projection of the correction into $\underline{h}$ would be OA if r were zero; for $r \neq 0$ the reduction factor is applied and suppose the projection is vector OB as shown in the figure. Taking a normal to $\underline{h}$ from

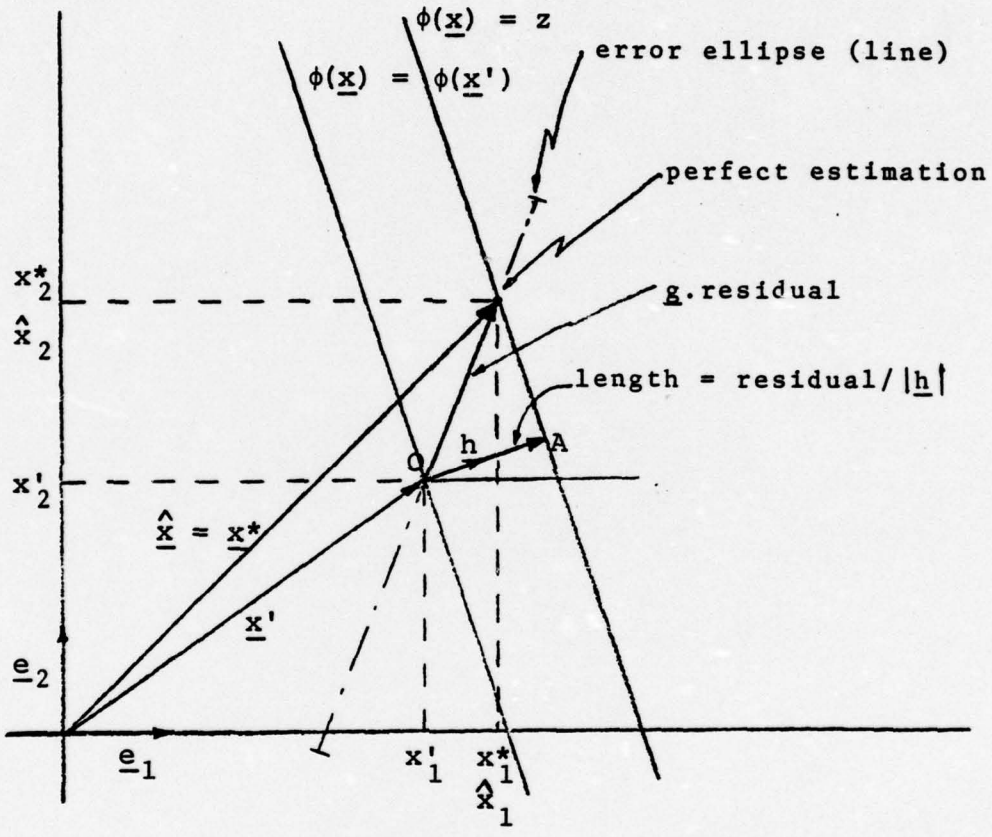

Figure 12 : Linear measurement - Perfect estimation for b=0 and r=0.

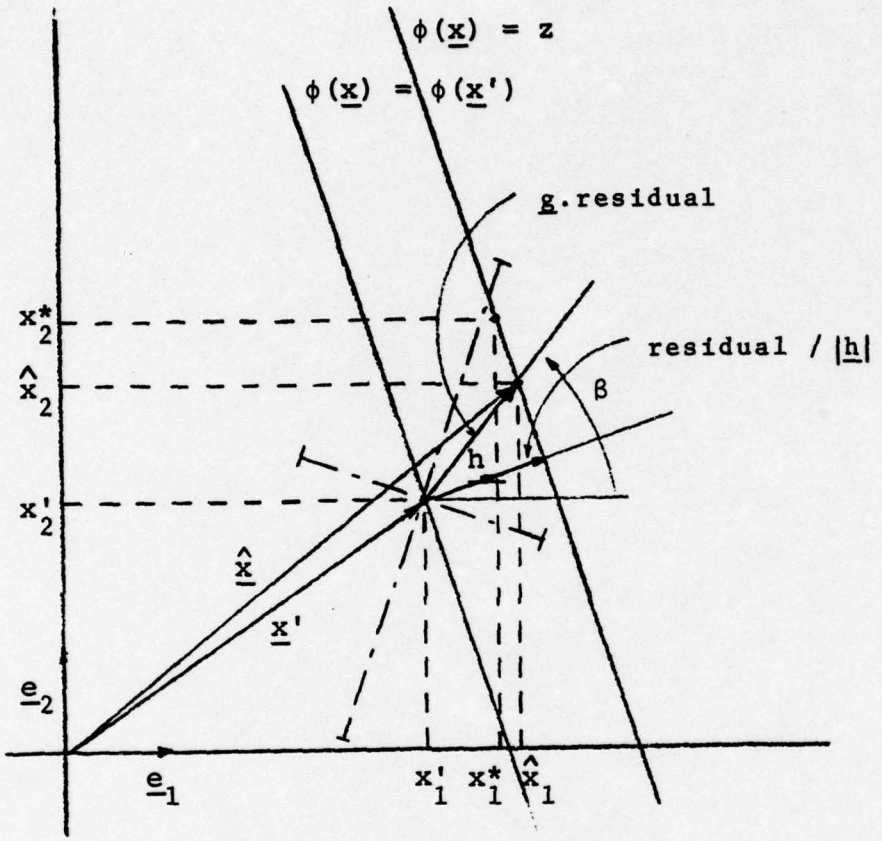

Figure 13 : Linear measurement - r=0.

point B, the point C where it cuts the direction of correction determines the final correction OC and the new estimate.

b. The Estimation Error Covariance Matrix

The effects on the estimation error covariance matrix can be seen in the following way. From Equation (4.7),

$$P(k) = [I - G(k)H(k)]P(k|k-1)$$

or

$$\begin{bmatrix} p_{11} & p_{12} \\ p_{12} & p_{22} \end{bmatrix} = \begin{bmatrix} 1 - g_1 h_1 & - g_1 h_2 \\ - g_2 h_1 & 1 - g_2 h_2 \end{bmatrix} \begin{bmatrix} p'_{11} & p'_{12} \\ p'_{12} & p'_{22} \end{bmatrix}$$

Using the values of g_1 and g_2 from (4.32) one finds that

$$p_{11} = [h_2^2(p'_{11} p'_{22} - p'^2_{12}) + p'_{11} r^2] / c \qquad (4.43a)$$

$$p_{12} = [h_1 h_2(p'^2_{12} - p'_{11} p'_{22}) + p'_{12} r^2] / c \qquad (4.43b)$$

$$p_{22} = [h_1^2(p'_{11} p'_{22} - p'^2_{12}) + p'_{22} r^2] / c \qquad (4.43c)$$

where

$$c = [p'_{11} h_1^2 + 2p'_{12} h_1 h_2 + p'_{22} h_2^2 + r^2] \qquad (4.43d)$$

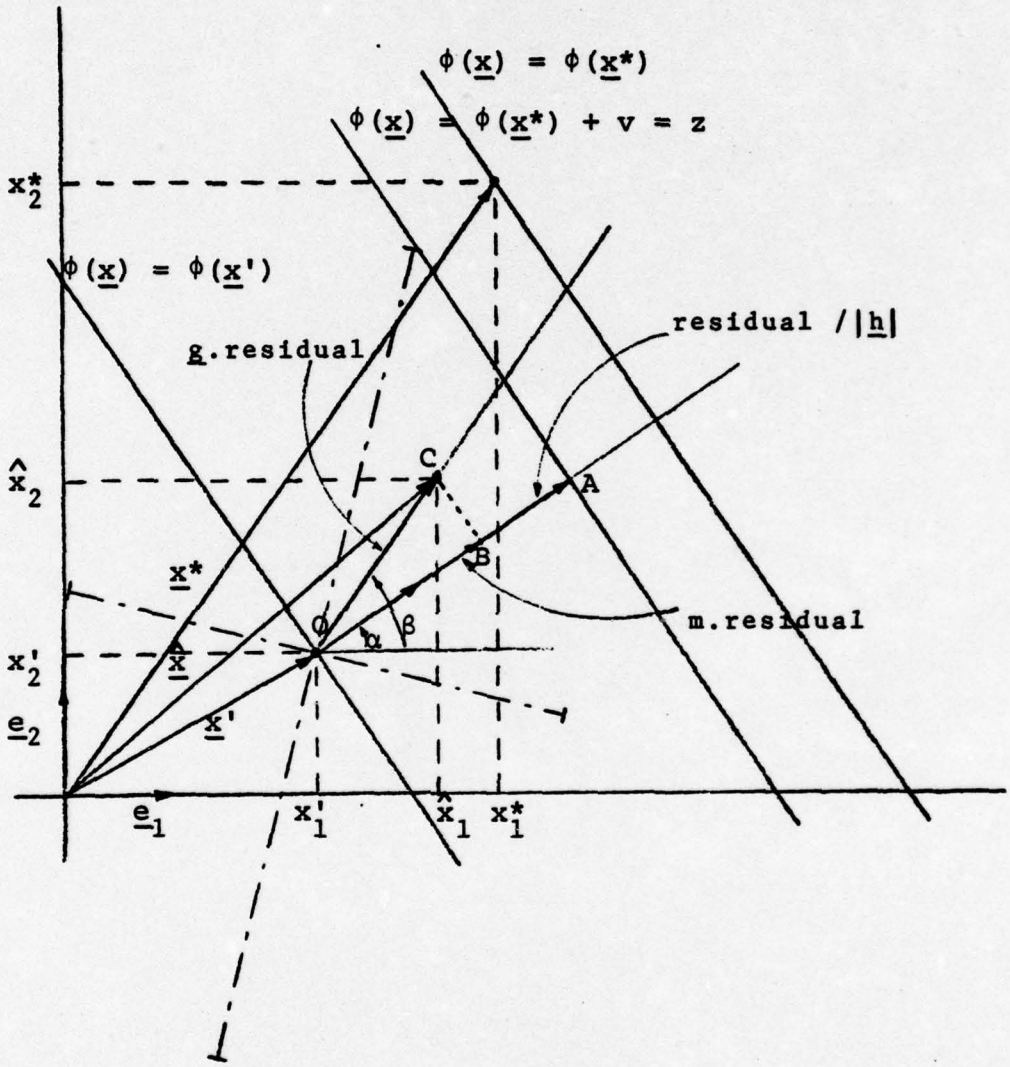

Figure 14 : Linear measurement - General correction.

And the estimation error ellipse has the orientation

$$\tan 2\delta = 2p_{12} / (p_{11} - p_{22}) =$$

$$= \frac{2h_1 h_2 (p'^2_{12} - p'_{11} p'_{22}) + 2p'_{12} r^2}{(h_1^2 - h_2^2)(p'^2_{12} - p'_{11} p'_{22}) + (p'_{11} - p'_{22}) r^2} \qquad (4.44)$$

The limiting situations occur in the special cases when (i) $r \to \infty$ and (ii) $r = 0$.

Case (i) - When r is relatively large, little information is provided to the filter; the estimate is essentially the same as the prediction, and the estimation error ellipse is essentially the same as the prediction error ellipse. This can be seen from Equations (4.43a) - (4.43d), as $r \to \infty$.

Case (ii) - When $r = 0$, all errors in the prediction, in the direction of the gradient of the measurement function, are corrected and the estimation error ellipse becomes a line colinear with the measurement line. As shown below, this result is obtained from Equations (4.43) and (4.44) when r is made equal zero.

From (4.43a) - (4.43d), $p_{11} \cdot p_{22}$ is easily shown to be equal to p_{12}^2 when $r = 0$, indicating that P(k) becomes singular. From (4.44),

$$\tan 2\delta = 2h_1 h_2 / (h_1^2 - h_2^2) =$$

$$= 2(h_2/h_1) \,/\, [1 - (h_2/h_1)^2] =$$

$$= 2 \tan\alpha \,/\, (1 - \tan^2\alpha) = \tan 2\alpha$$

From analysis of the individual terms of (4.43a) - (4.43d), this result is to be interpreted as

$$2\delta = 2\alpha \pm \pi$$

or

$$\delta = \alpha \pm \pi/2$$

When the minor axis of the prediction ellipse is already zero, as in Figure 12, i.e., $p_{12}^{\prime 2} = p_{11}^{\prime}\, p_{22}^{\prime}$, and the measurement is noiseless, then P(k) = 0 and complete certainty about the system state is obtained.

These two last paragraphs show a very interesting situation: if two perfect measurements are made on a two-state plant and the filter is aware of this (i.e. r = 0 is used in the Kalman equations), then an exact estimate is obtained --- the estimation error covariance matrix collapses into the zero matrix.

For a general situation with normal measurement noise values, the estimation error ellipse is rotated toward the measurement line, away from the gradient, with δ occupying a position between θ and $\alpha \pm \pi/2$.

The general expressions for the lengths of the major and the minor axis of the estimation error ellipse can be obtained by the application of Equations (4.28) and (4.29) to (4.43a) - (4.43c).

c. The Important Points

Summarizing the principal points seen up to now,

--- the direction of correction in the estimate is defined at the end of the prediction phase and doesn't depend on the measurements.

--- if the measurement is noiseless and r = 0 is used in the Kalman filter equations, the projection of the correction on the gradient of the measurement function is (residual / $|\underline{h}|$), independent of P(k|k-1). The estimation error covariance matrix becomes singular indicating, in a two-dimensional problem, that the estimation error ellipse becomes a line --- a point when the prediction error ellipse is already a line.

--- if the measurement is noisy, the projection of the correction on the gradient is multiplied by the reducing factor $[1 / (1 + \gamma^2)]$. The error ellipse is rotated toward the measurement line, away from the gradient of the measurement function.

--- if the measurement is too noisy, the reducing factor tends to zero and the estimation is the same as the

prediction.

2. The Nonlinear Measurement Case

Assume the same two-dimensional system as before but with nonlinear observations of the form

$$z(k) = h(\underline{x}(k), t_\kappa) + v(k)$$

a. The Extended Kalman Filter Approach

The prediction phase is the same as before but the estimation equations are now (3.18), (3.19) and (3.21) for an Extended Kalman Filter.

Let's again define a measurement function by

$$\phi(\underline{x}) = h(\underline{x})$$

and redefine $\underline{h}$ as the gradient of θ with respect to $\underline{x}$.

Now the components of $\underline{h}$ are no longer constants but depend on $\underline{x}$. At the predicted point these components will be

$$h = \frac{\partial}{\partial x_1} h(\hat{\underline{x}}(k|k-1)) \quad , \quad h = \frac{\partial}{\partial x_2} h(\hat{\underline{x}}(k|k-1))$$

Equations (4.27) through (4.44) are all still valid.

Let's consider two typical measurement functions and observe graphically how the new estimate is obtained.

Case (i) - assume the measurement function is of the form

$$\phi(\underline{x}) = \arctan\left[(x_1 - a_1) / (x_2 - a_2)\right] \qquad (4.45)$$

The measurement lines will be as shown in Figure 15.

Suppose now a noiseless measurement is obtained and is to be processed. Fig. 16 shows the situation when the prediction error ellipse is a line (b = 0). In Appendix C it is shown that for this special measurement function the vector OA of length [residual]/|h| will end somewhere before a point B on the curve $\phi(\underline{x}) = z$. Supposing its length is as shown, it can be seen that an imperfect estimate is obtained. Nevertheless the estimation error covariance matrix, given also by Equations (4.43), will collapse into the zero matrix indicating, falsely, that a perfect estimate was obtained.

Figure 17 shows a typical situation for a general prediction error and a noise-free measurement. The tip of the correction vector can be seen to follow the line A - A' parallel to the line $\phi(\underline{x}) = \phi(\underline{x}')$ instead of being along the line $\phi(\underline{x}_*) = \phi(\underline{x}^*)$. As seen in the previous section, the estimation error ellipse will erroneously be determined as a line also along A - A', indicating falsely the direction of the true state.

Case (ii) - assume the measurement function is of the form

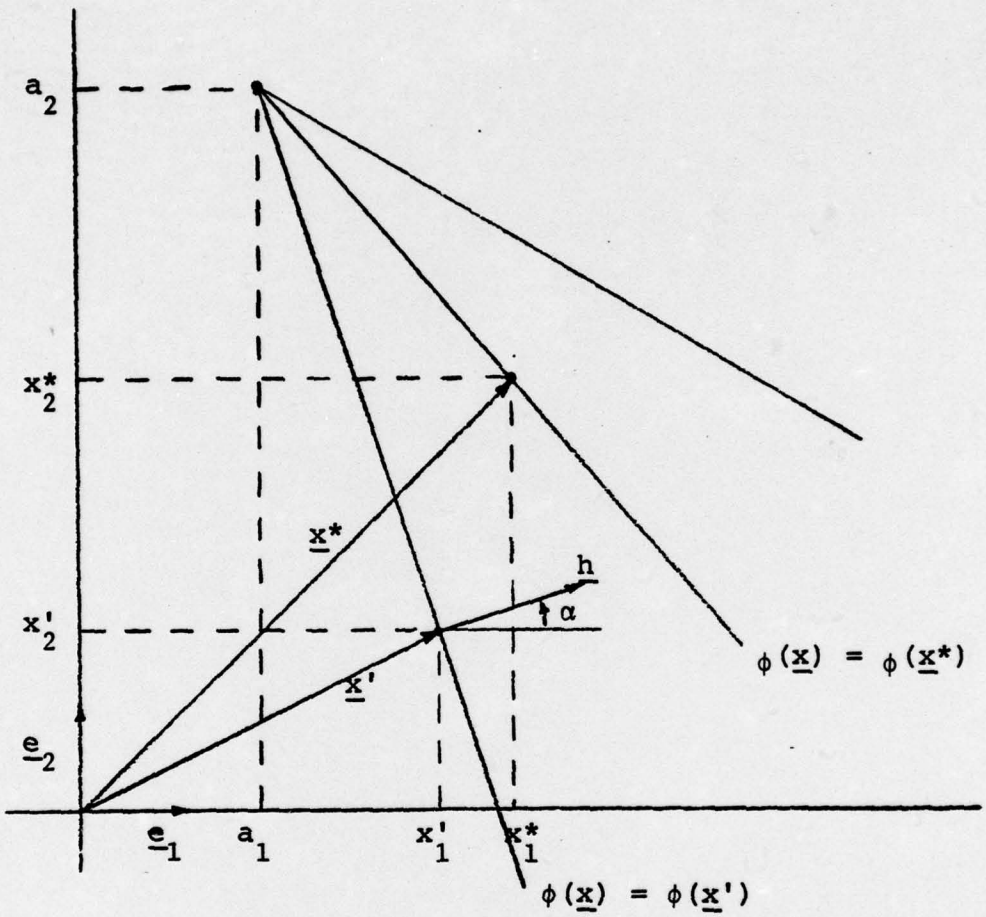

Figure 15 : Nonlinear measurement lines I.

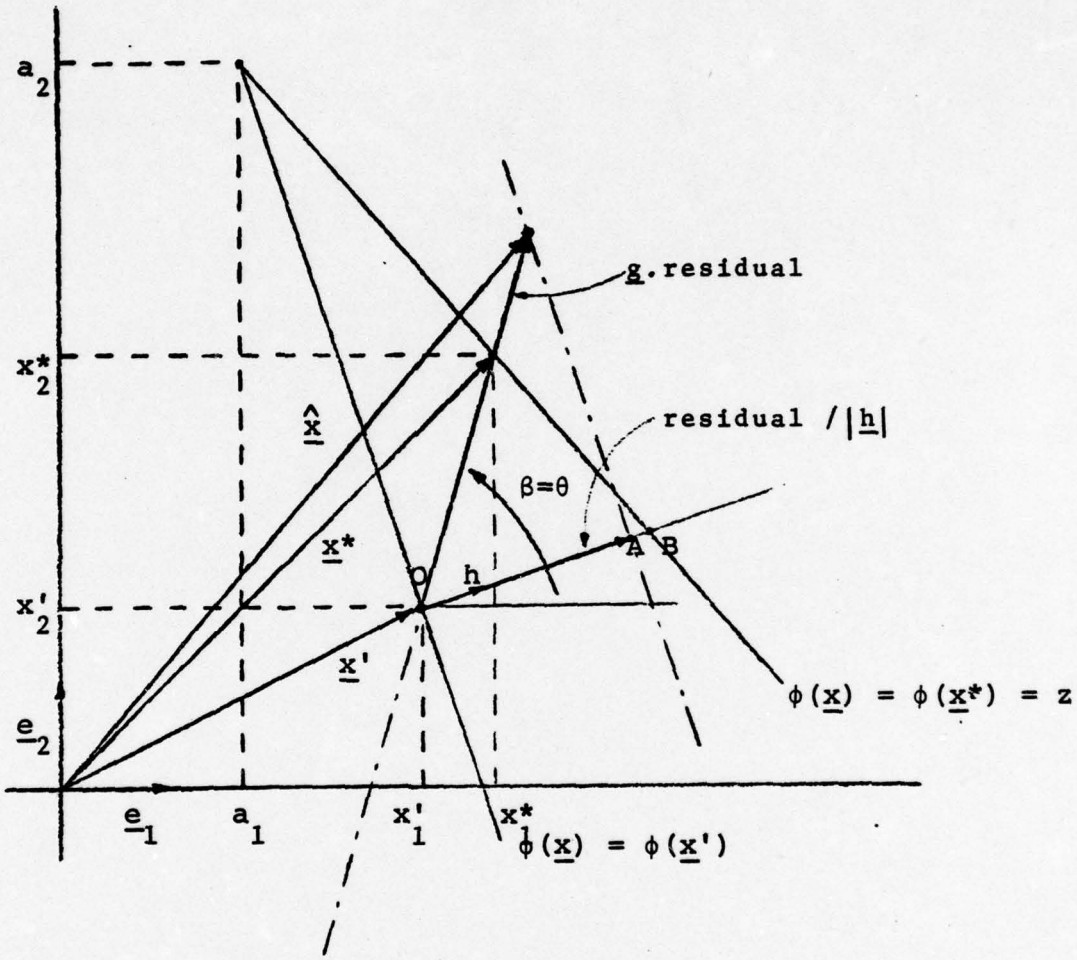

Figure 16 : Nonlinear measurement I - Imperfect correction for b=0 and r=0.

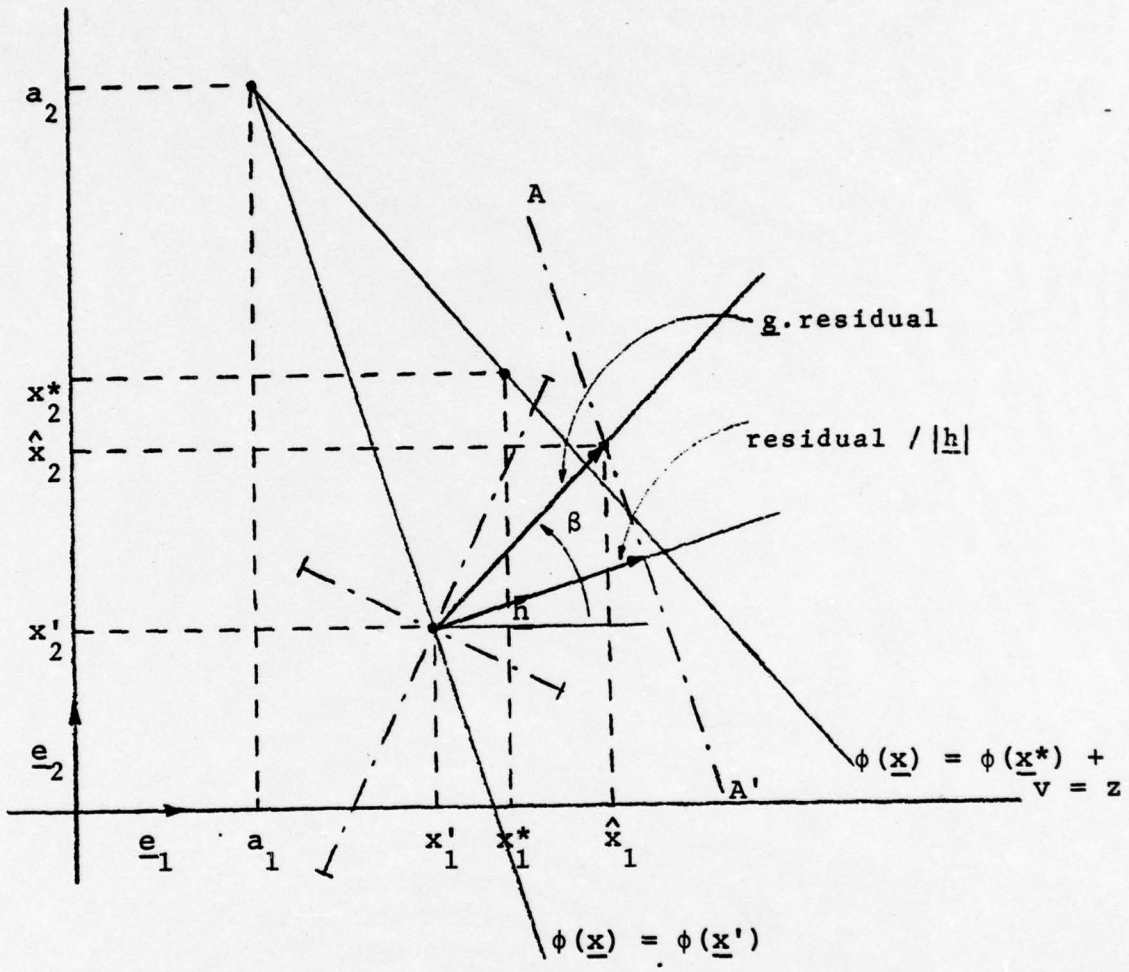

Figure 17 : Nonlinear measurement I - General correction for r=0.

$$\phi(\underline{x}) = \left[(x_1 - a_1)^2 + (x_2 - a_2)^2 \right]^{1/2} \qquad (4.46)$$

The measurement lines are as shown in Figure 18. This same figure shows the new estimate obtained when the measurement is noiseless ($r = 0$) and the prediction error ellipse is a line ($b = 0$). The same observations of Case (i) are valid. As shown in Appendix C the point A is on the curve $\phi(\underline{x}) = z$ for this special measurement function.

These figures have their values mostly because they show, in a simple way, the large errors that can be made in the processing of nonlinear measurements by an Extended Kalman Filter. Two types of errors are generated: one in the determination of the new state estimate; the other is seen in the fact that the estimation error covariance matrix P becomes a poor approximation to the true error covariance, making the filter non-optimal. These difficulties are a function of the nonlinearities involved and, apparently, are more significant when the predicted values are poor and when the measurement noise is assumed to be small when evaluating the extended Kalman filter equations.

b. The Iterative Approach

A way of correcting, in part, these deficiencies is the adoption of iterative procedures. The first improvements can be obtained if, after the Extended Kalman Filter has been applied to correct the prediction, the filtering process is repeated but with the linearizations made about

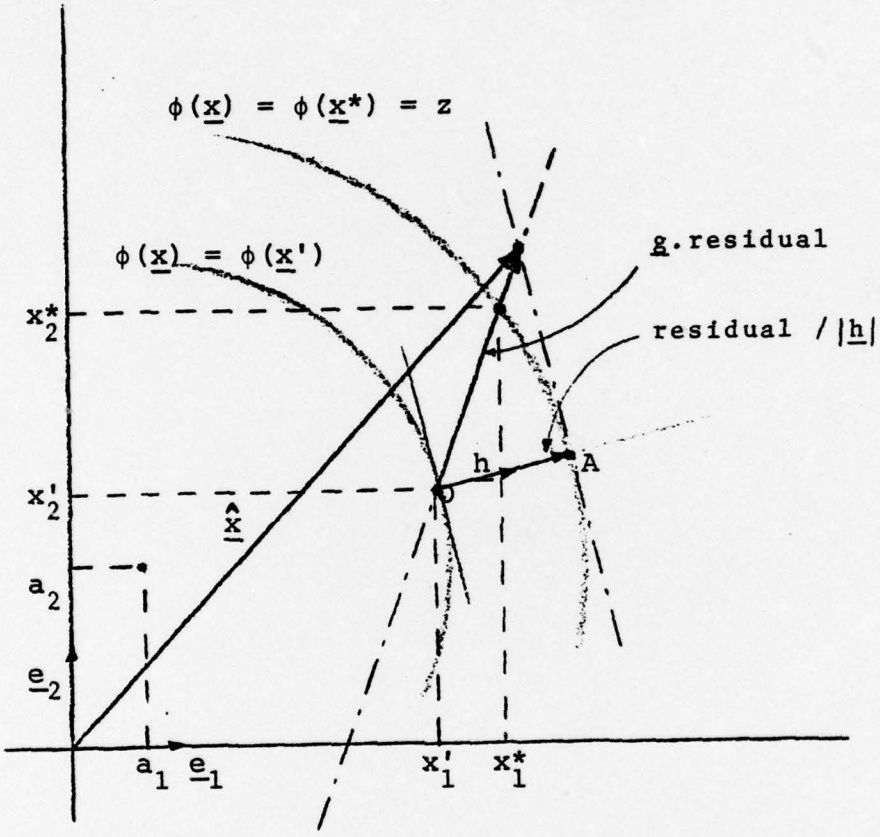

Figure 18 : Nonlinear measurement II - Imperfect correction for b=0 and r=0.

the just obtained estimate, hopefully a better approximation to the true state than the crude prediction.

Analytically the process consists of replacing the estimation equations (3.18), (3.19) and (3.21) by the iterative equations

$$\underline{\hat{x}}_{i+1} = \underline{\hat{x}}(k|k-1) + G_i [\underline{z}(k) - \underline{h}(\underline{\hat{x}}(k|k-1))] \qquad (4.47)$$

$$G_i = P(k|k-1)H_i^T (H_i P(k|k-1)H_i^T + R)^{-1} \qquad (4.48)$$

$$H_i = \frac{\partial}{\partial \underline{x}} h(\underline{\hat{x}}_i) \quad , \quad i = 0, 1, 2, \ldots, f$$

where

$$\underline{\hat{x}}_0 = \underline{\hat{x}}(k|k-1) \quad , \quad \underline{\hat{x}}_f = \underline{\hat{x}}(k)$$

$$P(k) = [I - G_f H_f] P(k|k-1) \qquad (4.49)$$

For our two-dimensional problem Equation (4.47) can be expressed as

$$\underline{\hat{x}}_{i+1} = \underline{x}' + \underline{g}_i \cdot [\text{residual}] \qquad (4.50)$$

where

$$\text{residual} = z - h(\underline{x}') = \phi(\underline{x}^*) - \phi(\underline{x}') + v(k) \qquad (4.51)$$

Adding and subtracting $\phi(\underline{\hat{x}}_i)$ to the residual,

$$\hat{\underline{x}}_{i+1} = \underline{x}' + \underline{g}_i.[z - \phi(\hat{\underline{x}}_i) + \phi(\hat{\underline{x}}_i) - \phi(\underline{x}')]$$

or

$$\hat{\underline{x}}_{i+1} = \underline{x}' + \underline{g}_i.[z - \phi(\hat{\underline{x}}_i)] - \underline{g}_i.[\phi(\underline{x}') - \phi(\hat{\underline{x}}_i)] \quad (4.52)$$

These equations can be applied until there is no significant difference between consecutive estimates, and 2 or 3 iterations are normally enough.

The effect of these equations can be easily visualized for the simple case of $b = 0$ and $r = 0$. The sequence of Figures 19 - 21 show this effect for one of the special measurement functions already studied. In Figure 19 the first estimate is obtained as done previously in Figure 16. The vector OA, which is smaller than OB as shown in Appendix C, represents the projection of the correction on the gradient $\underline{h}_o$. A normal to $\underline{h}_o$ from point A cuts the prediction error line ($b = 0$) at the first estimate $\hat{\underline{x}}_1$.

In Figure 20 the terms of Equation (4.52) are shown for $i = 1$. Two correction terms are applied to the prediction $\underline{x}'$, both in the direction of $\underline{g}_1$ but with different residuals. The direction of $\underline{g}_1$ is again along the prediction error line ($b = 0$).

The gradient of the measurement function at the first estimate is $\underline{h}_1$. The projection of the first correction ($\underline{g}_1[z - \phi(\hat{\underline{x}}_1)]$) into $\underline{h}_1$ is smaller than CE, say CD. Taking the normal at D one gets the first correction term

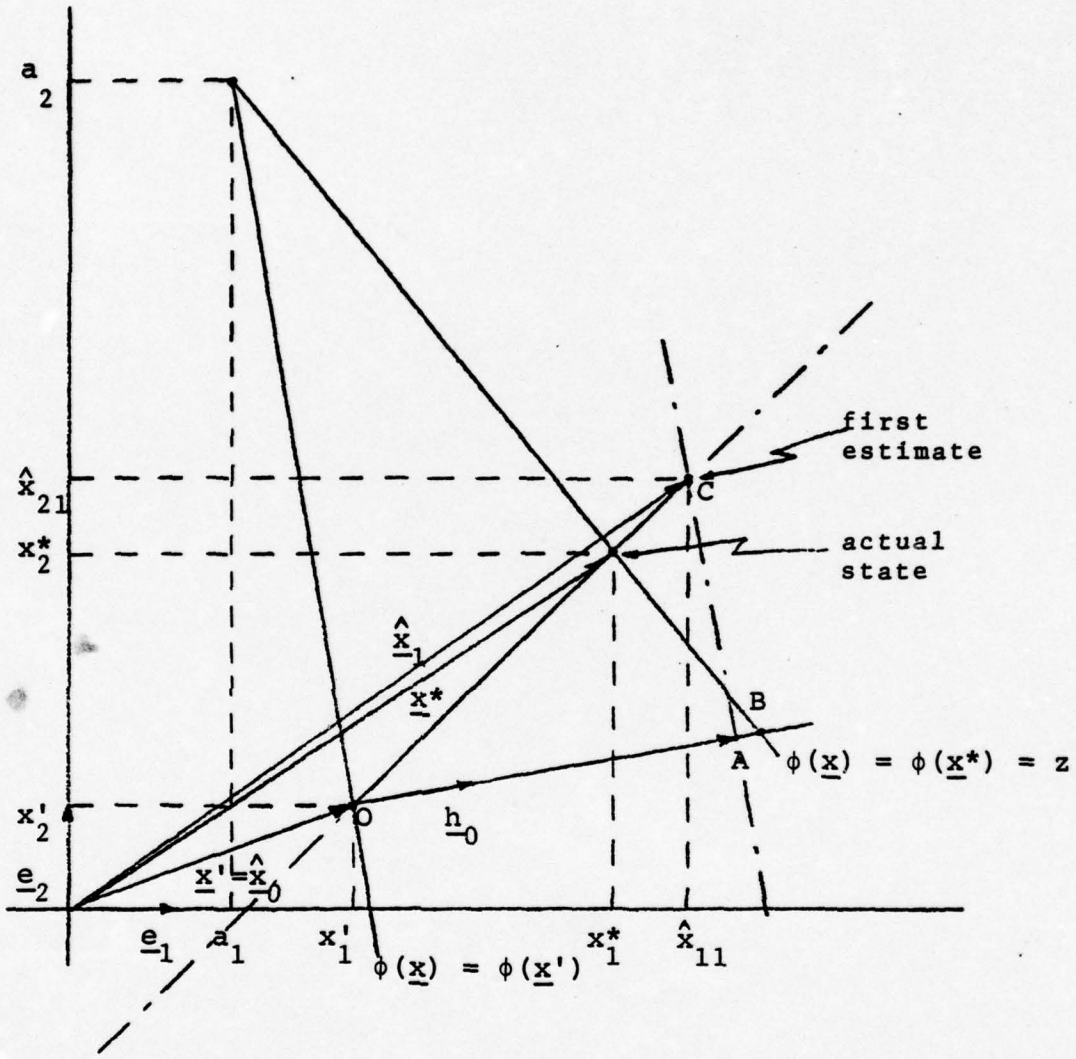

Figure 19 : Iterative process - First estimate.

CH.

The projection of the second correction term, $(-\underline{g}_1 [\phi(\underline{x}') - \phi(\underline{\hat{x}}_i)])$, into $\underline{h}_1$ is smaller than CG, say CF. The normal from point F determines the second correction term (IC).

Adding the three vectors $\underline{x}'$, CH and IC one has the second estimate, shown in Figure 21, and the next iteration can be processed.

If in Equation (4.47) one modifies the residual by

$$\underline{z}(k) - \underline{h}(\underline{\hat{x}}(k|k-1)) = \underline{z}(k) - [\underline{h}(\underline{\hat{x}}_i) + H_i.(\underline{\hat{x}}(k|k-1) - \underline{\hat{x}}_i) + \ldots] =$$

$$\tilde{=} \underline{z}(k) - \underline{h}(\underline{\hat{x}}_i) - H_i.[\underline{\hat{x}}(k|k-1) - \underline{\hat{x}}_i]$$

then Equation (4.47) becomes

$$\underline{\hat{x}}_{i+1} = \underline{\hat{x}}(k|k-1) + G_i[\underline{z}(k) - \underline{h}(\underline{\hat{x}}_i) - H_i[\underline{\hat{x}}(k|k-1) - \underline{\hat{x}}_i]] \quad (4.53)$$

This variation in the residual is very small to affect considerably the estimates but in [11] it is shown that its use produces a better agreement between the calculated estimation error covariance matrix and the true error covariance, when processing a noisy measurement.

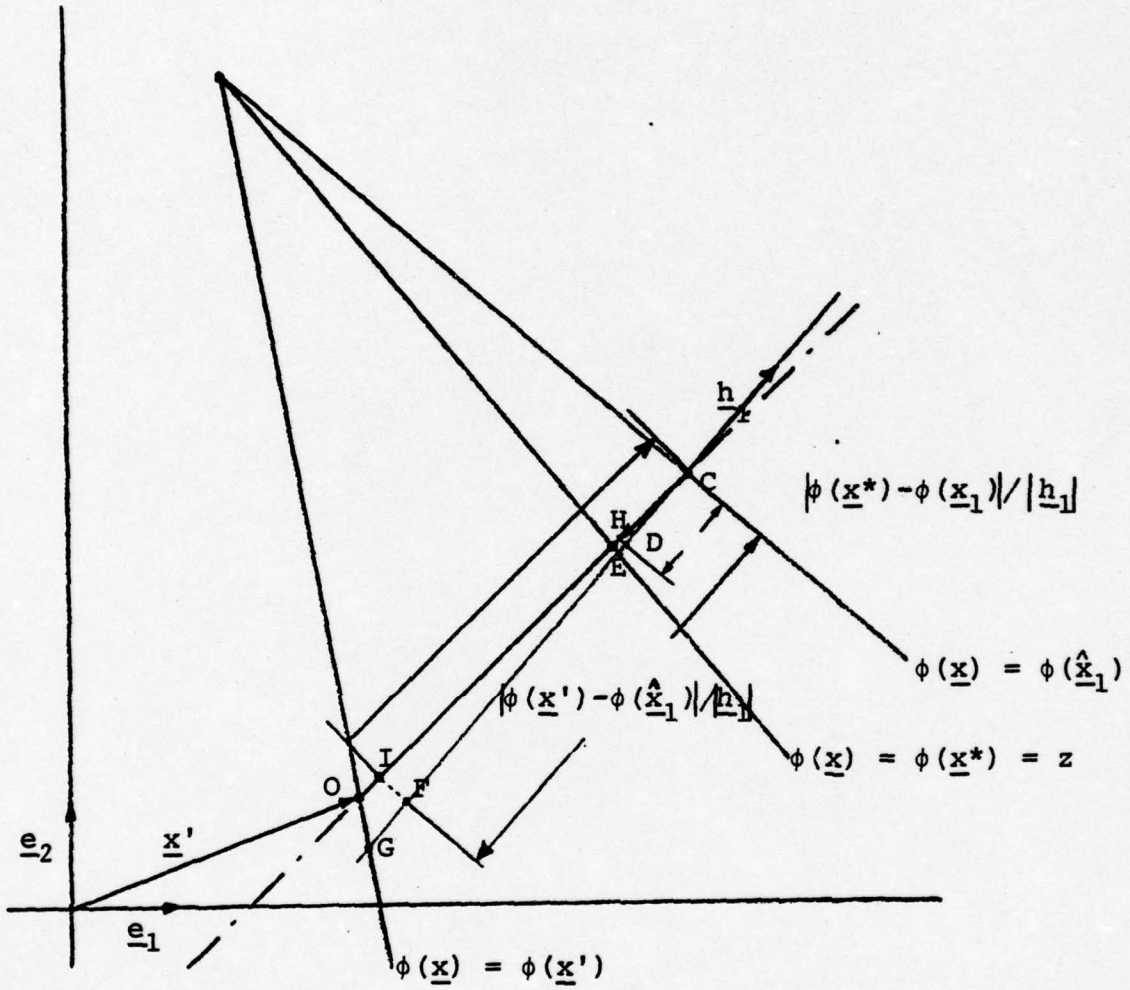

Figure 20 : Iterative process - Correction terms.

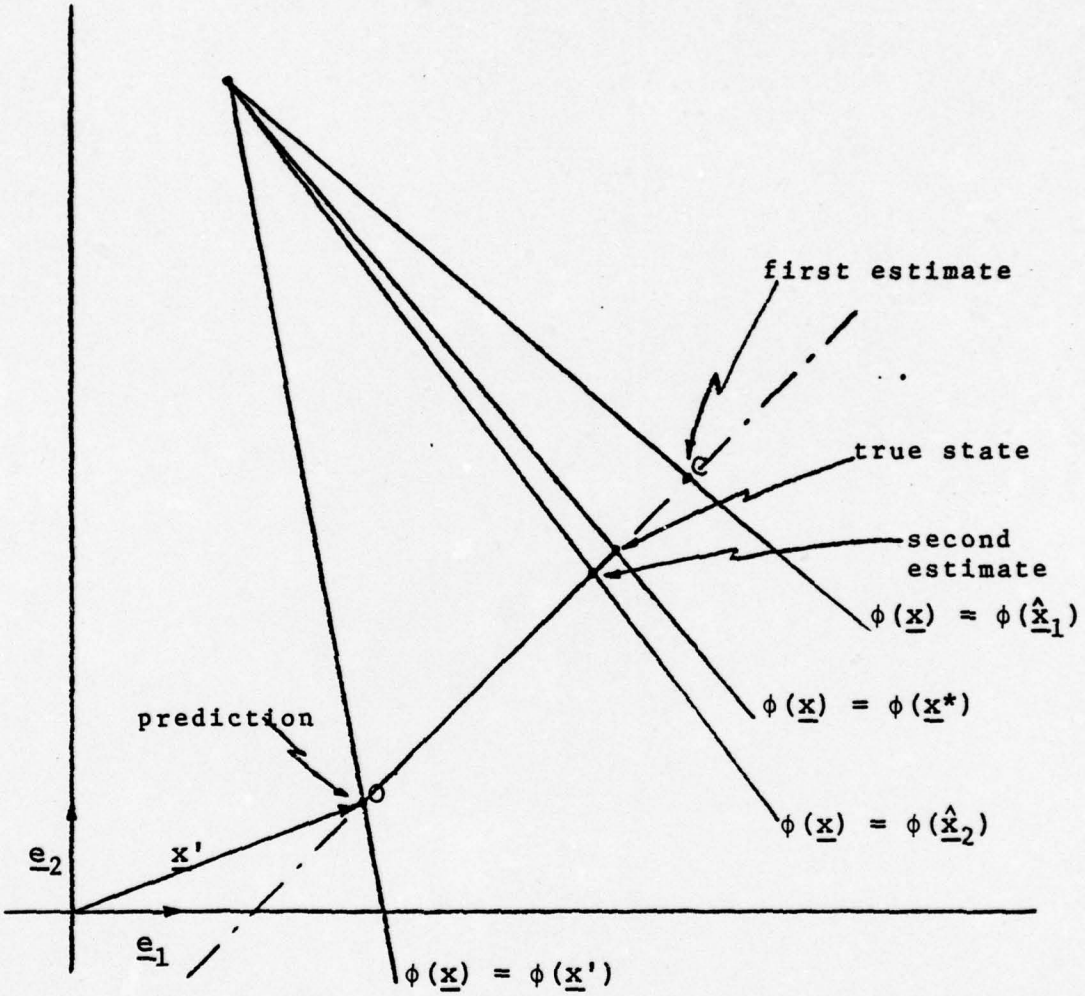

Figure 21 : Iterative process - Second estimate.

3. Summary

The direct application of these graphical interpretations to a general problem is impractical. Nevertheless the basic points observed here can be generalized for Kalman Filters:

--- the "direction" of correction in the estimation is defined by the predicted quantities and doesn't depend on the measurements.

--- the amount of correction in an estimation, along the direction defined, is the result of a weighting process between the uncertainty in the measurement and the confidence in the predicted values. This correction is a function of the factor $[1 / (1 + \gamma^2)]$ where, in general, for a n-dimensional system

$$\gamma^2 = r^2 / \sum_{i=1}^{n} \sum_{j=1}^{n} p'_{ij} h_i h_j \qquad (4.51)$$

--- the errors in the estimate from the processing of a nonlinear measurement can be large and, most important, the estimation error covariance matrix may become a very poor approximation of the true error covariance, forcing the filter to inaccurately weight future measurements. This problem depends on the nonlinearities involved and seems to be worse when the predicted values are poor and/or the measurements are considered by the filter to have relatively low noise.

--- the errors indicated above may be reduced with the use of the iterative equations (4.48), (4.49) and (4.47) or (4.53), instead of the standard approach given by the Equations (3.18),(3.19) and (3.21), at the expense of greater computing effort.

V. COMPUTER SIMULATION

A. GENERAL CONSIDERATIONS

A computer simulation was implemented in a Unix Operating System running on a PDP 11/50 with the FP 11B floating point processor, located at room 506 of Spanagel Hall, NPS. The whole program is interactive and is expected to be self-explanatory to a user. Its block diagrams and coding are presented in Appendix E.

The graphical outputs were generated on a Tektronix 4014-1 terminal. The presentation of the results of the various simulations is simplified by the adoption of the following conventions.

The metric system was used in all calculations and outputs. The axes are dimensioned in kilometers. Heading and bearing angles, expressed in radians, are measured counterclockwise from the positive X-axis.

Figure 22 shows a typical plot. Points of the true track are represented by the sysmbol "+" and interconnected by a solid line. Buoys are represented by a distinctive boxed symbol. The portion of the true track that is in the range of a buoy is bounded, if necessary, by dash-dotted lines.

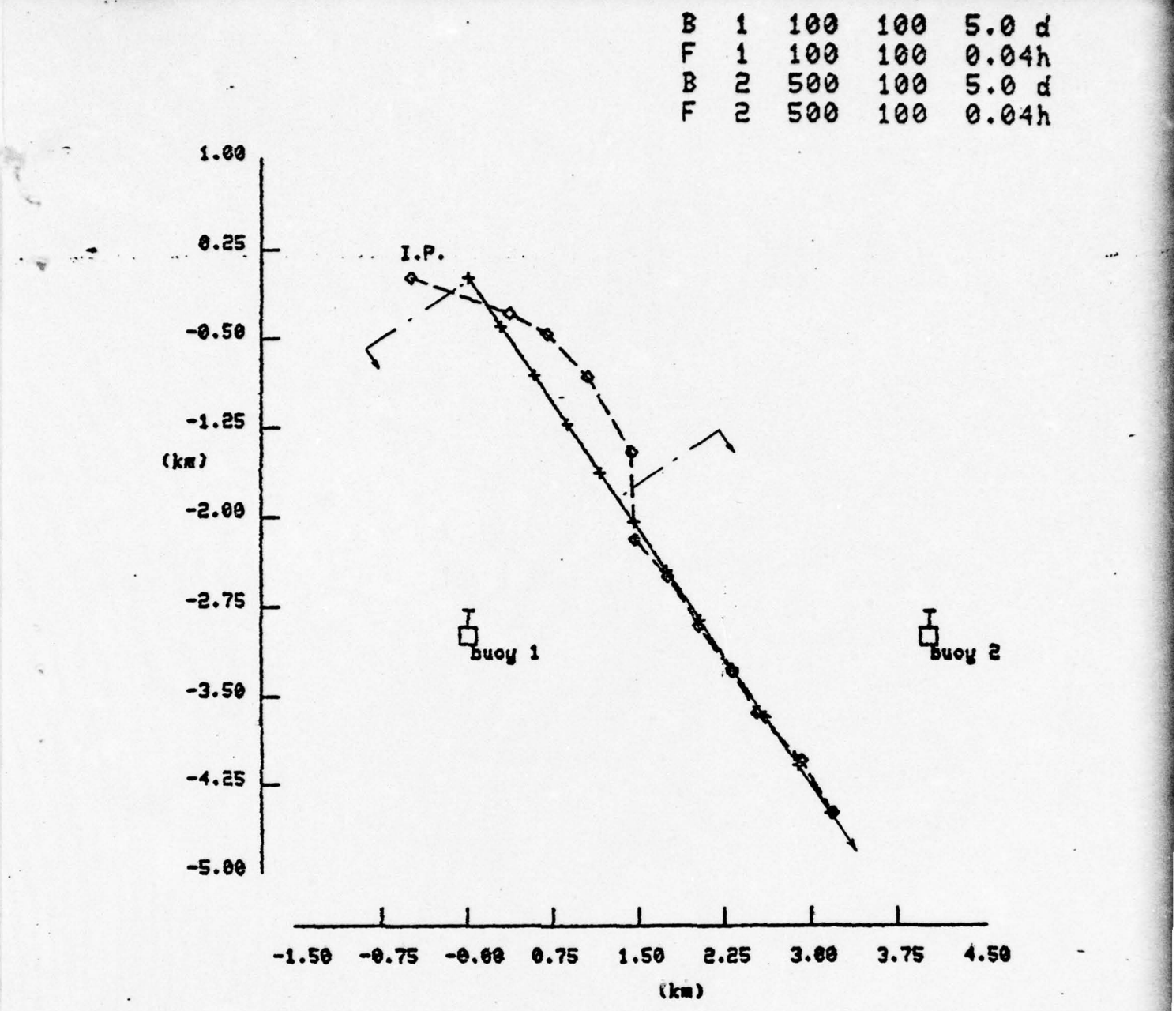

Figure 22 : True and estimated trajectories - A typical run.

The signals received by the sonobuoys are assumed to be sent to a ship or aircraft where they are processed by specialized equipment to generate certain measurements. The major characteristics of these measurements are printed on top of each figure and obey a code whose general form is

L N1 N2 N3 S

where

L - a capital letter indicating a type of measurement. B stands for bearing; F for frequency; D for frequency difference; R for frequency ratio; and T for time delay.

N1 - an optional number indicating, when necessary, the buoy that generates the measurement. If this number has two digits it identifies two buoys, thus, T 12 indicates a time delay measurement between buoys 1 and 2.

N2 - a number indicating how many seconds after the start of the problem this measurement will be first obtained. It is also optional.

N3 - a number indicating the period between consecutive measurements.

S - a number indicating the standard deviation of the simulated zero-mean Gaussian noise that is associated with this measurement, followed by an optional small letter indicating dimension: d for degrees, h for Hertz and s for seconds.

The interpretation of the code presented in Figure 22 is then that both buoys 1 and 2 provide bearing and frequency measurements with a period of 100 seconds between consecutive set of measurements. Buoy 1 provides its first set of measurements 100 seconds after the start of the problem; buoy 2, perhaps because of its limited range, provides its first set of measurements only after 500 seconds of the start of the problem. The standard deviation of the measurement noise is 5 degrees for the bearings and 0.04 Hertz for the frequencies.

The filter receives the measurements for processing. It is given some initial conditions and the initial position is marked in the figures by the first diamond with the letters I.P. on top.

As the target moves and the measurements are simulated, the filter generates estimates of the target parameters which are represented by small diamonds, interconnected by dashed lines to represent the estimated path. The diamonds and the "+" symbols correspond to the same time points.

Associated with each estimated point the filter provides an estimation error covariance matrix which indicates the amount of confidence or, conversely, uncertainty that should be given to this estimate. An interesting way to show this in a trajectory plot like Figure 22 is by plotting the one-sigma error ellipses associated with each estimated point. These error ellipses have their orientation and axis dimen-

sions given by Equations (4.27) - (4.29), and can be seen in Figure 23.

These figures were obtained by running the simulation once. They may represent a typical real-time result. Nevertheless they do not give the expected or average behavior of the filter to the situation simulated. To obtain this average behavior many Monte Carlo runs have to be executed and their individual results processed to generate the sample statistics. The sample statistics formulas for obtaining the sample means and covariances can be found, for example, in page 86 of Ref. [2].

In this work all the statistical results were obtained from 200 MonteCarlo runs. Figure 24 shows the average behavior of the filter after these runs. Now the small diamonds represent the sample mean estimated position and the ellipses show the spreading of the results about the mean values. Note that at the initial position point, since in all runs it was the same, the ellipse is the point itself.

To observe the errors in the estimation of the speed and heading of the target different plots have to be used. Figure 25 shows the sample mean error in the estimation of speed as a function of time. Figure 26 shows the sample mean error in the estimation of the heading of the target.

Other types of plots or outputs could be generated from the results given by the program simulation, like the sample covariance between estimated velocity and bearing, if it

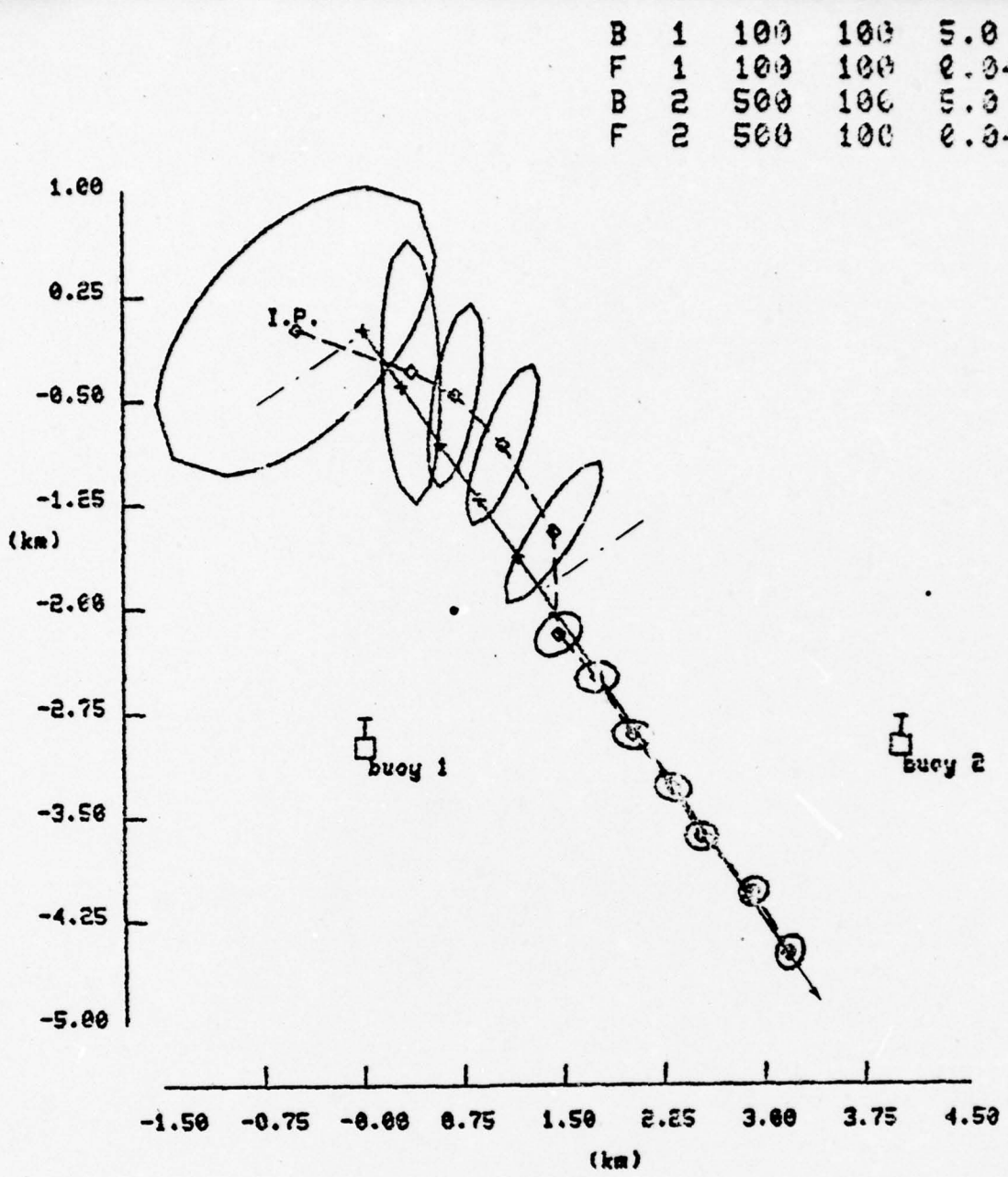

Figure 23 : True and estimated trajectories
Typical estimation error ellipses.

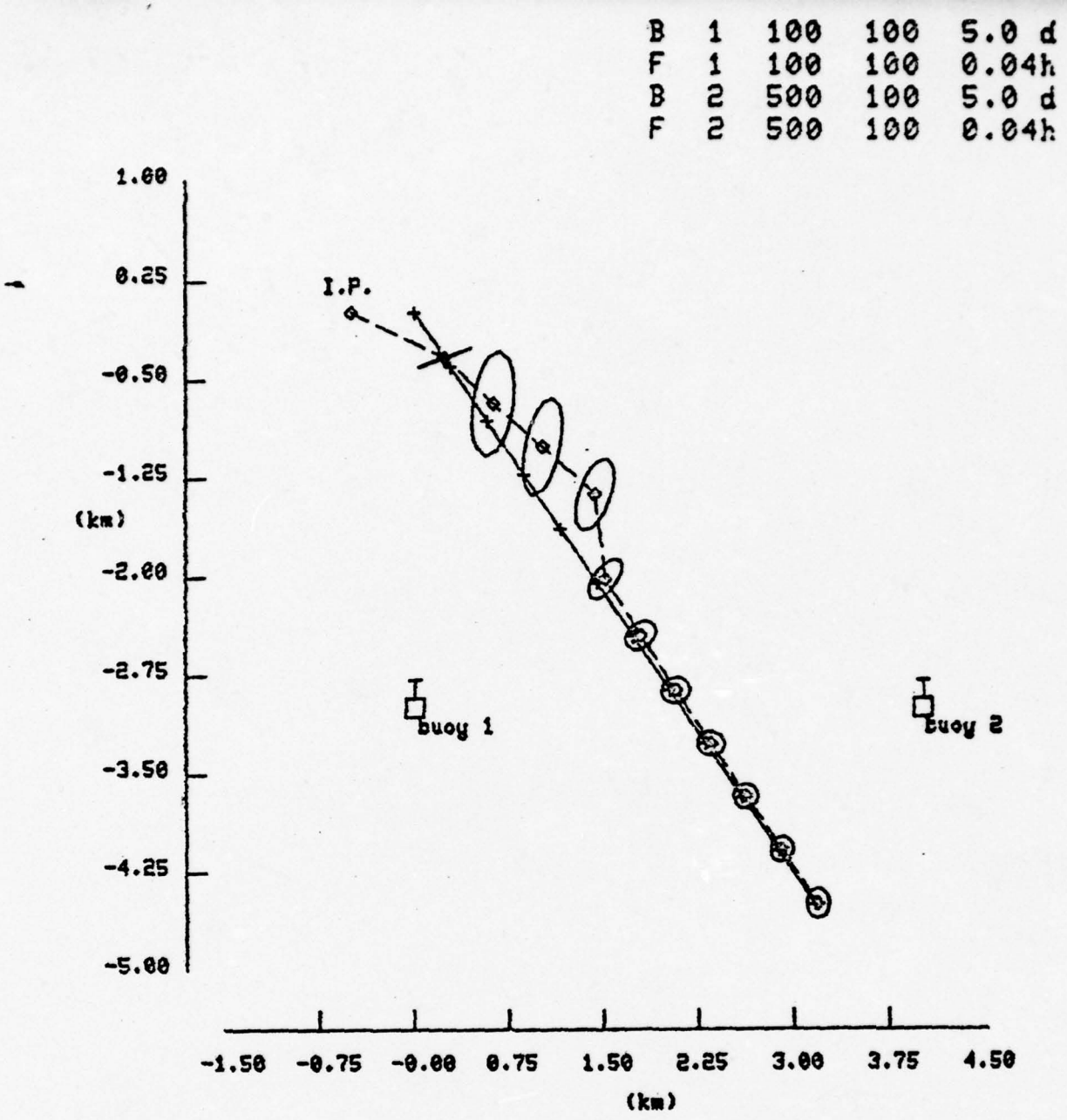

Figure 24 : True and estimated trajectories
Sample means and ellipses.

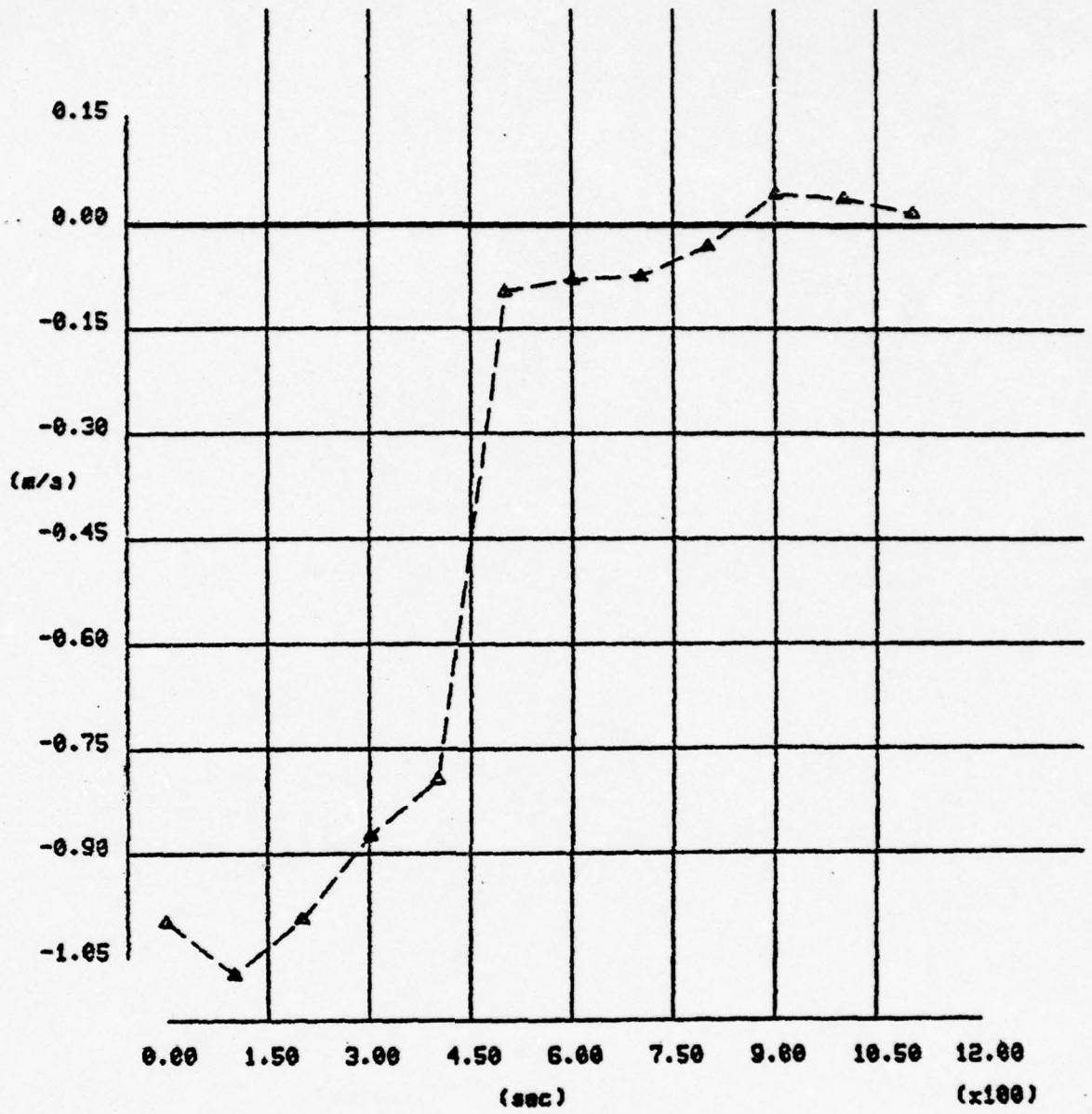

Figure 25 : Error in speed estimation - Sample means.

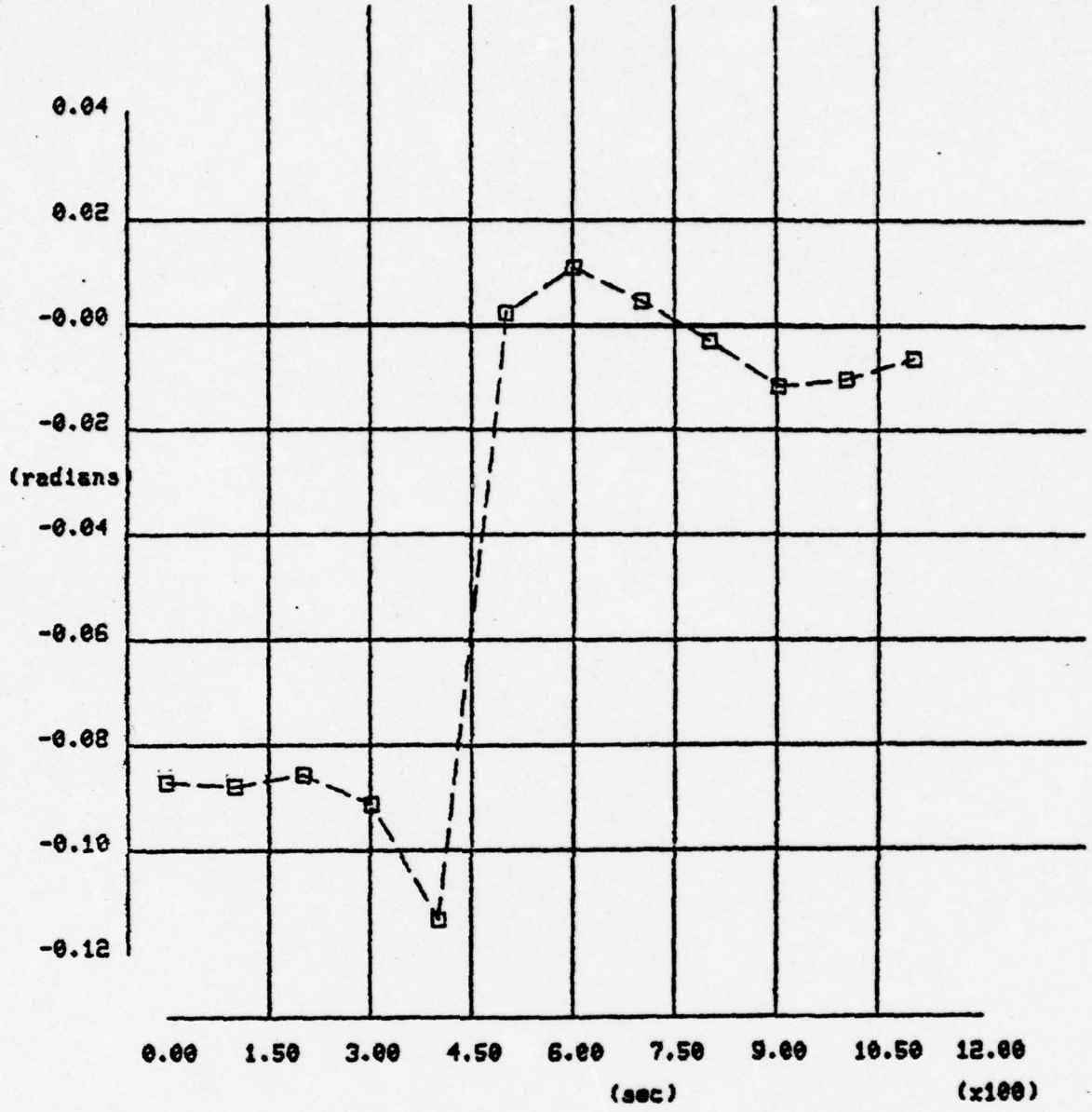

Figure 26 : Error in heading estimation - Sample means.

ever becomes necessary.

B. SELECTED RESULTS

As has been seen in this work, the number of variables in the passive tracking problem is very large. Some specify the true target track and the true position and characteristics of the sonobuoys; others define the measurement scheduling and noise characteristics. The nonlinear filter that processes the measurements has its own variables and must also assume values for the other variables, which may be different from the true ones.

For any combination of these variables a new problem is formed and its simulation may generate a number of interesting conclusions. The results presented are representative of those obtained from the execution of the simulation program described in Appendix E. In most of the results presented a certain reasonable initial condition for the filter was assumed; the position of the buoys was assumed constant and known; the ranges within which reliable bearing, frequency and time delay measurements could be obtained were assumed equal.

1. Non-maneuvering Target

a. One Buoy in Action at a Time

Figure 27 shows the behavior of the filter in a situation where only one buoy is in contact with the target

at any instant. The range and position of the buoys were pre-arranged to satisfy this requirement. Target speed is 5.0 m/s; its heading is 315 degrees measured from the positive X-axis. The initial assumptions of the filter include 6.0 m/s for speed and 325 degrees for heading. The measurements were processed as suggested in [2]. Frequency and bearing measurements are available every 100 seconds and processed simultaneously; standard deviations of 5 degrees and 0.04 Hertz were assumed for the noise components.

The frequency measurement provides, indirectly, some range information and, this way, complements the bearing measurement. This range information can also be obtained by judiciously positioning the next buoys or by having two or more buoys in contact with the target at one time.

In Figure 28 the frequency measurement was eliminated and the simple bearing measurement allowed the estimator to track the non-maneuvering target almost as well as before, because of the special position of the buoys. Note that the ellipses tend to align with the measurement lines. This can be explained from the discussions of Section IV,B and Appendix D.

There are many ways to improve this tracking. A very small improvement can be obtained if less noisy or more frequent frequency measurements could be obtained. To get more precise frequency indication one needs better resolution from the FFT processors; to obtain better resolution

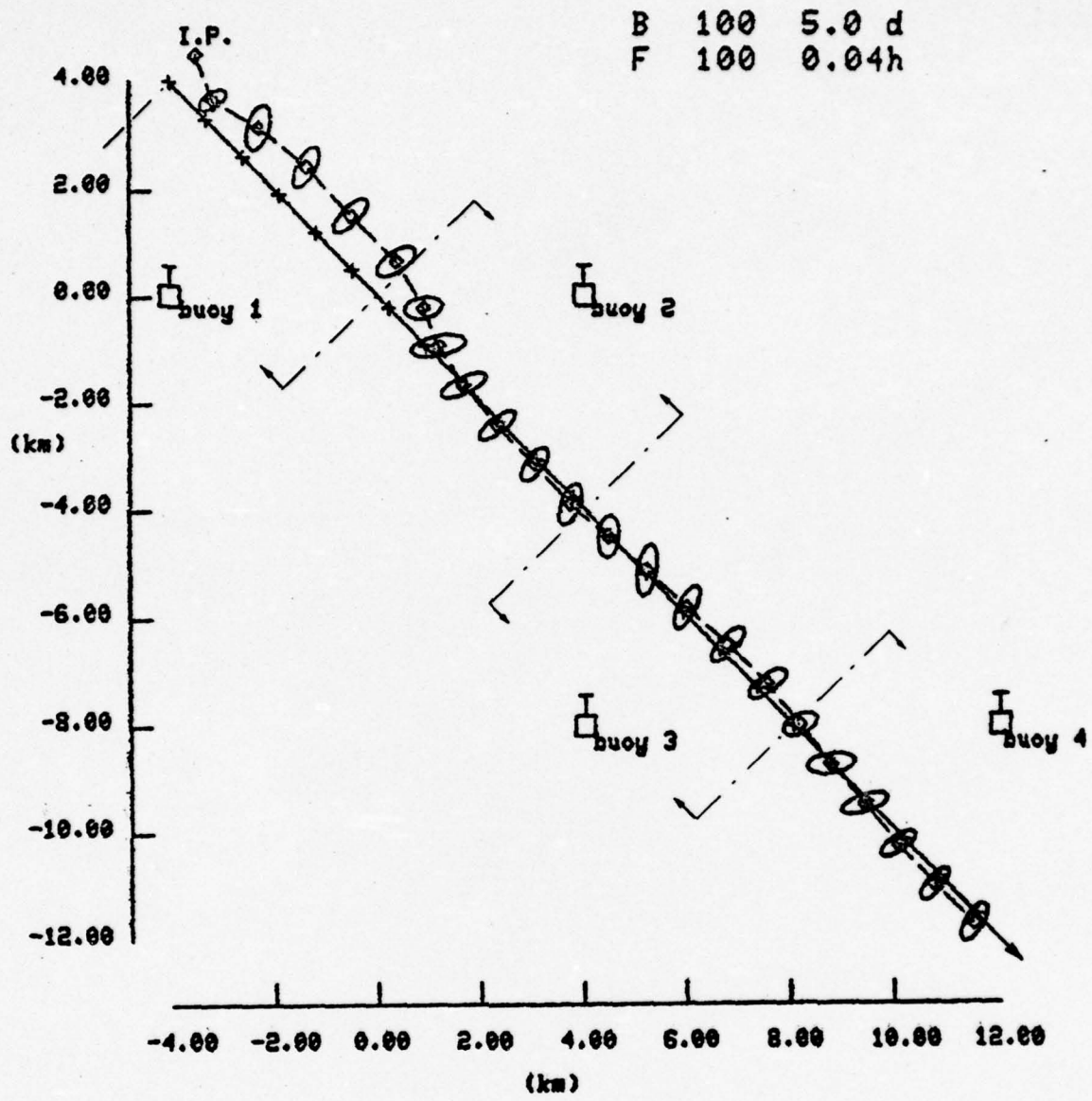

Figure 27 : True and estimated trajectories for a non-maneuvering target - Simultaneous frequency and bearing measurements.

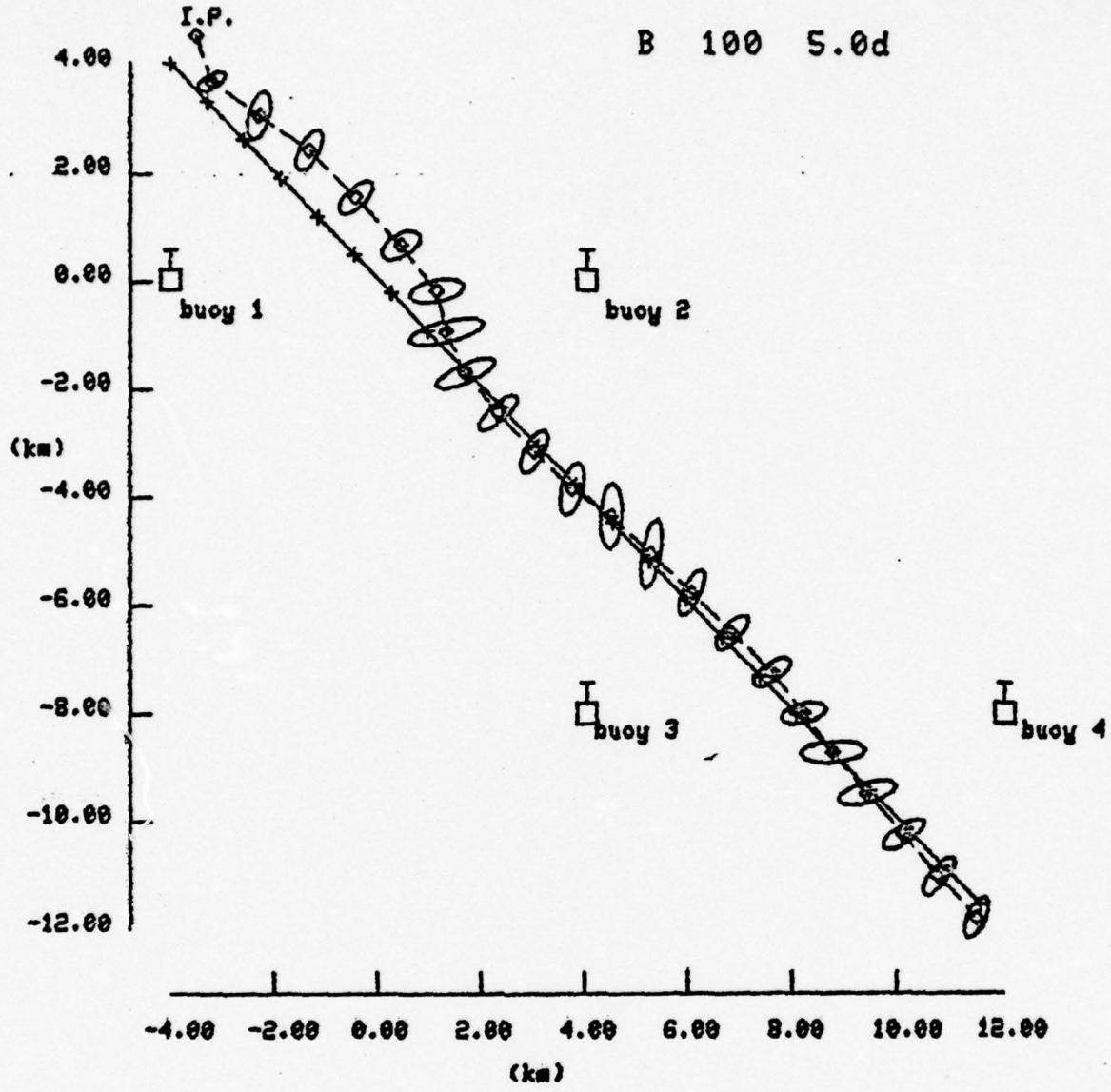

Figure 28 : True and estimated trajectories for a non-maneuvering target - Bearing measurements only.

one needs longer records which, in turn, introduce more errors due to target-sensor geometry variations during record time. To reduce the period between consecutive independent frequency indications one has to sacrifice resolution but this would reduce even more the effect of the frequency measurement on tracking accuracy. Besides, an emitted frequency of 300 Hertz from a target with a relative velocity of 5 knots toward a buoy is shifted by only about 0.5 Hertz and it can be seen that not much resolution can be spared.

The bearing information is basically continuous and it seems reasonable to admit that only economical limitations exist for obtaining less noisy or, equivalently, more frequent bearing measurements. Figure 29 shows the effect of processing only bearing measurements, but more frequently (at 25-second intervals). In Figure 30 the standard deviation of the measurement noise was reduced to 1 degree. Note that the alignment of the ellipses with the measurement lines is more pronounced with less noisy measurements. Note also that the error in range while the first buoy is in contact with the target is not corrected by improving the accuracy of the bearing measurements.

Figures 31 and 32 show the mean errors in estimating the velocity and bearing of the target. The symbol "+" is associated with Fig 27, the triangles with Fig 28 and the diamonds with Fig 29.

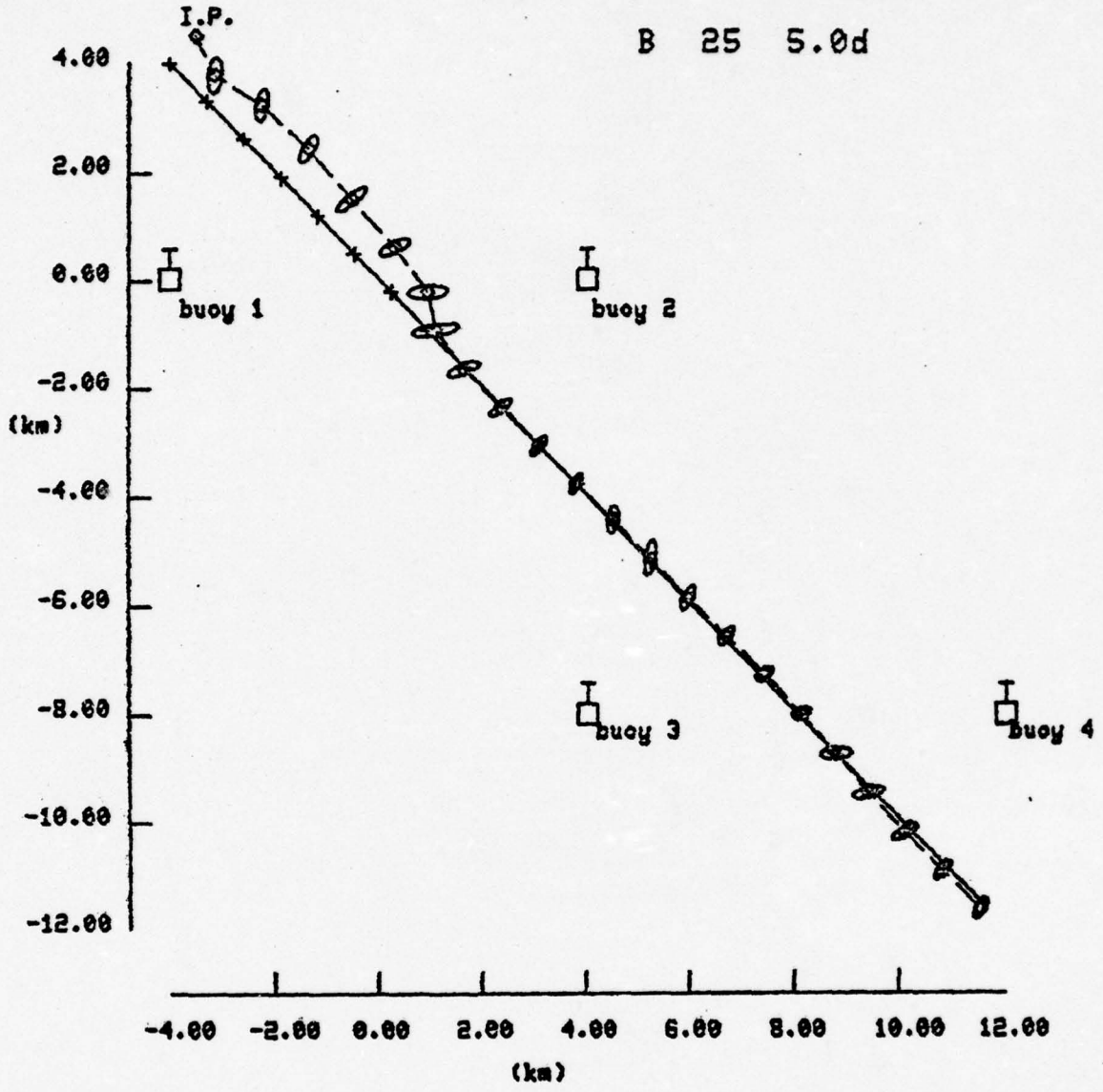

Figure 29 : True and estimated trajectories for a non-maneuvering target - Reduced interval between consecutive measurements.

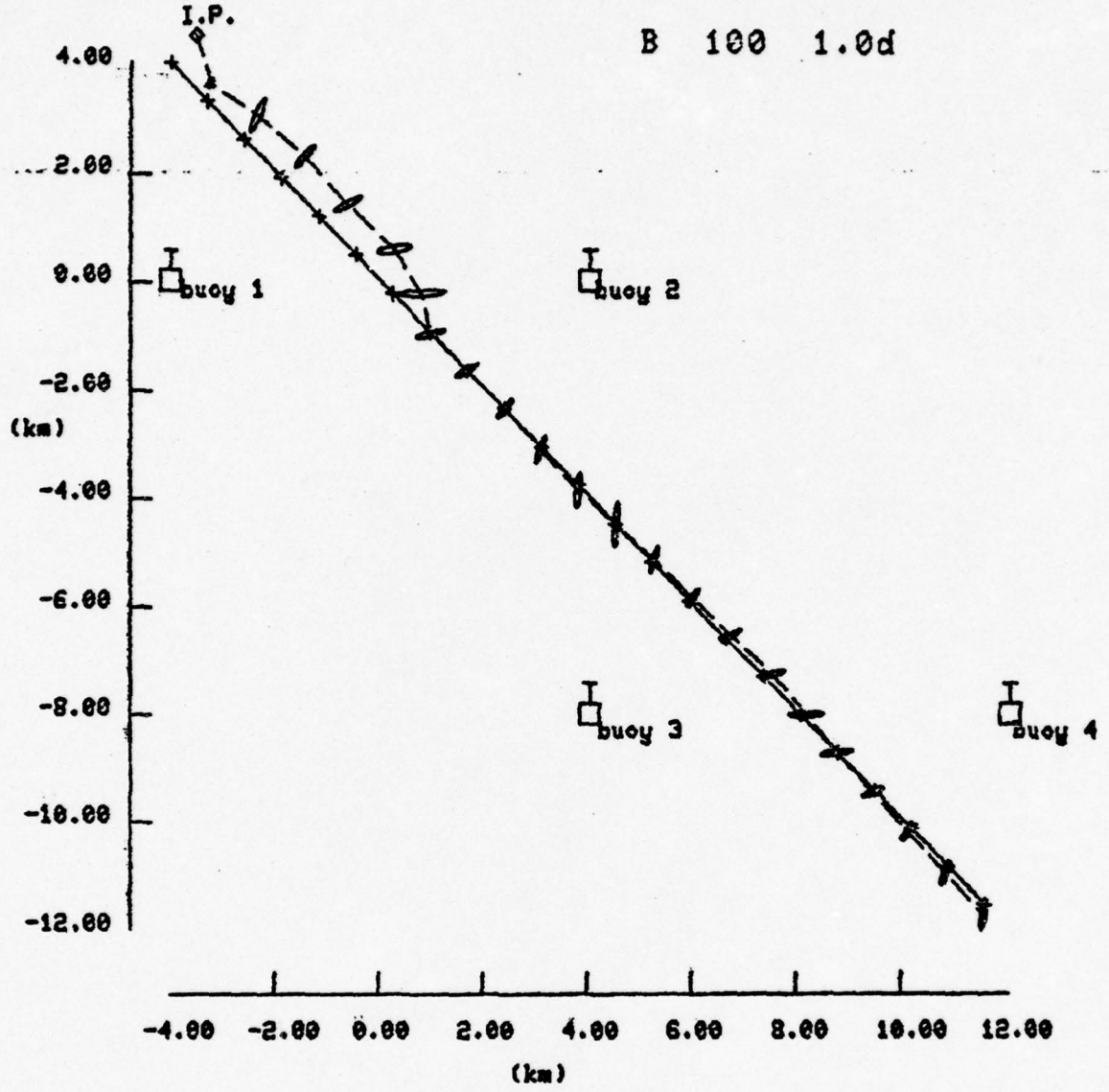

Figure 30 : True and estimated trajectories for a non-maneuvering target - More precise bearing measurements.

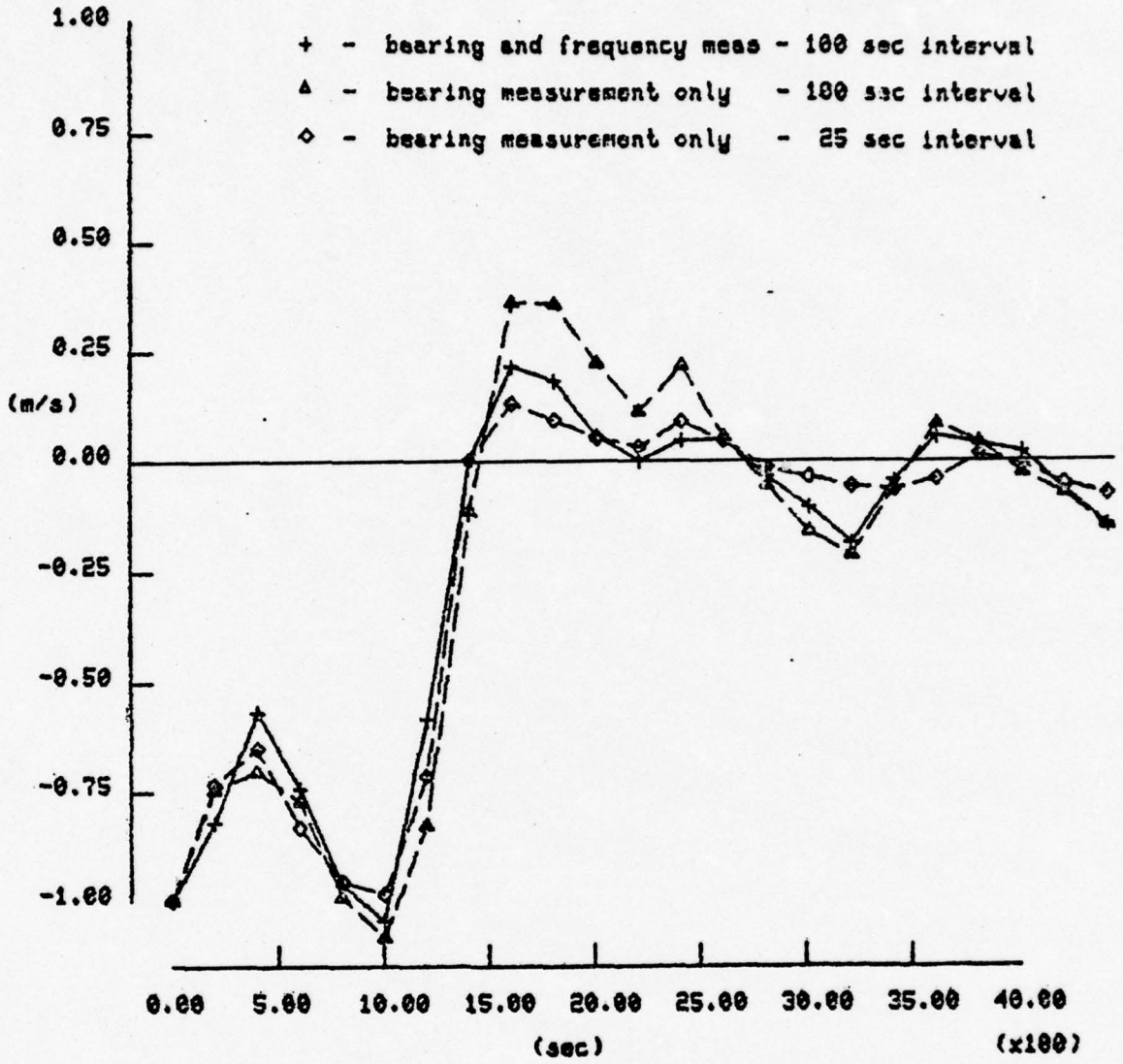

Figure 31 : Error in speed estimation - Comparison of results.

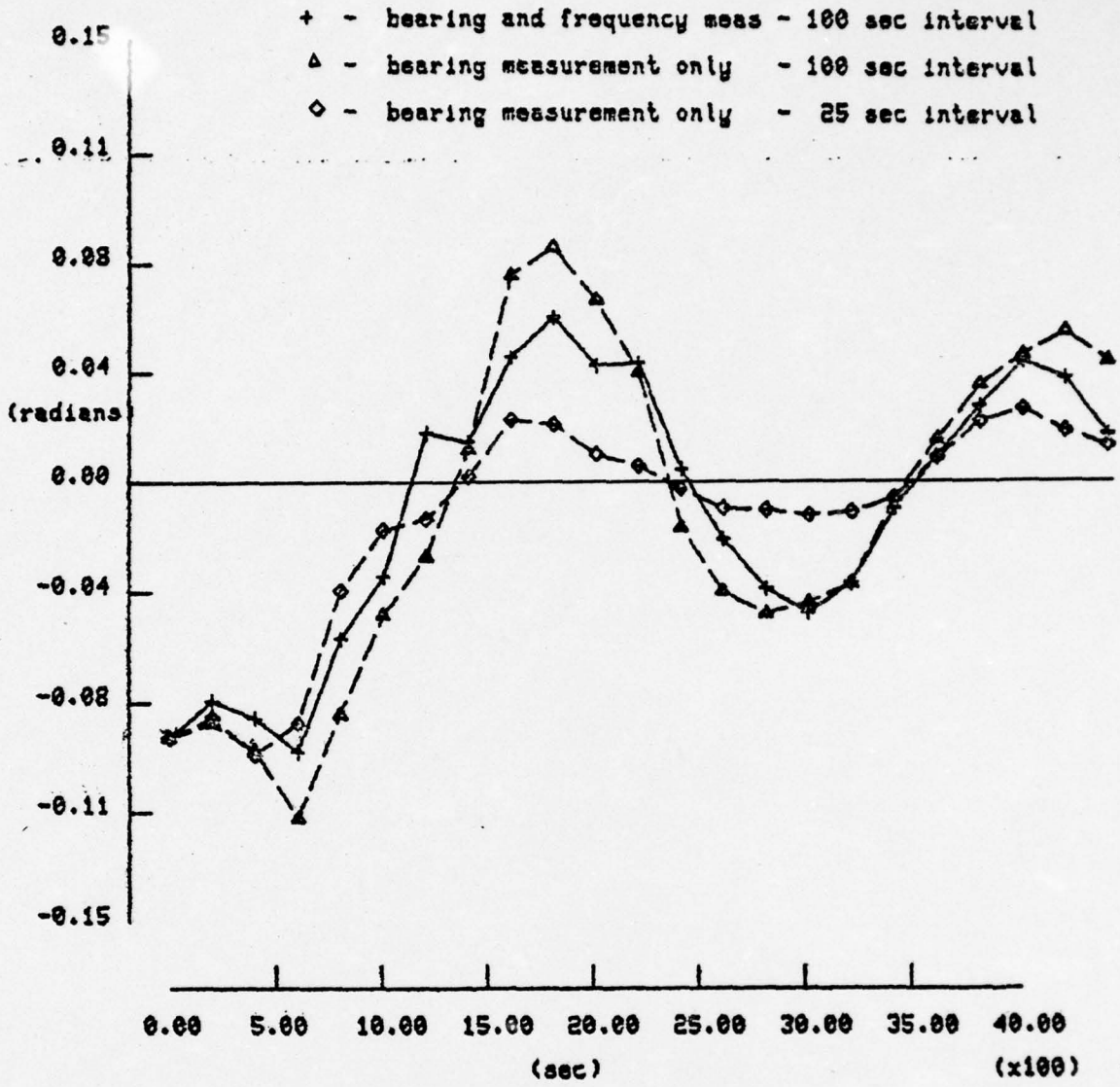

Figure 32 : Error in heading estimation - Comparison of results.

Since the contribution of the frequency measurements is so small compared to that of the bearing indications in this case, the partitioning of the measurements has very little effect on tracking accuracy. Also the iterative techniques suggested in Section IV,B,2 have no marked effect on the processing of the frequency measurements for the same reason.

b. Two Buoys in Action at a Time

The placement of another buoy in action can greatly improve the tracking accuracy, as shown in the next figures. The buoys are now arranged so that two buoys, instead of one, are in contact with the target at any time. The scaling is changed so that the estimation errors may be better appreciated.

In Figure 33 the added buoy is a Lofar buoy that can only provide frequency measurements. The two frequency and one bearing measurements available every 100 seconds were processed simultaneously. Note the improvement in accuracy when buoys 3 and 4 gain contact with the target in replacement of buoys 1 and 2. This also is explained from the discussions of Section IV,B.

In Figure 34 all buoys contribute with frequency and bearing measurements which are still processed simultaneously every 100 seconds. The position of the buoys, in a line perpendicular to the true track, is not a very good

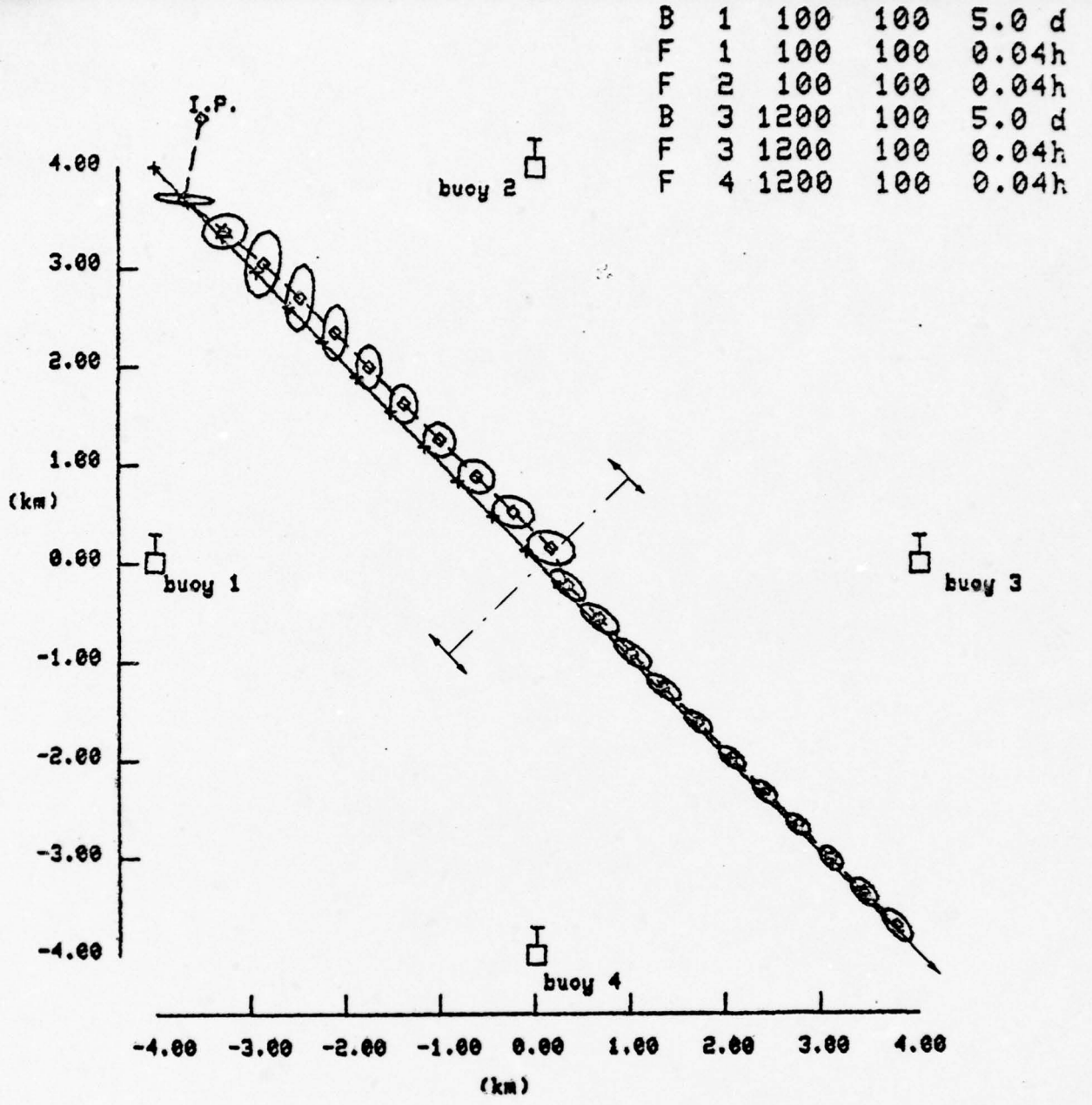

Figure 33 : True and estimated trajectories for a non-maneuvering target - Simultaneous processing of one bearing and two frequency measurements.

position for two Difar buoys. Nevertheless the resulting tracking accuracy is good for this non-maneuvering target.

In Figure 35 the two frequency measurements, which require a five-state plant for their processing, were replaced by a frequency difference measurement with 0.04 Hertz of standard deviation in its noise component, which requires only a four-state plant, as discussed in Section II,D,2. The results are basically the same, mainly because they are mostly dependent on the bearing measurement and not on the frequency information. The use of the frequency ratio measurement also gave the same kind of results when a very low noise measurement, with about 0.0001 units of standard deviation, was considered.

In Figure 36 the frequency measurements were eliminated and only bearing measurements were processed. Because of the bad position of the buoys, on a line perpendicular to the true track, the accuracy of the tracking along that line is not good. The ellipses show a reasonable spreading of the estimates along perpendiculars to the true track. Figure 37 shows the same plot, with different scaling, for the first 1000 seconds of the path.

For different positions of the buoys, especially if one moves the buoys off the perpendicular to the true track, better tracking can be obtained as shown in Figure 38. The tendency of the ellipses to align with the measurement lines explains the improvement obtained.

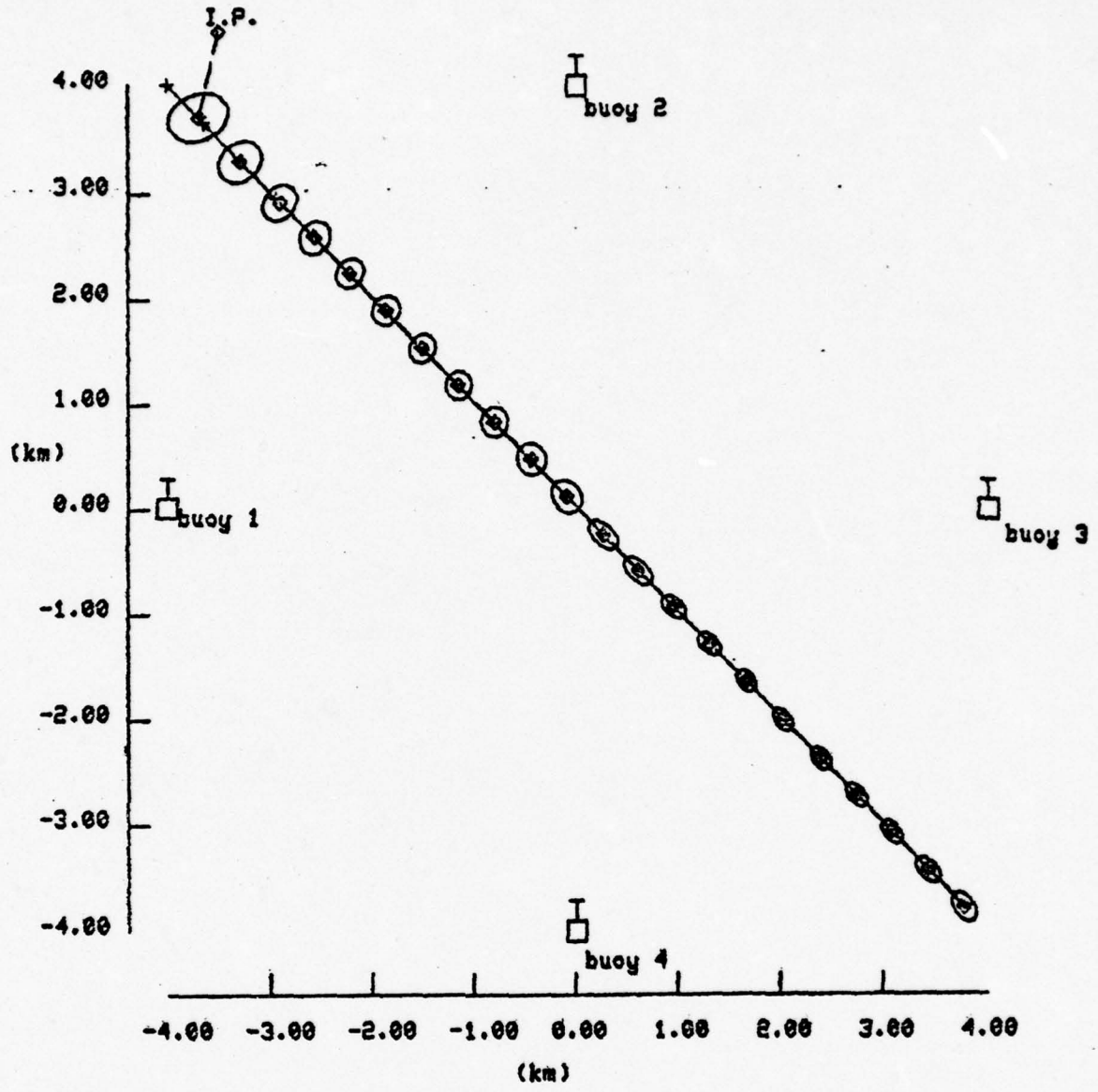

Figure 34 : True and estimated trajectories for a non-maneuvering target - Simultaneous processing of two bearing and two frequency measurements.

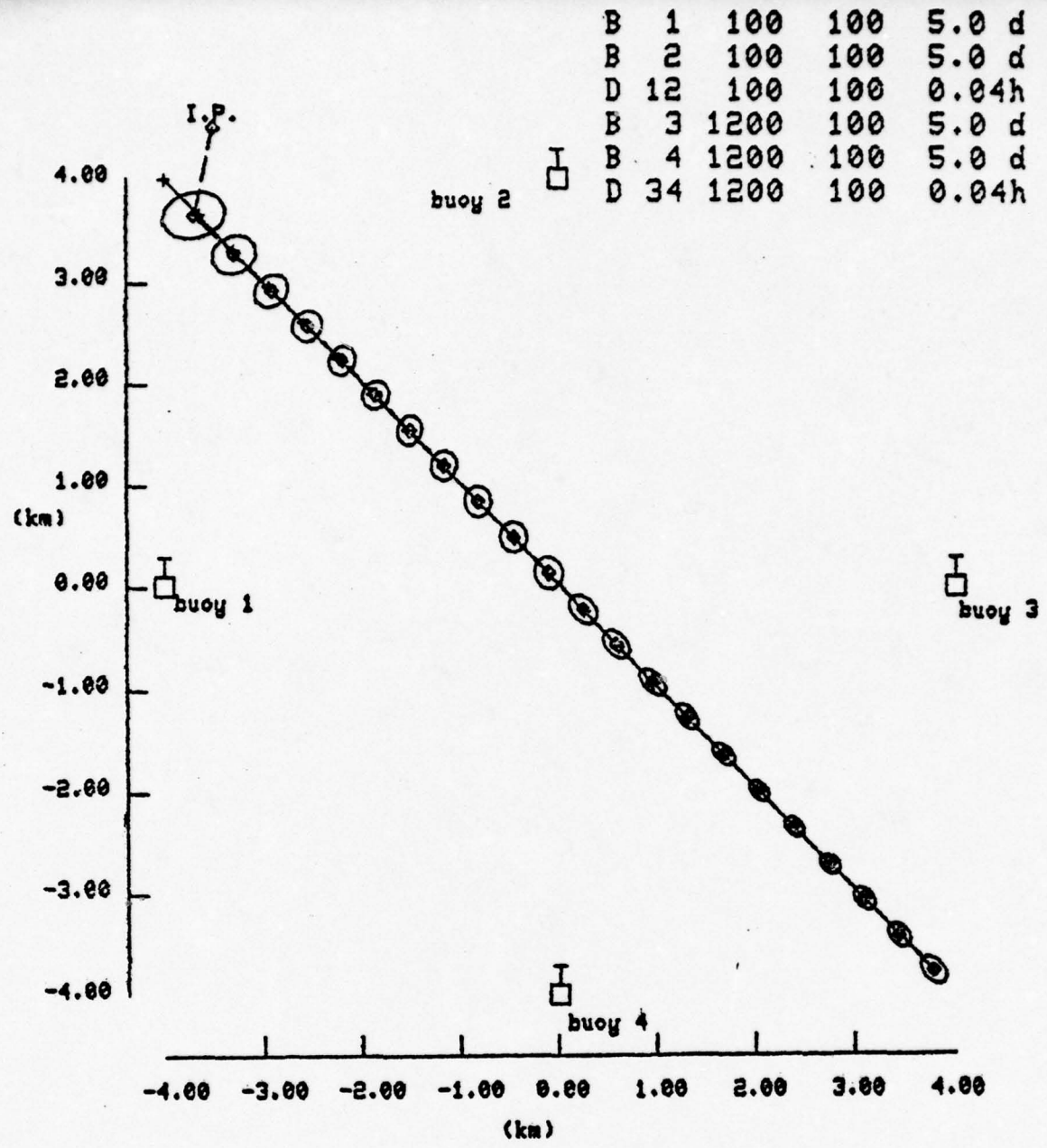

Figure 35 : True and estimated trajectories for a non-maneuvering target - Simultaneous processing of bearing and frequency-difference measurements.

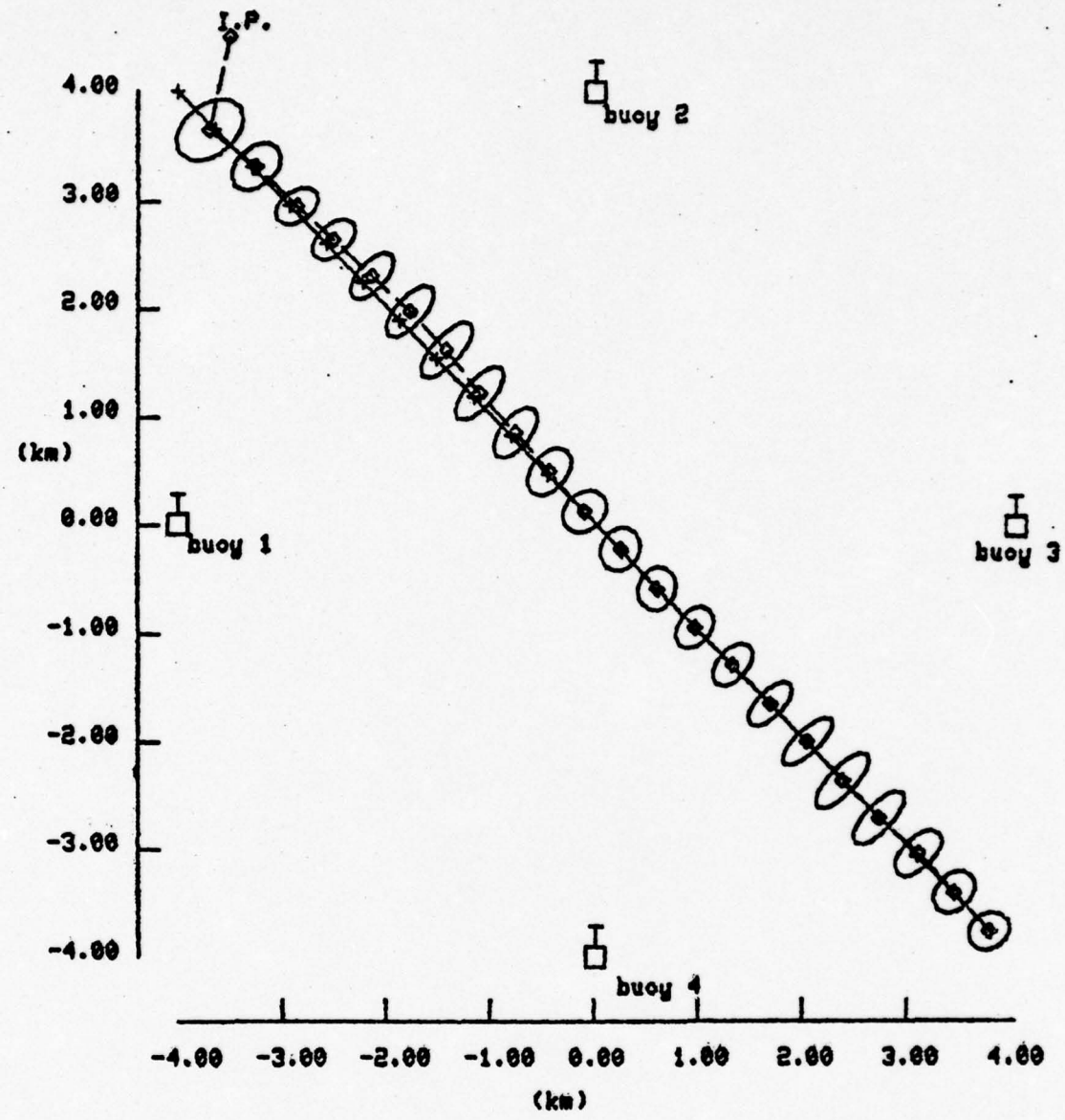

Figure 36 : True and estimated trajectories for a non-maneuvering target - Separate processing of bearing measurements.

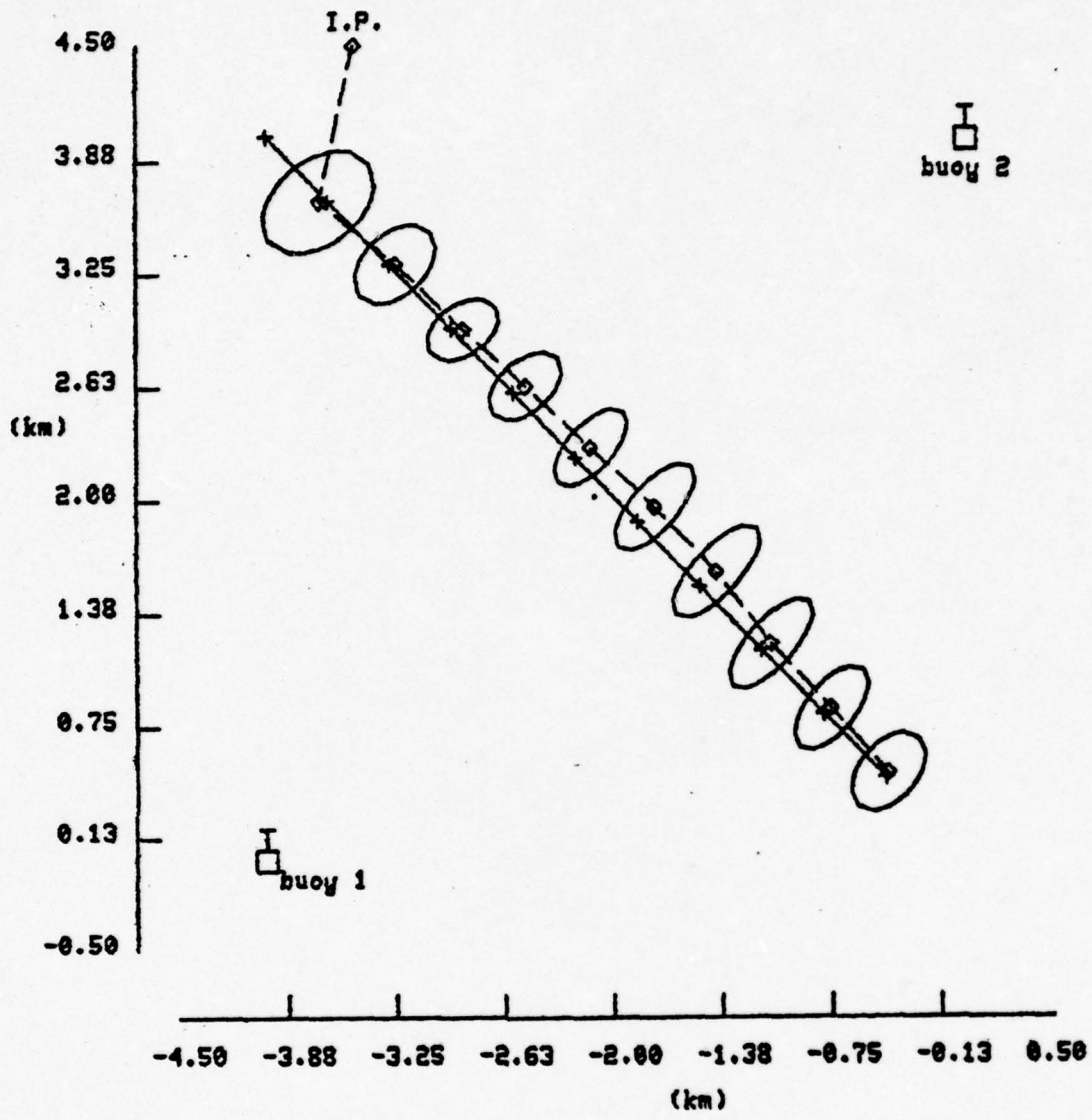

Figure 37 : True and estimated trajectories for a non-maneuvering target - Separate processing of bearing measurements - Reduced scale.

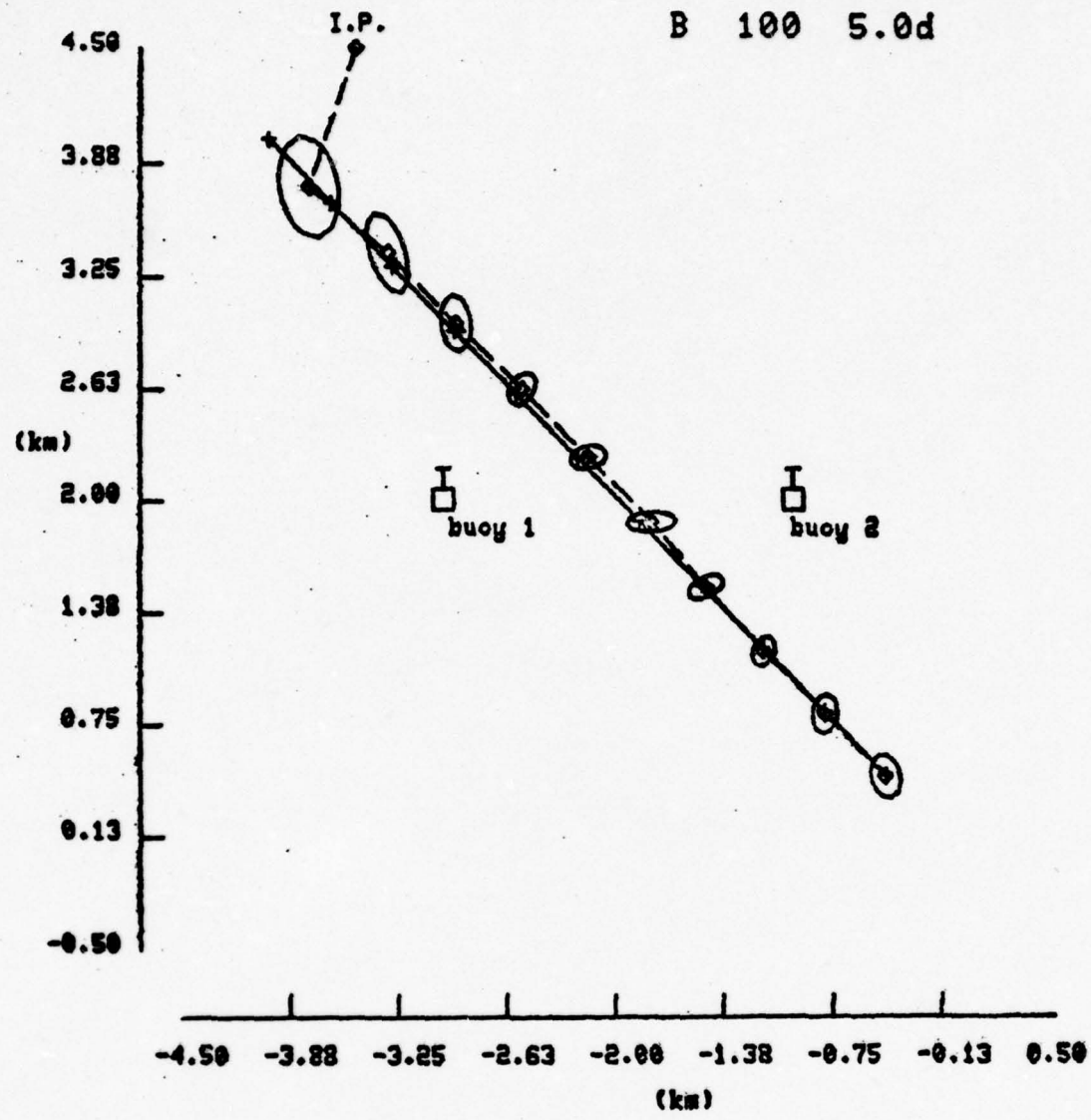

Figure 38 : True and estimated trajectories for a non-maneuvering target - Separate processing of bearing measurements - Buoys in different position.

By reducing the period between consecutive bearing measurements and processing them separately one may obtain the accuracy shown in Figure 39. The ellipses are like the ones of Figure 38 but with reduced dimensions.

Good results can also be obtained if one includes the time delay measurements. Figure 40 shows the result when they are applied to this situation. Notice that the ellipses are very small reflecting the fact that very good information about the position of the target is given by a low-noise time delay measurement. Also the ellipses tend to align with the tangent to the measurement lines defined in Section IV,B which, in this case of time delay measurements, are hyperbolas.

2. Maneuvering Target

The next paragraphs discuss results obtained when a selected target maneuver is simulated --- a total turn of 180 degrees at 9 degrees per minute with a constant speed of 5.0 m/s.

a. One Buoy in Action at a Time

Figure 41 shows the tracking obtained by processing frequency and bearing measurements provided by a single buoy located close to the center of curvature of the target path. The filter takes some time to react to the target maneuver and, when it does, an over-correction is

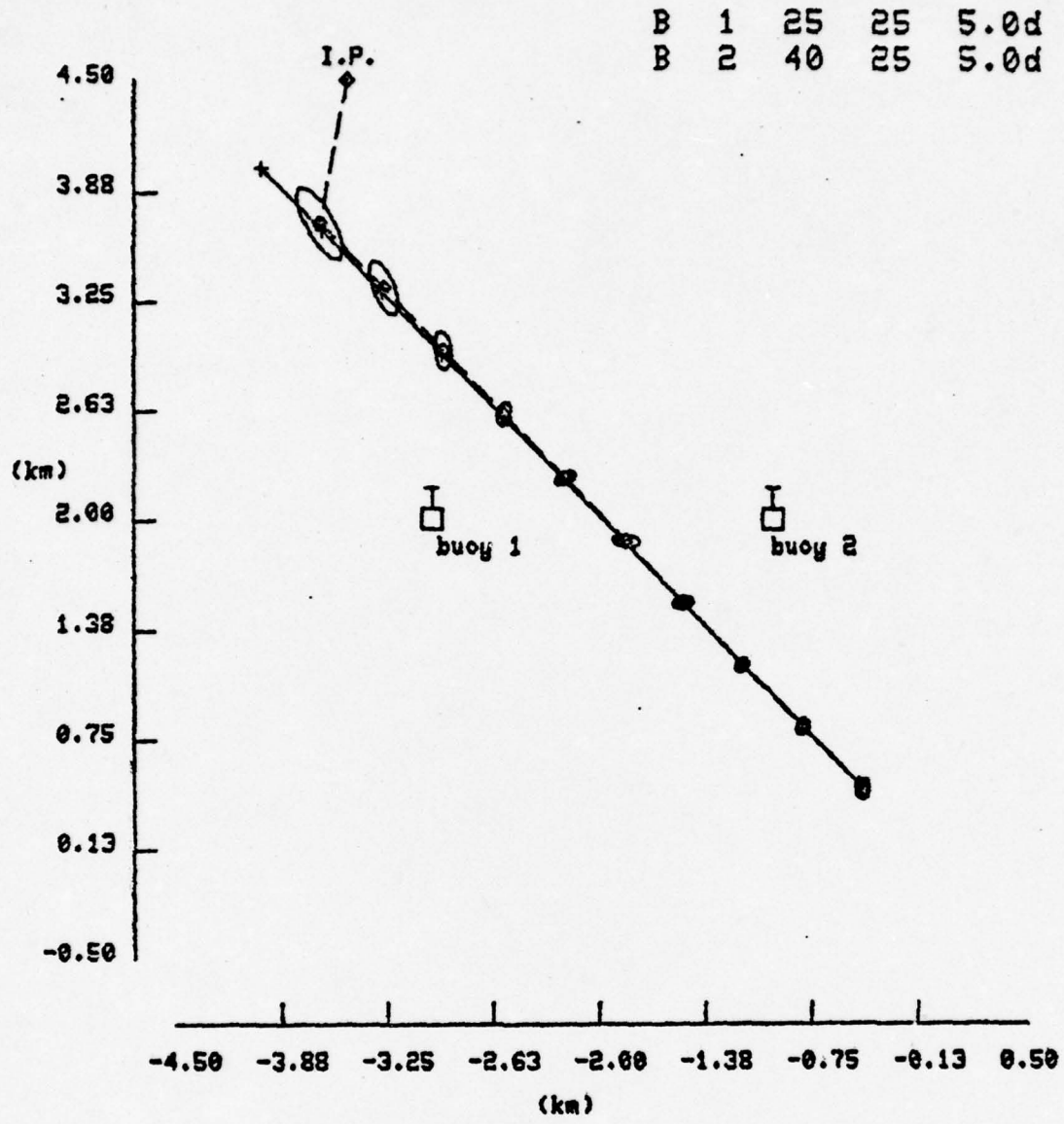

Figure 39 : True and estimated trajectories for a non-maneuvering target - Reduced period between consecutive measurements.

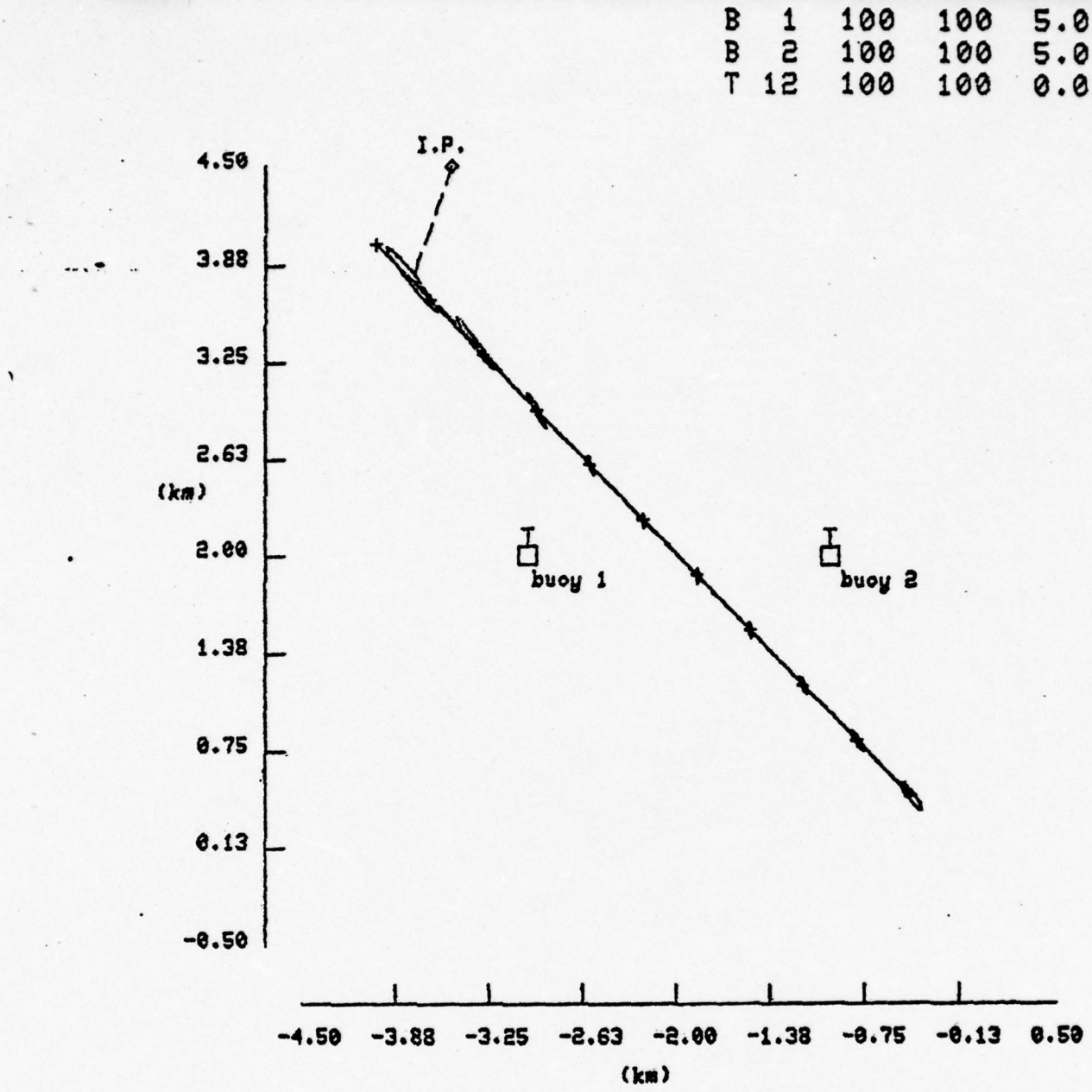

Figure 40 : True and estimated trajectories for a non-maneuvering target - Separate processing of bearing and time delay meas.

applied. The result is that the estimated path is very different from the true path of the target. About the same result is obtained when the buoy is placed on the other side of the track, i.e., a small delay to react to the maneuver followed by an over-correction.

In Figure 42 the frequency measurements were eliminated and only bearing indications were processed to generate an estimated track very close to the one of Figure 41. The alignment of the ellipses with the measurement lines is again very clear and may suggest where two buoys should be placed in order to improve the tracking.

b. Two Buoys in Action at a Time

Figure 43 shows what can be obtained by processing the measurements provided by two buoys. The range of the buoys was adjusted so that both are in contact with the target during all the path shown. Both are Difar buoys and provide bearing and frequency measurements with a period of 100 seconds, which are processed simultaneously by the filter.

In Figure 44 the measurements were processed separately and a small improvement in the tracking was obtained at the end of the path, although during the maneuver the simultaneous processing worked better. It was observed in other simulations that the degree of improvement obtained by partitioning the bearing and the time delay measurements is dependent on the maneuver of the target and

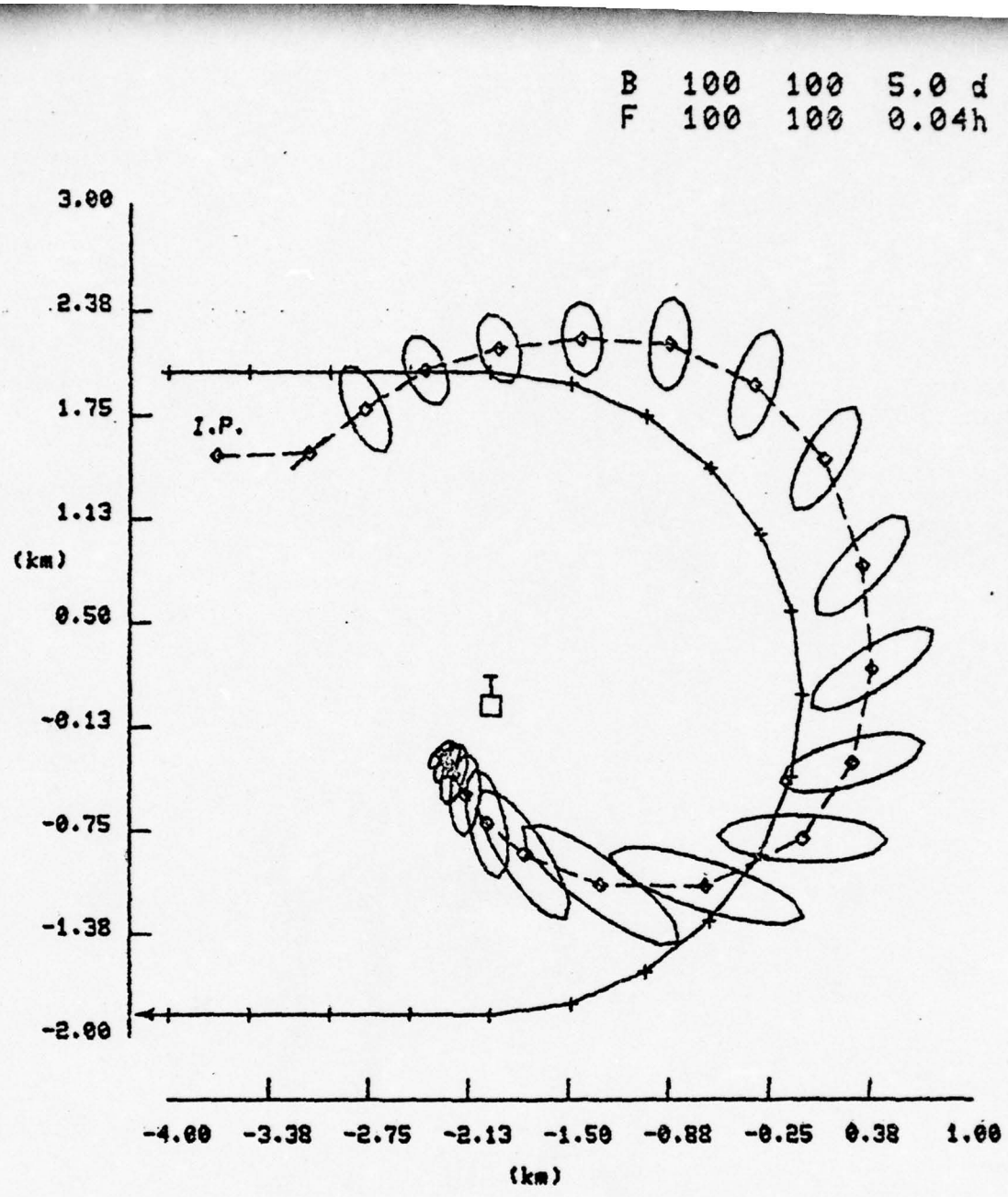

Figure 41 : True and estimated trajectories for a maneuvering target - Simultaneous frequency and bearing measurements.

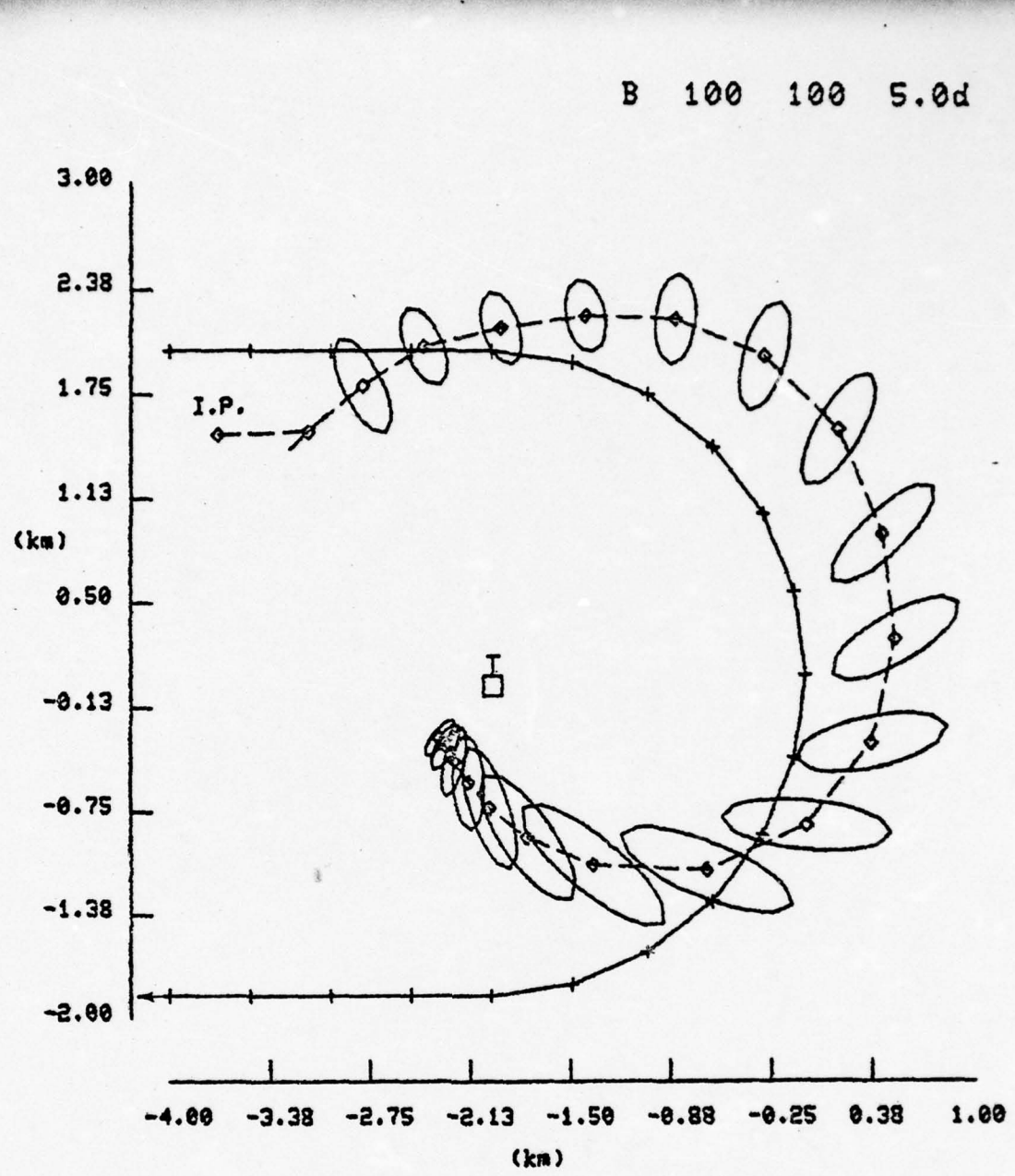

Figure 42 : True and estimated trajectories for a maneuvering target - Bearing measurements only.

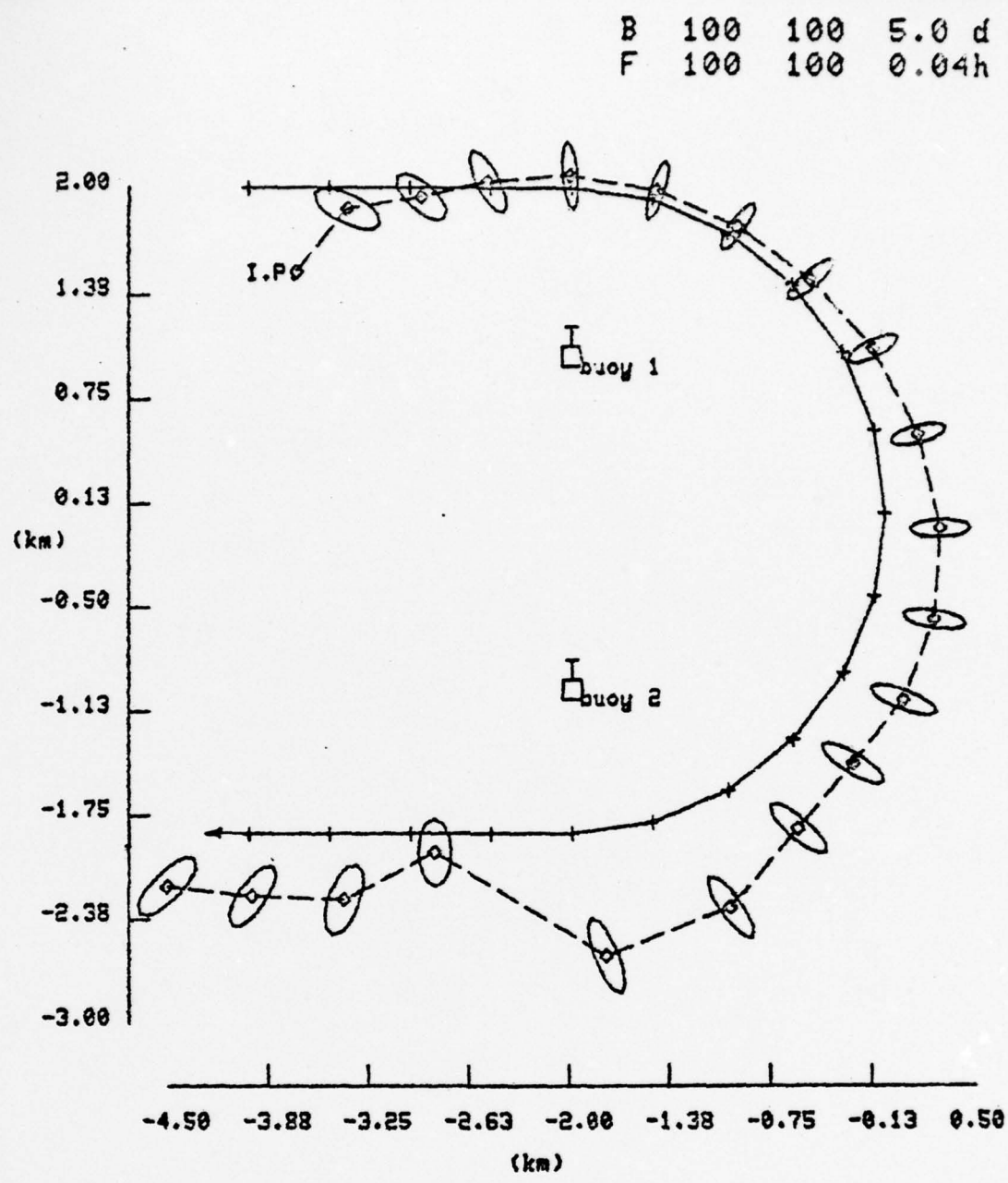

Figure 43 : True and estimated trajectories for a maneuvering target - Simultaneous processing of frequency and bearing measurements.

the relative position of the buoys. The worst situation is when the target maneuvers toward the buoys. This happens when the partial estimates are worse than the predicted values and occur sometimes during fast maneuvers, or slow maneuvers with long intervals between consecutive measurements.

In Figure 45 the low-noise time delay measurement was added and, instead of reducing the errors, the tracking became worse. The direction of the ellipses is clearly along the tangent to the hyperbolas of position, indicating that the filter is uncertain about the range of the target to the buoys during all the maneuver. This characteristic of the measurement lines in this case, and the fact that the target is modelled by the filter as following basically a straight path, explain the form of the estimated track. As soon as the target reassumes a constant path the filter starts to recover.

In Figures 46 and 47 the iterative techniques described in Section IV,B,2,b were applied to the frequency and time delay measurements. In Figure 46 only one iteration was executed; in Figure 47 the iterated formulas were applied three times. The improvement is clearly seen by comparing with Figure 45.

As with the partitioning of the measurements, it was observed from other similar simulations that the application of the iterative techniques does not always provide

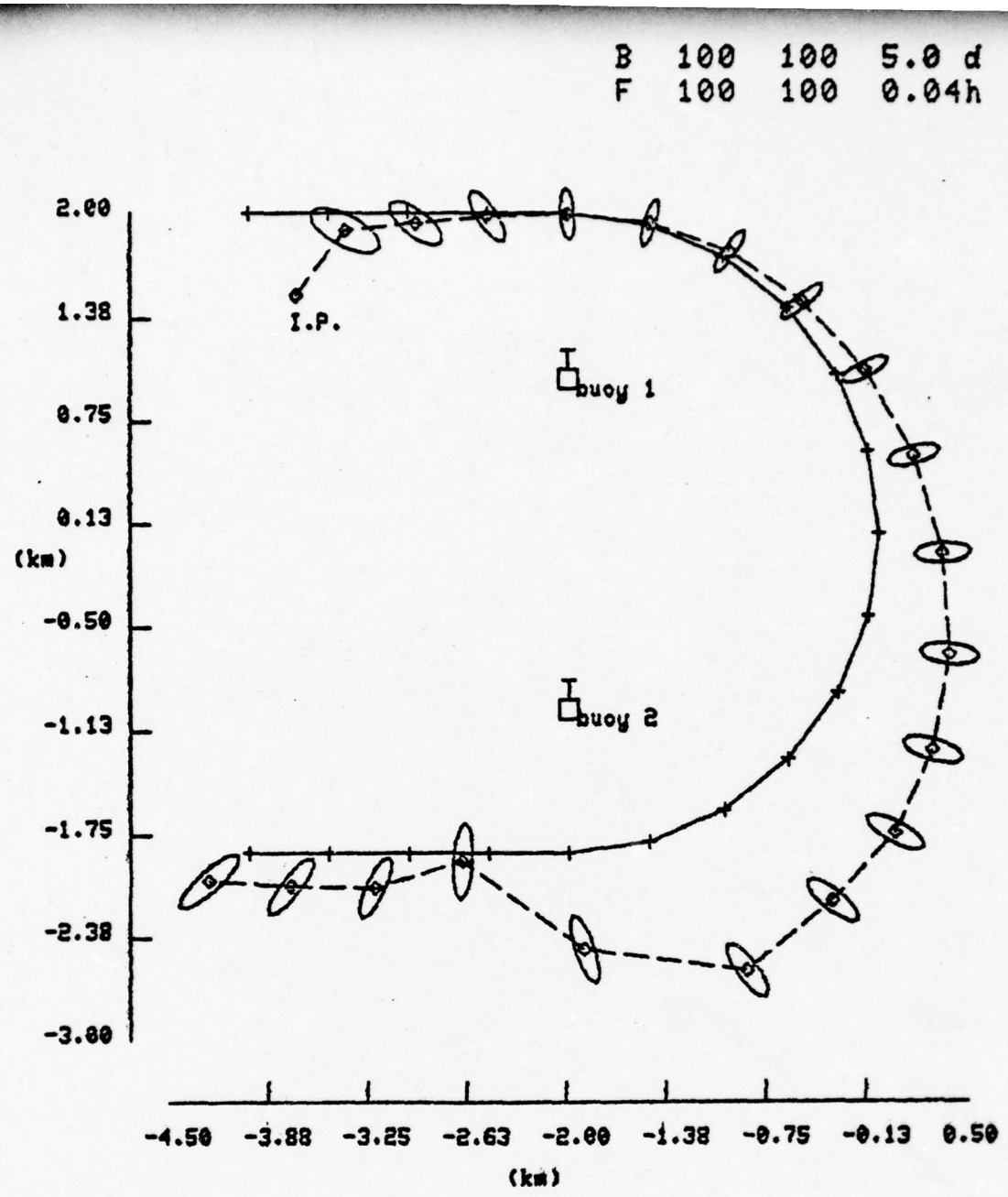

Figure 44 : True and estimated trajectories for a maneuvering target - Separate processing of frequency and bearing measurements.

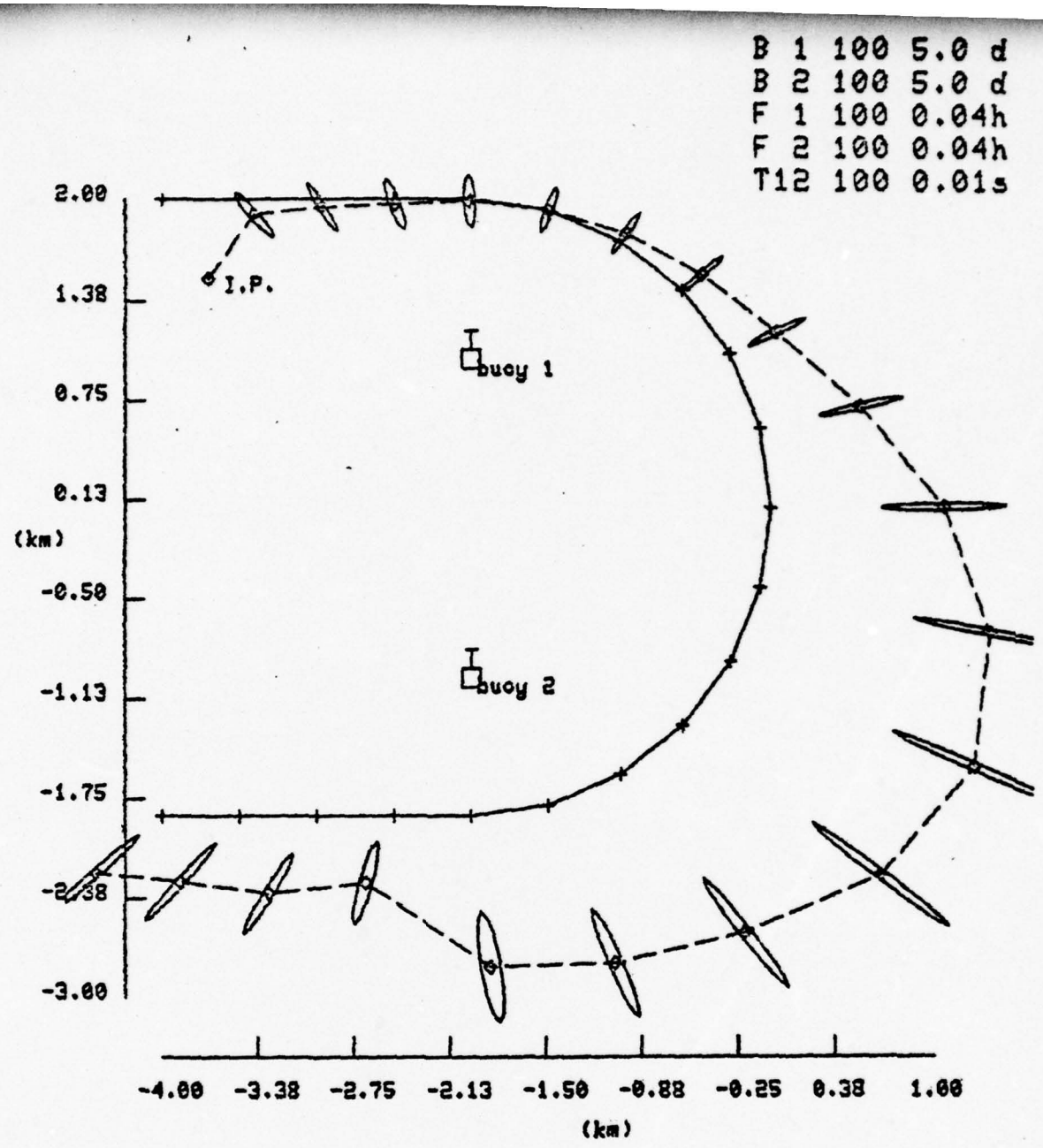

Figure 45 : True and estimated trajectories for a maneuvering target - Separate processing of bearing, frequency and time delay measurements.

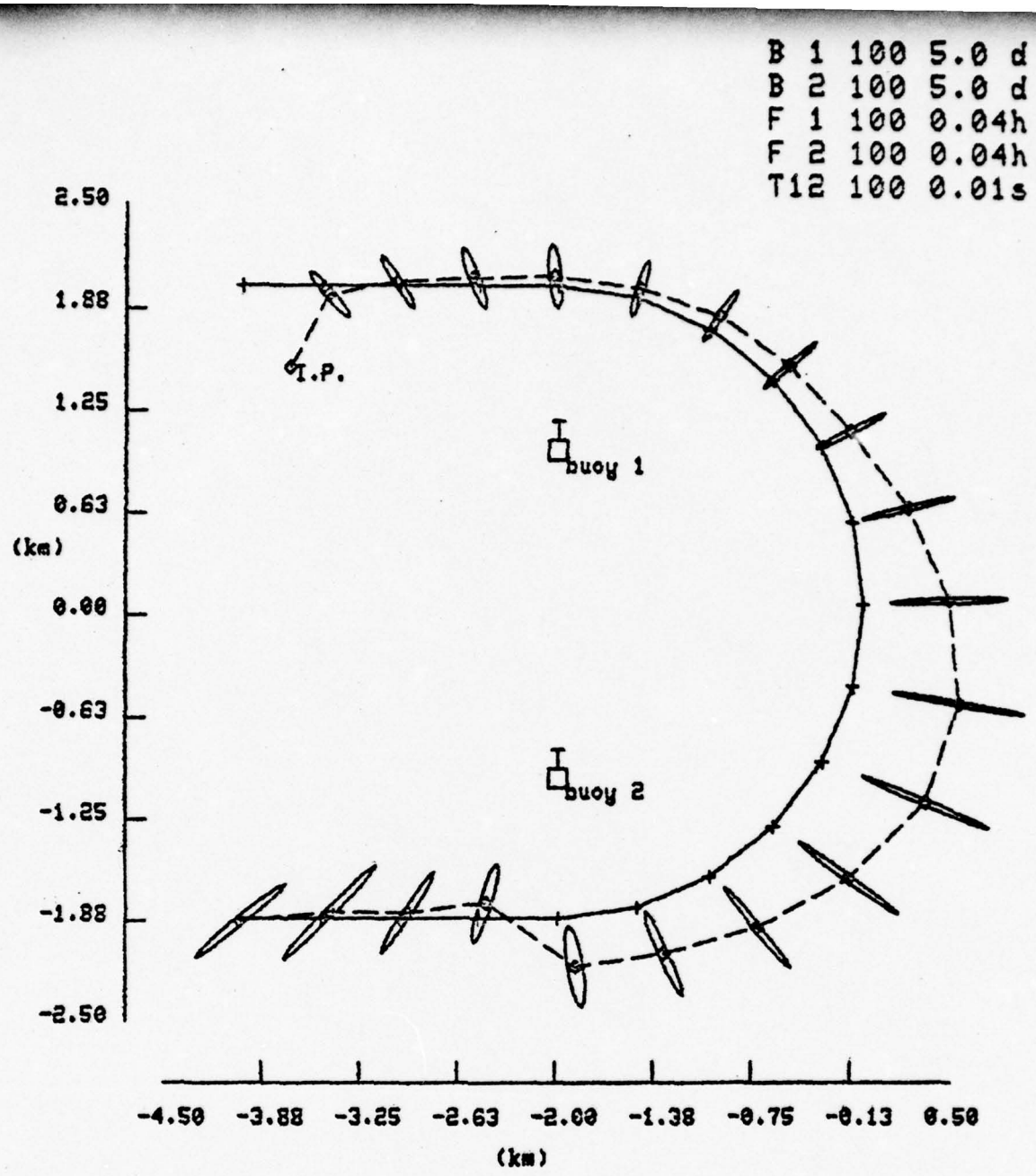

Figure 46 : True and estimated trajectories for a maneuvering target - One iteration on frequency and time delay measurements.

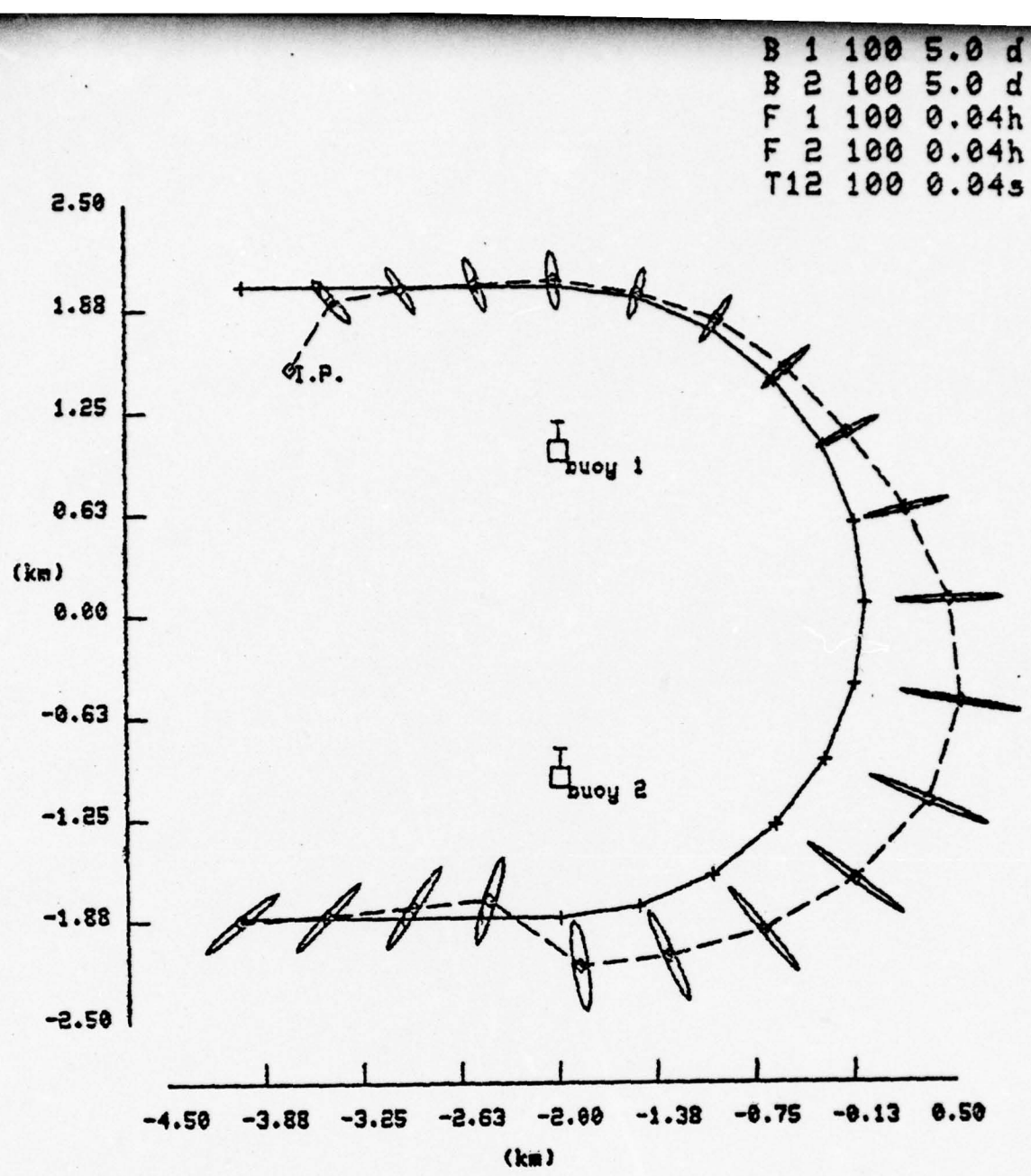

Figure 47 : True and estimated trajectories for a maneuvering target - Three iterations on frequency and time delay measurements

better tracking. It depends on the type and direction of the maneuvers, the position of the buoys and, consequently, on the position of the measurement lines.

In the case of the non-maneuvering target the use of two buoys instead of only one was almost always sufficient to provide good tracking. If for the maneuvering target one uses three buoys judiciously positioned, instead of only one or two, one can also obtain good tracking as clearly shown in Figure 48.

C. SUMMARY

Below are listed the most important facts observed from the simulations:

--- The tendency of the error ellipses to align with the measurement lines was observed in Section IV,B. The simulations show that the sample covariance ellipses also follow this trend.

--- The tendency of the error ellipses to align with the measurement lines can be of great help in the practical solution of filtering situations. If, for example, the error ellipse is very thin, i.e., have a very high ratio a/b, then the best measurement to process is the one whose measurement line is approximately perpendicular to the major axis of the ellipse. In the tracking problem this can be obtained by a bearing measurement from a buoy placed along the perpendicu-

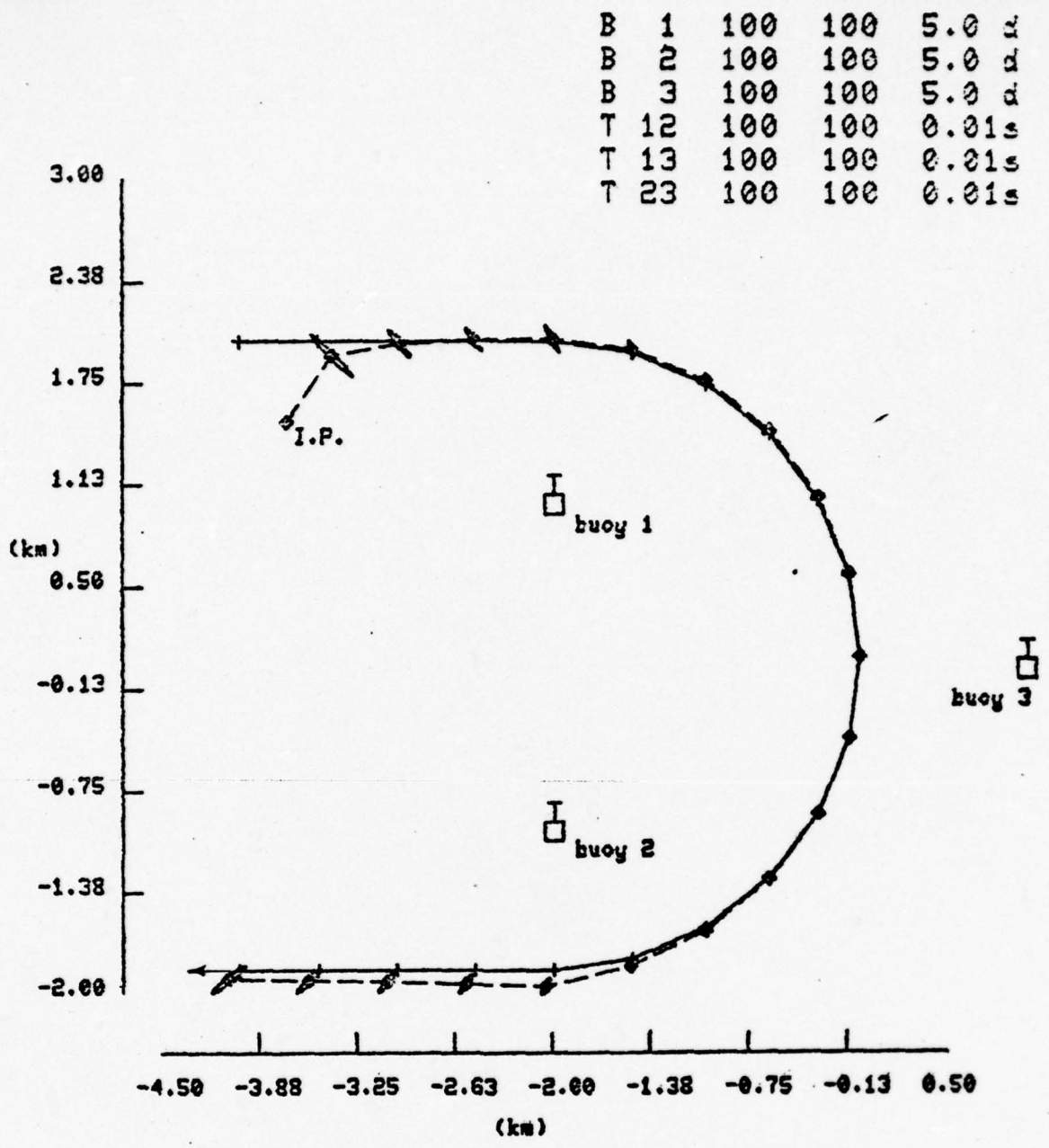

Figure 48 : True and estimated trajectories for a maneuvering target - The influence of a third buoy.

lar to the major axis of the ellipse, or by a time delay measurement from two buoys placed along the direction of the major axis of the ellipse.

--- The frequency measurement have a very small effect on the tracking accuracy.

--- The use of frequency difference or frequency ratio measurements improve computing efficiency (by eliminating the need for having the rest frequency as a state in the filter model) without noticeable effect on accuracy.

--- The partitioning of the measurements improves computing efficiency, may provide better tracking accuracy and allows the processing of measurements as they occur, and thus is of great practical importance.

--- For low noise measurements the iterative techniques, although requiring an increase in computing, are capable of providing better tracking for maneuvering targets.

--- Tracking with only one buoy is acceptable only for non-maneuvering targets.

--- The relative position of the buoys is one of the most important factors which influences the quality of the tracking.

VI. CONCLUSIONS

A. SUMMARY OF RESULTS

The optimal estimation of characteristics and/or parameters of a certain class of nonlinear, dynamic, stochastic systems has been studied in a probabilistic environment using Bayes formulation concepts. Approximate solutions and filtering algorithms were generated and, among them, the known Extended Kalman Filter equations and higher order filtering equations have been obtained through this method.

The problem of tracking submarine targets using special passive sonobuoys was modelled and with this model extensive simulations were executed to allow the study of the problem in detail.

Most of the results indicate that the frequency measurements have minimal effect on the filtering process. The small contribution to range information that they do provide, when associated with bearing measurements, can normally be obtained otherwise by judicious placement of subsequent buoys.

The utilization of other types of measurements such as the frequency difference, the frequency ratio and the time delay measurements, proves to be a great help in improving computing efficiency by eliminating the rest frequency as a

necessary state, and thus reducing the dimensionality by one. Also, especially with the time delay measurement, a great improvement in tracking accuracy is possible.

The concept of partitioning the measurements and processing them separately, even if they occur simultaneously, is shown to bring advantages in computing efficiency and also, for nonlinear measurements, in tracking accuracy. This concept is of great practical importance, for, in situations where the measurements are sporadically and non-periodically received it is most important to be able to process the measurements as they naturally occur.

The graphical interpretation of the action of Kalman filters, developed in this work, provides insight into the importance of each variable of the problem in the filtering process. The direction and magnitude of the correction which is applied to the predicted values to generate the new estimate values can now be anticipated as a function of the measurement.

Nonlinearity errors have been graphically presented and iterative techniques, including the known Iterated Extended Kalman Filter equations, have been suggested to counteract their disruptive effect. The application of these techniques to the tracking problem shows that improvement in tracking accuracy is possible.

The graphical interpretation also indicates the very practical conclusion that the error ellipses tend to align

with the measurement lines, as defined in Chapter IV. This provides guidance for optimal positioning of the buoys and the types of measurements to process. This observation is reinforced by the simulation results of Chapter V.

B. SUGGESTIONS FOR FUTURE RESEARCH

The concept of partitioning the measurements allows one to process the measurements separately and opens some questions for future research, such as, in which order should nonlinear measurements be processed to obtain maximum efficiency?

The graphical interpretation of the filtering process allows anticipation of the direction and magnitude of the corrections which are then applied to predictions to generate new estimates. This situation suggests future research in the determination of the optimum characteristics of the measurement functions which in turn can determine the optimum positions and characteristics of sensors.

The expansion of the model to include accelerations should be considered if maneuvering targets have to be tracked efficiently and the increase in computing power can be obtained. Consideration of the depth of the target and the inclusion of uncertainty about the position of the buoys are additional ways to extend this study.

The model and simulation implemented herein, without benefit of classified information, is very flexible, but many idealizing assumptions have been made. Thus, a natural extension of this work is to apply the algorithms and concepts developed to a real problem using actual sensor data.

APPENDIX A : PROBABILITY RELATIONS

The relation

$$\underline{x} = \underline{a} + G.\underline{v} \qquad (A.1)$$

is given where $\underline{x}$ and $\underline{v}$ are random vectors of dimensions n and q, respectively, $\underline{a}$ is a n-dimensional deterministic vector and G is a (nxq) matrix of deterministic coefficients.

The joint density $p_v(\underline{v})$ is given and the joint density $p_x(\underline{x})$ is wanted.

Case (i) - If $n = q$ and G^{-1} exists, the solution is given by [13],

$$\underline{v} = G^{-1}[\underline{x} - \underline{a}] = \underline{f}(\underline{x}) \qquad (A.2)$$

and

$$p_x(\underline{x}) = \left|\det\left[\frac{\partial}{\partial \underline{x}}\underline{f}\right]\right| \cdot p_v(\underline{f}(\underline{x})) \qquad (A.3)$$

Case (ii) - If $n < q$ one could add dummy variables

$$x_{n+1} = v_{n+1},\ x_{n+2} = v_{n+2},\ \ldots,\ x_q = v_q$$

and create

$$\underline{x}' = \underline{a}' + G'.\underline{v}$$

where

$$\underline{x}' = \begin{bmatrix} \underline{x} \\ \hline x_{n+1} \\ \vdots \\ x_q \end{bmatrix} \qquad \underline{a}' = \begin{bmatrix} \underline{a} \\ \hline \underline{0} \end{bmatrix}$$

$$G' = \begin{bmatrix} & G & \\ - & - & - \\ \underline{0} & | & \underline{I} \end{bmatrix}$$

Now, if G'^{-1} exists,

$$\underline{v} = G'^{-1} [\underline{x}' - \underline{a}'] = \underline{f}(\underline{x}') \qquad (A.4)$$

From Case (i), the solution is

$$p_{x'}(\underline{x}') = \left| \det \left[\frac{\partial}{\partial \underline{x}'} \underline{f} \right] \right| \cdot p_v (\underline{f}(\underline{x}')) \qquad (A.5)$$

and

$$p_x (\underline{x}) = \int p_{x'}(\underline{x}') . dx_{n+1} . dx_{n+2} \cdots dx_q \qquad (A.6)$$

Case (iii) - If $n > q$ the following development applies.

Let

$$\underline{x} = \begin{bmatrix} x_1 \\ x_2 \\ \cdot \\ \hline x_{q+1} \\ \cdot \\ x_n \end{bmatrix} \begin{bmatrix} \underline{x}' \\ \hline x_{q+1} \\ \cdot \\ x_n \end{bmatrix} \quad , \qquad \underline{a} = \begin{bmatrix} \underline{a}' \\ \hline a_{q+1} \\ \cdot \\ a_n \end{bmatrix}$$

$$G = \begin{bmatrix} G' \\ - - - - - - - - - \\ g_{q+1,1} \cdots \quad \cdots \; g_{q+1,q} \\ \cdots \cdots \quad \cdots \; \cdots \\ g_{n,1} \cdots \quad \cdots \; g_{n,q} \end{bmatrix} \begin{bmatrix} G' \\ - - - \\ \underline{g}_{q+1} \\ \cdots \\ \underline{g}_n \end{bmatrix}$$

From (A.1), one also has that

$$\underline{x}' = \underline{a}' + G' \cdot \underline{v}$$

and then, if G'^{-1} exists,

$$\underline{v} = G'^{-1} [\underline{x}' - \underline{a}'] = \underline{f}(\underline{x}') \tag{A.7}$$

From Case (i) one then has

$$p_{x'}(x_1, x_2, \ldots, x_q) = \left| \det \left[\frac{\partial}{\partial \underline{x}'} \underline{f} \right] \right| \cdot p_v(\underline{f}(\underline{x}')) \tag{A.8}$$

Now consider the variable x_{q+1}. Given (A.7),

$$p(x_{q+1} | x_1, x_2, \ldots, x_q) = p(x_{q+1} | v_1, v_2, \ldots, v_q)$$

but

$$x_{q+1} = a_{q+1} + g_{q+1,1} v_1 + g_{q+1,2} v_2 + \ldots + g_{q+1,q} v_q =$$

$$= a_{q+1} + \underline{g}_{q+1} \cdot \underline{v}$$

or

$$\underline{x}_{q+1} = a_{q+1} + \underline{g}_{q+1} \cdot \underline{f}(\underline{x}') = l_{q+1} \qquad (A.9)$$

From (A.9) comes

$$p(x_{q+1} | x_1, x_2, \ldots, x_q) = \delta(x_{q+1} - l_{q+1})$$

and

$$p(x_1, x_2, \ldots, x_{q+1}) = \delta(x_{q+1} - l_{q+1}) \cdot p_{x'}(x_1, x_2, \ldots, x_q)$$

Doing the same thing for $x_{q+2}, \ldots, x_n$, one finally gets

$$p_x(\underline{x}) = \prod_{i=q+1}^{n} \delta(x_i - l_i) \cdot \left| \det\left[\frac{\partial f}{\partial x'}\right] \right| \cdot p_v(\underline{f}(\underline{x}')) \qquad (A.10)$$

For the special case of $q = 1$, the vectors $\underline{x}'$, $\underline{a}'$ and $\underline{g}'$ become scalars and the above equations lead to

$$\underline{f}(\underline{x}') = f(x_1) = (x_1 - a_1) / g_1$$

$$\frac{\partial}{\partial x_1} f = 1 / g_1 \quad , \qquad l_r = a_r + (x_1 - a_1) g_r / g_1$$

and Equation (A.10) becomes

$$p_x(\underline{x}) = \prod_{i=2}^{n} \delta(x_i - l_i) \cdot \left| 1/g_1 \right| \cdot p_v((x_1 - a_1)/g_1) \qquad (A.11)$$

Another similar formula can be obtained for this special $q = 1$ situation. The matrix G in (A.1) is now a n-dimensional vector and, if one breaks (A.1) into its n

individual scalar equations one can obtain

$$p(x_i|v) = \delta(x_i - a_i - g_i v)$$

Also note that

$$p(x_i|x_j,v) = p(x_i|v) \qquad i \neq j$$

and

$$p(x_i,x_j|v) = p(x_i|x_j,v).p(x_j|v) = p(x_i|v).p(x_j|v)$$

And from these relations,

$$p_{x/v}(x|v) = \prod_{i=1}^{n} p(x|v) = \prod_{i=1}^{n} \delta(x_i - a_i - g_i v)$$

and finally,

$$p_x(\underline{x}) = \int \prod_{i=1}^{n} \delta(x_i - a_i - g_i v).dv \qquad (A.12)$$

APPENDIX B : COMPONENTS OF COVARIANCE MATRIX

For a single measurement of the form $z = H.\underline{x} + v$, the observation matrix becomes the vector

$$H = [h_1 \quad h_2 \quad \cdots \quad h_n]$$

where n is the dimension of the system.

The Kalman gain is given by

$$G = P'H^T[HP'H^T + r^2] \tag{B.1}$$

where P' is used to represent the prediction error covariance matrix, which is symmetric, and r is the standard deviation of the measurement error.

Since H is in this case a vector, the product $HP'H^T$ will be a scalar.

Let $$c = [HP'H^T + r^2]^{-1} \tag{B.2}$$

The vector P'H can be shown to be

$$P'H^T = \begin{bmatrix} \sum_{j=1}^{n} p'_{1j} h_j \\ \sum_{j=1}^{n} p'_{2j} h_j \\ \vdots \\ \sum_{j=1}^{n} p'_{nj} h_j \end{bmatrix} \tag{B.3}$$

and thus the constant c is given by

$$c = 1 \Big/ \left[\sum_{i=1}^{n} \sum_{j=1}^{n} p'_{ij} h_i h_j + r^2 \right] \qquad (B.4)$$

From (B.1) one now sees that the Kalman gain is a vector whose components are the components of $P'H^T$ multiplied by the constant c, i.e. the components of the gain vector are

$$g_g = \sum_{j=1}^{n} p'_{mj} h_j \Big/ \left[\sum_{i=1}^{n} \sum_{j=1}^{n} p'_{ij} h_i h_j + r^2 \right] \qquad (B.5)$$

The estimation error covariance matrix is computed from the equation

$$P = [I - G.H].P' = P' + \Delta P' \qquad (B.6)$$

where

$$\Delta P' = - GHP' = - cP'H\, HP' \qquad (B.7)$$

Let's define

$$a_i = \sum_{j=1}^{n} p'_{ij} h_j = p'_{i1} h_1 + p'_{i2} h_2 + \ldots + p'_{in} h_n \qquad (B.8)$$

Then, from (B.3),

$$HP' = [P'H^T]^T = [a_1 \;\; a_2 \;\; \ldots \;\; a_n] \qquad (B.9)$$

and from (B.4),

$$c = \left[\sum_{i=1}^{n} h_i a_i + r^2 \right]^{-1} \qquad (B.10)$$

From (B.7) the increment $\Delta P'$ to the error covariance matrix is then

$$\Delta P' = - c \cdot \begin{bmatrix} a_1^2 & a_1 a_2 & a_1 a_3 & \cdots & a_1 a_n \\ a_1 a_2 & a_2^2 & a_2 a_3 & \cdots & a_2 a_n \\ \vdots & \vdots & \vdots & \vdots & \vdots \\ a_1 a_n & a_2 a_n & a_3 a_n & \cdots & a_n^2 \end{bmatrix} \tag{B.11}$$

The individual terms of the estimation error covariance matrix will be given by

$$p_{ij} = p_{ji} = p'_{ij} - c \cdot a_i \cdot a_j = p'_{ij} - a_i \cdot a_j \Big/ \left(\sum_{i=1}^{n} \sum_{j=1}^{n} p'_{ij} h_i h_j + r^2 \right)$$

or

$$p_{ij} = \frac{\sum_{k=1}^{n} \sum_{m=1}^{n} h_k h_m (p'_{ij} p'_k - p'_{ik} p'_{jm}) + p'_{ij} r^2}{\sum_{k=1}^{n} \sum_{m=1}^{n} h_k h_m p'_k + r^2} \tag{B.12}$$

APPENDIX C : CHARACTERISTICS OF MEASUREMENT FUNCTIONS

In Figure C-1 some curves of the form $f(\underline{x})$ = constant are shown, where $f(\underline{x})$ is assumed given. The vector $\underline{x}^a$ and a constant value d are also given. The vector $\underline{x}^b$ is defined by the equation

$$\underline{x}^b = \underline{x}^a + \frac{d}{|\underline{h}|} \cdot \frac{\underline{h}}{|\underline{h}|} \qquad (C-1)$$

or

$$\underline{x}^b = \underline{x}^a + \underline{h} \cdot [d/|\underline{h}|^2] \qquad (C-2)$$

where $\underline{h}$ is the gradient of $f(\underline{x})$ with respect to $\underline{x}$ taken at point $(\underline{x}^a, \underline{x}^a)$, and $\underline{h}/|\underline{h}|$ is a unit vector along $\underline{h}$.

$$\underline{h}_1 = h_1 \underline{e}_1 + h_2 \underline{e}_2 \qquad |h| = [h_1^2 + h_2^2]^{1/2}$$

$$h_1 = \frac{\partial}{\partial x_1} f(\underline{x}^a) \qquad h_2 = \frac{\partial}{\partial x_2} f(\underline{x}^a)$$

To determine the location of $\underline{x}^b$ numerical data is required. However, it is possible to determine qualitatively whether $\underline{x}^b$ ends on the curve $f(\underline{x}^a) + d$, or on one side or the other of this curve. This is done in the following paragraphs for three special functions.

Case (i) - For linear $f(\underline{x})$, $\underline{x}^b$ always ends on the curve $f(\underline{x}) = f(\underline{x}^a) + d$, as shown below

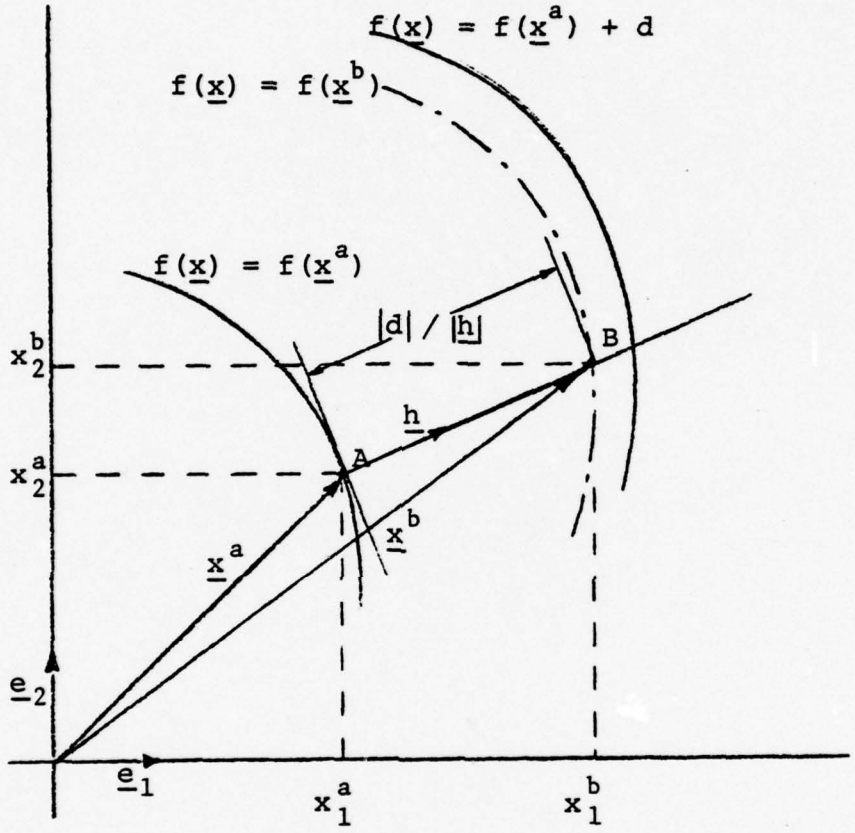

Figure C - 1 : Problem geometry.

Let $f(\underline{x}) = px_1 + qx_2$

then $h_1 = p$, $h_2 = q$ and $|h|^2 = p^2 + q^2$

From Equation (C-2),

$$\underline{x}^b = \underline{x}^a + (p\underline{e}_i + q\underline{e}_2).d/(p^2 + q^2)$$

so

$$x_1^b = x_1^a + pd/(p^2 + q^2)$$
$$x_2^b = x_2^a + qd/(p^2 + q^2)$$

Now,

$$f(\underline{x}^b) = px_1^b + qx_2^b = px_1^a + p^2 d/(p^2 + q^2) +$$
$$+ qx_2^a + q^2 d/(p^2 + q^2) =$$
$$= px_1^a + qx_1^a + d = f(\underline{x}^a) + d$$

Case (ii) - For $f(\underline{x})$ defined as below, $\underline{x}^b$ always ends on top of $f(\underline{x}^a) + d$, as in the Case (i).

$$f(\underline{x}) = [(x_1 - p)^2 + (x_2 - q)^2]^{1/2}$$

Now,

$$h_1 = (x_1^a - p)/m \qquad h_2 = (x_2^a - q)/m$$

where

$$m = [(x_1^a - p)^2 + (x_2^a - q)^2]^{1/2} = f(\underline{x}^a)$$

and

$$|h|^2 = h_1^2 + h_2^2 = 1$$

From (C-2),

$$\underline{x}^b = \underline{x}^a + \underline{h}.d = \underline{x}^a + [(x_1^a - p)\underline{e}_1 + (x_2^a - q)\underline{e}_2].d/m$$

so

$$x_1^b = x_1^a + h_1 d = x_1^a + (x_1^a - p)d/m$$
$$x_2^b = x_2^a + h_2 d = x_2^a + (x_2^a - q)d/m$$

Now,

$$f(\underline{x}^b) = [(x_1^a + h_1 d - p)^2 + (x_2^a + h_2 d - q)^2]^{1/2} =$$

$$= [(x_1^a - p)^2 + 2h_1 d(x_1^a - p) + h_1^2 d^2 +$$

$$+ (x_2^a - q)^2 + 2h_2 d(x_2^a - q) + h_2^2 d^2]^{1/2}$$

Using the values of h_1 and h_2,

$$f(\underline{x}^b) = [(x_1^a - p)^2 + (x_2^a - q)^2 + d^2 +$$

$$+ 2d[(x_1^a - p)/m + (x_2^a - q)/m]]^{1/2} =$$

$$= [f(\underline{x}^a)^2 + 2d.f(\underline{x}^a) + d^2]^{1/2} =$$

$$= [(f(\underline{x}^a) + d)^2]^{1/2} =$$

$$= f(\underline{x}^a) + d$$

Case (iii) - For f(x) as defined below and shown in Figure C-2, $\underline{x}^b$ always ends before the curve $f(\underline{x}^a) + d$, for $|d| < \pi$.

$$f(\underline{x}) = \arctan[(x_2 - q)/(x_1 - p)]$$

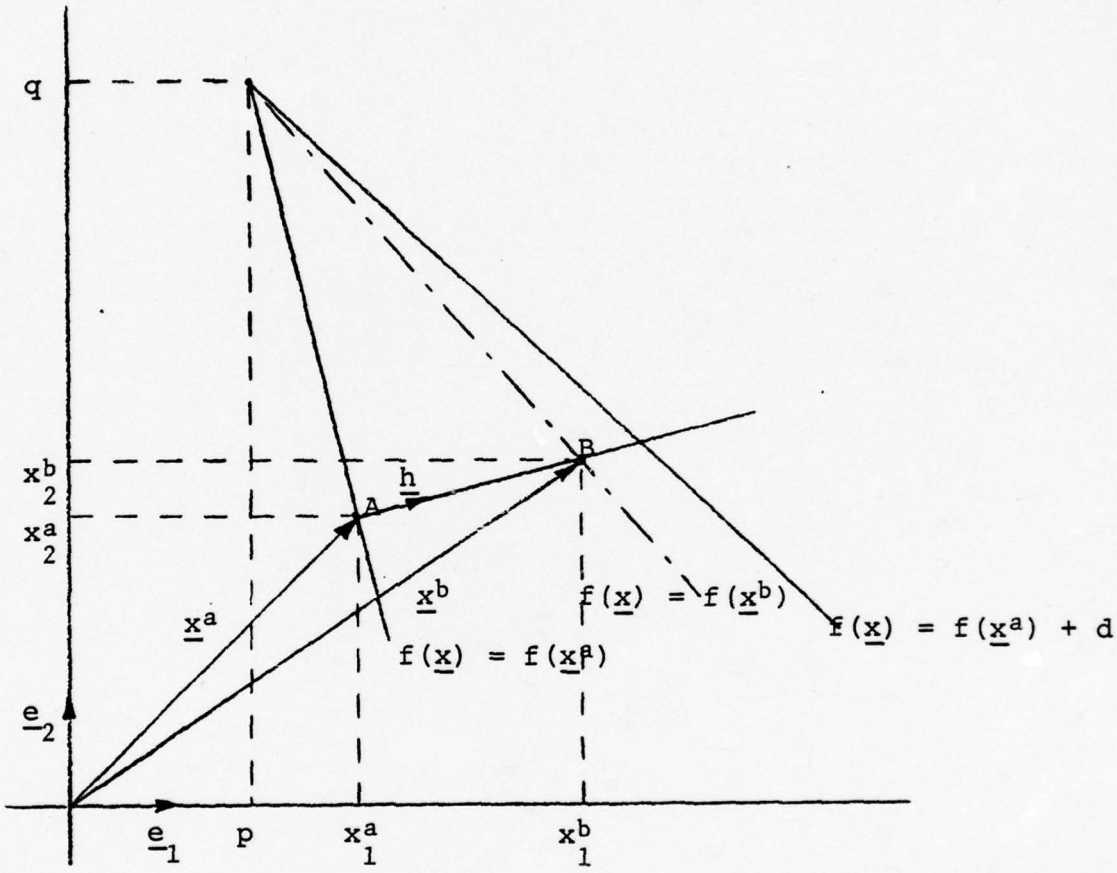

Figure C - 2 : Geometry for Case (iii).

The case $|d| > \pi/2$ is not of interest since the lines h and $f(\underline{x}) = f(\underline{x}^a) + d$ are diverging. For $|d| < \pi/2$,

$$h_1 = -(x_2^a - q)/n \qquad h_2 = (x_1^a - p)/n$$

where

$$n = (x_1^a - p)^2 + (x_2^a - q)^2$$

and

$$|h|^2 = h_1^2 + h_2^2 = 1/n$$

From Equation (C-2),

$$\underline{x}^b = \underline{x}^a + d.[-(x_2^a - q)\underline{e}_1 + (x_1^a - p)\underline{e}_2]$$

so,

$$x_1^b = x_1^a - (x_2^a - q)d$$
$$x_2^b = x_2^a + (x_1^a - p)d$$

Now,

$$f(\underline{x}^b) = \arctan[(x_2^b - q)/(x_1^b - p)] =$$

$$= \arctan[(x_2^a - q) + (x_1^a - p)d]/$$

$$[(x_1^a - p) - (x_2^a - q)d]$$

or

$$f(\underline{x}^b) = \arctan[(s + d)/(1 - sd)]$$

where

$$s = (x_2^a - q)/(x_1^a - p) = \tan[f(\underline{x}^a)]$$

so,

$$\tan[f(\underline{x}^b)] = (s + d)/(1 - sd) =$$

$$= [\tan[f(\underline{x}^a)] + d] \; / \; [1 - d.\tan[f(\underline{x}^a)]] =$$

$$= \tan[f(\underline{x}^a) + \arctan(d)]$$

or

$$f(\underline{x}^b) = f(\underline{x}^a) + \arctan(d)$$

Since $|d| < \pi/2$, then $\arctan(d) < d$ and $\underline{x}^b$ will not reach the line $f(\underline{x}^a) + d$.

APPENDIX D : ANALYTICAL EVALUATION OF KALMAN FILTERS

After the design of a filter an analysis phase is necessary to verify its behavior in various representative situations.

A "filtering situation" is considered here to be completely specified by:

--- the true parameters and initial conditions of the system which generate a unique track $x(0), x(1), \ldots, x(t)$.

--- the true parameters of the sensors and their measurement schedules.

--- the parameters and initial conditions assumed by the filter for the system and for the sensors.

The approach normally used to determine filter behavior is to simulate the desired situation and execute hundreds or thousands of Monte Carlo runs and compute sample statistics. The most useful results of this process are:

$\underline{a}^m(k)$ - the sample mean of the estimated state vector at time t_k obtained from m Monte Carlo runs.

$\underline{e}^m(k) = \underline{a}^m(k) - \underline{x}(k)$ - the sample mean of the estimated error vector at time t_k.

$\underline{b}^m(k)$ - the sample second central moment of the state (or error) estimates about $\underline{a}^m(k)$, at t_k.

The objective of this section is to study the possibility of obtaining values of $\bar{a}(k)$, $\bar{e}(k)$ and $\bar{b}(k)$, which are approximately the values of $a^m(k)$, $e^m(k)$ and $b^m(k)$ when m is very large, without the use of the time consuming Monte Carlo operations.

1 --- Theoretical Solution

Once a "filtering situation", as stated above, is defined, the operation of a Kalman Filter is described by the recursive equations below where only the dependence of each term on the previous estimates is stressed.

$$\hat{x}(k+1|k) = f(\hat{x}(k)) \qquad (D.1)$$

$$P(k+1|k) = \phi(\hat{x}(k)).P(k).\phi^T(\hat{x}(k)) + g(\hat{x}(k)).Q(k).g^T(\hat{x}(k)) \qquad (D.2)$$

$$G(\hat{x}(k+1|k),P(k+1|k)) = P(k+1|k).H^T(\hat{x}(k+1|k)).[H(\hat{x}(k+1|k)).P(k+1|k).H^T(\hat{x}(k+1|k)) + R(k)]^{-1} \qquad (D.3)$$

$$\hat{x}(k+1) = \hat{x}(k+1|k) + G(\hat{x}(k+1|k),P(k+1|k)).[h(x(k+1)) + v(k+1) - h(\hat{x}(k+1|k))] \qquad (D.4)$$

$$\underline{P}(k+1) = [I - G(\underline{\hat{x}}(k+1|k), P(k+1|k)).H(\underline{\hat{x}}(k+1|k))].P(k+1|k) \qquad (D.5)$$

In this case these equations describe a deterministic process were it not for the random measurement noise $\underline{v}(k+1)$, the only random input to the "filter dynamics" since a unique track is considered. The initial condition of the filter, $\underline{x}(0)$ and $P(0)$ are also deterministically given.

Equations (D.4) and (D.5) can be rewritten as

$$\underline{\hat{x}}(k+1) = \phi(\underline{\hat{x}}(k+1|k), P(k+1|k)) + \Psi(\underline{\hat{x}}(k+1|k), P(k+1|k)).\underline{v}(k+1)$$

$$P(k+1) = \Gamma(\underline{\hat{x}}(k+1|k), P(k+1|k))$$

where ϕ, Ψ and Γ are generally nonlinear matrix functions of the variables indicated.

Considering (D.1) and (D.2) one can then write

$$\underline{\hat{x}}(k+1) = \underline{f}^*(\underline{\hat{x}}(k), P(k)) + \underline{g}^*(\underline{\hat{x}}(k), P(k)).\underline{v}(k+1) \qquad (D.6)$$

$$\underline{P}(k+1) = \underline{h}^*(\underline{\hat{x}}(k), P(k)) \qquad (D.7)$$

where $\underline{f}^*$, $\underline{g}^*$, $\underline{h}^*$ are also generally nonlinear matrix functions. From (D.6) and (D.7) one can clearly see now that, if $\underline{v}$ is a discrete white Gaussian noise process, the joint process $\{\underline{\hat{x}}, P\}$ is Markov.

If one considers a new vector $\underline{y}$ formed with the n elements of $\underline{\hat{x}}$ and the $n.(n+1)/2$ distinct elements of the (nxn)

symmetric matrix P, $\underline{y}$ is an [n.(n+3)/2]-dimensional process. Equations (D.6) and (D.7) can then be combined into

$$\underline{y}(k+1) = A(\underline{y}(k)) + B(\underline{y}(k)).\underline{v}(k+1) \qquad (D.8)$$

where A is a vector function and B a R to R^m matrix function, m = n.(n+3)/2.

The complete behavior of the filter can be described by the probability law of $\underline{y}$, which is obtained from

$$p(\underline{y}(k+1)) = \int p(\underline{y}(k+1)|\underline{y}(k)).p(\underline{y}(k)).d\underline{y}(k) \qquad (D.9)$$

and $p(\underline{y}(k+1)|\underline{y}(k))$ is obtained from $p(\underline{v}(k+1))$ and Equation (D.8) in the manner shown in Appendix A. The initial value $\underline{y}(0)$ is deterministic since it contains the initial condition of the filter which is given.

2 --- The Linear Case

For the special case of linear dynamics and observations, the solution can be obtained in a simpler way. In this case the functions ϕ, $\underline{g}$ and H are not functions of the state estimates and so neither is G.

Equations (D.1) - (D.5) can be grouped now into

$$\hat{\underline{x}}(k+1) = \phi(\hat{\underline{x}}(k+1|k), P(k+1,k)) + \Psi(P(k+1|k)).\underline{v}(k+1)$$

$$P(k+1) = \Gamma(P(k+1|k))$$

and finally, in a recursive way,

$$\underline{\hat{x}}(k+1) = \underline{f}^*(\underline{\hat{x}}(k),P(k)) + \underline{g}^*(P(k)).\underline{v}(k) \qquad (D.10)$$

$$\underline{P}(k+1) = \underline{h}^*(P(k)) \qquad (D.11)$$

From (D.11) it is clear that the estimation error covariance matrix is now a deterministic process and can be precomputed, together with the gains.

Equation (D.10) then becomes

$$\underline{\hat{x}}(k+1) = \underline{f}^*(\underline{\hat{x}}(k)) + \underline{g}^*(k+1).\underline{v}(k+1)$$

From (D.1) - (D.5) the values of $\underline{f}^*$ and $\underline{g}^*$ can be found to be, for this linear case,

$$\underline{\hat{x}}(k+1) = [I + G(k+1).H(k+1)].\phi(k).\underline{\hat{x}}(k) +$$

$$+ G(k+1).H(k+1).\underline{\bar{x}}(k+1) + G(k+1).\underline{v}(k+1)$$

or

$$\underline{\hat{x}}(k+1) = S(k+1).\underline{\hat{x}}(k) + F(k+1) + G(k+1).\underline{v}(k+1) \qquad (D.12)$$

where

$$\underline{S}(k) = [I + G(k).H(k)].\phi(k)$$

$$\underline{F}(k) = G(k).H(k).\underline{x}(k)$$

The sought after behavior of the filter can be described by the moments below, which agree with [12]

$$\bar{a}(k+1) = E[\hat{x}(k+1)] = S(k+1).E[\hat{x}(k)] + F(k+1) +$$

$$+ G(k+1).E[v(k+1)] \qquad (D.13)$$

$$\bar{e}(k+1) = \bar{a}(k+1) - x(k+1) = S(k+1).E[\hat{x}(k)] +$$

$$+ [I - G(k+1).H(k+1)].x(k+1) +$$

$$+ G(k+1).E[v(k+1)] =$$

$$= S(k+1).\bar{e}(k) + D(k+1).x(k+1) - S(k+1).x(k) +$$

$$+G(k+1).E[v(k+1)] \qquad (D.14)$$

$$\bar{b}(k+1) = S(k+1).\bar{b}(k).S^T(k+1) +$$

$$+ G(k+1).E[v(k+1).v^T(k+1)]G^T(k+1) \qquad (D.15)$$

3 --- General Case

For the general nonlinear problem one returns to Equation (D.9) which cannot normally be solved in closed form.

Numerical techniques and approximations would be necessary that may use more computing power and present worse results than the Monte Carlo process that we are trying to avoid.

One way to simplify the problem is to assume that y(k) has an approximate Gaussian distribution, even with all the nonlinearities shown. Linearizing Equation (D.8) around the mean value of y(k) would give

$$\underline{y}(k+1) \cong A(\underline{\bar{y}}(k)) + \frac{\partial}{\partial \underline{y}} A(\underline{\bar{y}}(k)).[\underline{y}(k) - \underline{\bar{y}}(k)] +$$

$$+ B(\underline{\bar{y}}(k)).\underline{v}(k+1) \qquad (D.16)$$

Taking $\underline{\bar{y}}(0)$ as the deterministically known initial value $\underline{y}(0)$, and applying the expectation and variance operators to Equation (D.16), one gets the recursive equations for the moments of $\underline{y}(k)$:

$$\underline{\bar{y}}(k+1) = A(\underline{\bar{y}}(k)) + B(\underline{\bar{y}}(k)).E[\underline{v}(k+1)] \qquad (D.17)$$

$$Var[\underline{y}(k+1)] = [\frac{\partial}{\partial \underline{y}} A(\underline{\bar{y}}(k))].Var[\underline{y}(k)].[\frac{\partial}{\partial \underline{y}} A(\underline{\bar{y}}(k))]^T +$$

$$+ B(\underline{\bar{y}}(k)).Var[\underline{v}(k+1)].B^T(\underline{\bar{y}}(k)) \qquad (D.18)$$

The moments we are interested in, $\underline{\bar{a}}$, $\underline{\bar{e}}$ and $\underline{\bar{b}}$ are directly obtained from subvectors and submatrices of the above moments.

The primary difficulty with this approach, however, is in obtaining the functions A and B. This can be seen for the very simple case below, as an example.

Suppose a scalar system with a single observation is described by the equations

$$x(k+1) = x^2(k) + w(k)$$

$$z(k) = x(k) + v(k)$$

Equations (D.1) - (D.5) give

$$\hat{x}(k+1|k) = \hat{x}^2(k) \qquad ; \qquad \phi(k) = 2\hat{x}(k)$$

$$p(k+1|k) = 4\hat{x}^2(k).p(k) + q^2(k)$$

$$G(k+1) = \frac{4\hat{x}^2(k).p(k) + q^2(k)}{4\hat{x}^2(k).p(k) + q^2(k) + r^2(k)}$$

and, after the appropriate steps,

$$\begin{bmatrix} \hat{x}(k+1) \\ p(k+1) \end{bmatrix} = \begin{bmatrix} \hat{x}^2(k) + \dfrac{4\hat{x}^2(k).p(k) + q^2(k)}{4\hat{x}^2(k).p(k) + q^2(k) + r^2(k)}.[x(k) - \hat{x}(k)] \\ \dfrac{[4\hat{x}^2(k).p(k) + q^2(k)].r^2(k)}{4\hat{x}^2(k).p(k) + q^2(k) + r^2(k)} \end{bmatrix}$$

$$+ \begin{bmatrix} \dfrac{4\hat{x}^2(k).p(k) + q^2(k)}{4\hat{x}^2(k).p(k) + q^2(k) + r^2(k)} \\ 0 \end{bmatrix} .v(k+1)$$

The mean value given by Equation (D.17) can be obtained in a simpler way, however. It is the result obtained by running the filter in the simulated environment but making the measurement noise assume its mean value E[v(k)], normally zero.

If one uses more terms in the expansion of Equation (D.8), better results will be obtained at the expense of increased computing effort and time.

For this general case it is suggested that these equations be applied to a simple scalar or two-dimensional nonlinear problem and that the computing power required to find the sought after moments be compared with that required to run a Monte Carlo process yielding the same level of accuracy in the results.

APPENDIX E : COMPUTER PROGRAM

The basic structure of the computer program written for the simulation of the tracking problem, and the evaluation of models and filtering algorithms, is shown in Figure E-1. The solid lines represent the normal flow of control within the program; the dashed lines show the extra pathes that become available whenever an interruption is requested by the user.

After a brief introduction to the program a table called MENU is presented to the user, as shown in Figure E-2. If the user chooses actions number 1 or 5 the result is clear.

Choice number 3 provides access to all the problem variables. Since the number of variables that characterize each simulation is very large, a simple way to deal with these variables had to be devised. As it is implemented, the program always "remember" the values given to the variables at the last time the program was used, so that only the variables to have their values modified have to be addressed. The change of value of a variable is simply made by selecting the page where it appears, typing the letter associated with the variable and the new desired value. The program immediately responds by presenting back the entered value. A more detailed diagram of the actions resulting

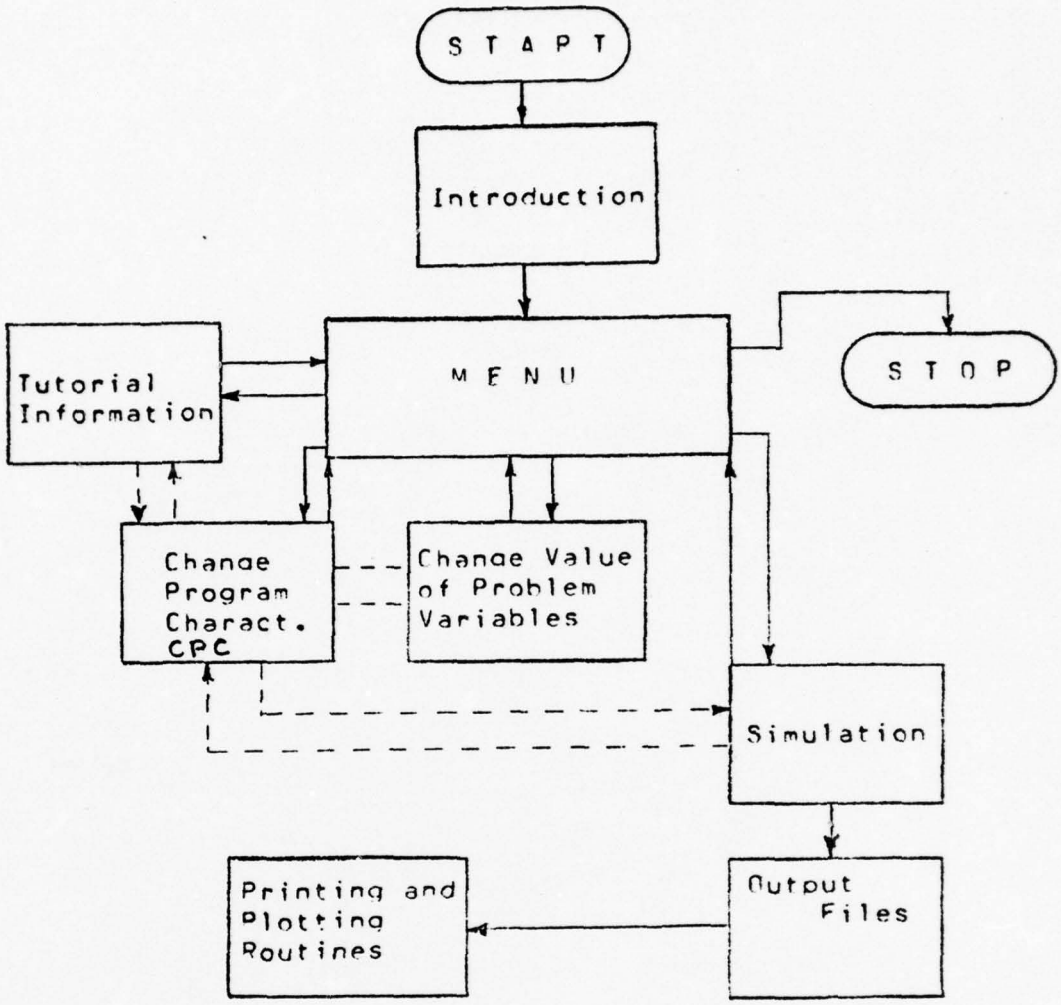

Figure E-1 : Basic structure of program.

MENU

Press the number corresponding to the action desired and c/r.

1 - PRESENT TUTORIAL INFORMATION

2 - MODIFY PROGRAM FLAGS

3 - FORMULATE OR MODIFY THE PROBLEM

4 - START THE SOLUTION OF THE PROBLEM

5 - END THE PROGRAM AND EXIT

Figure E-2 : The MENU table.

from choice number 3 is presented in Figure E-3. A typical page of variables is shown in Figure E-4.

Choice number 4 simulates the tracking problem according to the values defined in the previous step. A block diagram of the actions involved in the simulation is presented in Figures E-5, E-6 and E-7.

Initially all the important problem variables are printed with their current values in a form as shown in Figures E-8, E-9 and E-10. During the first run the scheduling of all the events involved in the simulation is also printed for future reference, as shown in Figure E-11.

With choice number 2 from the MENU a new table is presented as shown in Figure E-12. This table in also presented to the user whenever he requests an interruption, at any time or point within the program.

The extra choices that now become available are almost self-explanatory but it should be added that with choice number 7 the simulation is ended and the partial statistics are computed and written in the appropriate output files; choice number 6 allows the modification of any variable in the middle of the simulation, in the same way as explained before; choice number 0 transfer control back to MENU or to the point of interruption.

A listing of the program, in C language, is available at the Electrical Engineering Department, Naval Postgraduate

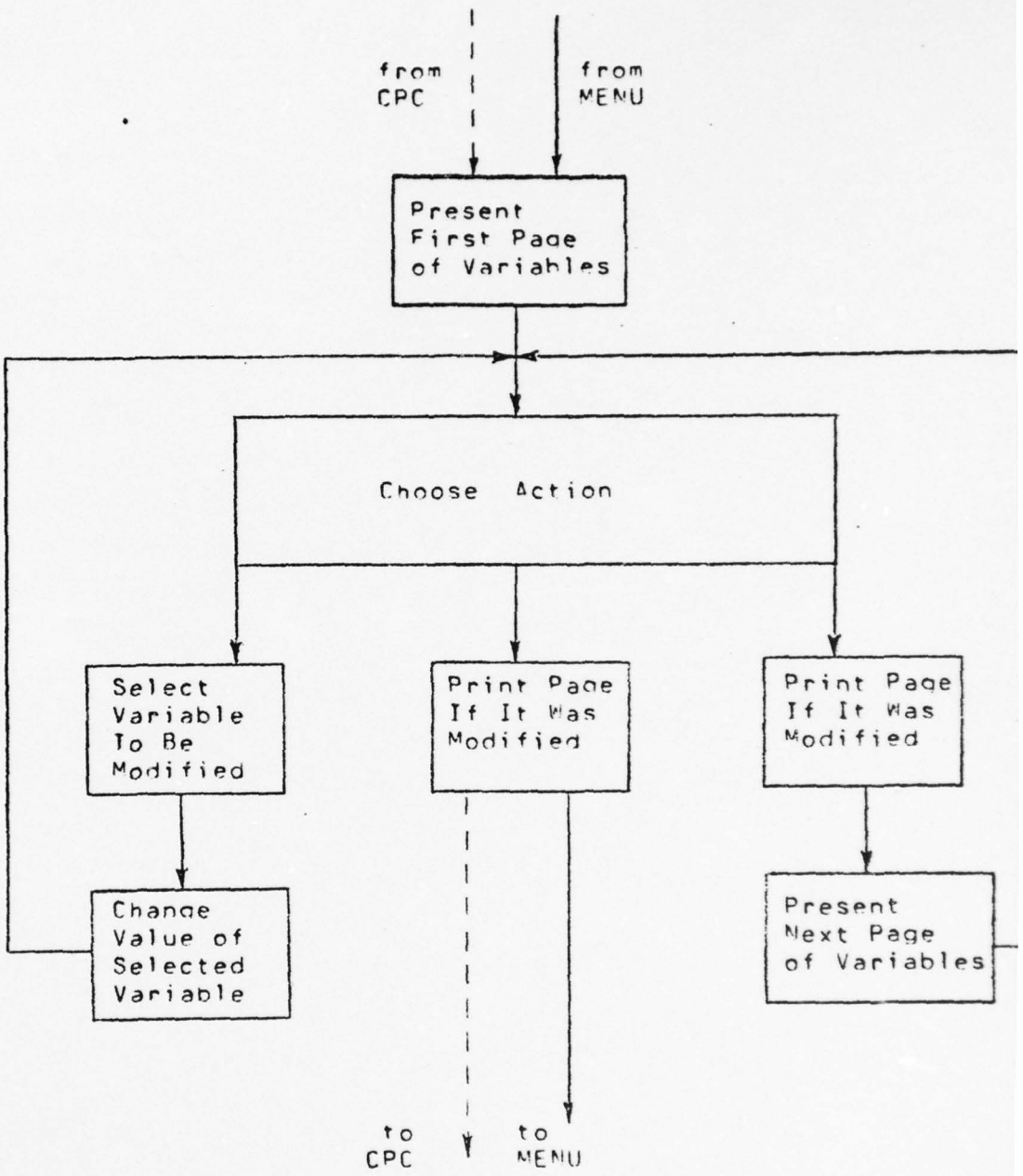

Figure E-3 : Changing the value of problem variables

To change the value of any variable, type the indicated letter, at least one space, the desired value and c/r.
To see the other variables of the problem, type 1 c/r.
To go back to menu, type 0 c/r.

(1 meter = 1.094 yards; 1 meter/sec = 1.94 knots)

TARGET INITIAL PARAMETERS

initial x - position	:	0.0	km	a
y - position	:	0.0	km	b
speed	:	7.0	m/sec	c
heading	:	305.0	deg	d
frequency	:	500.8	hertz	e

standard deviation of forcing functions

speed/sec	:	0.0	m/sec/sec	f
heading/sec	:	0.0	deg/sec	g
frequency/sec	:	0.0	hertz/sec	h

Figure E-4 : Typical page of variables.

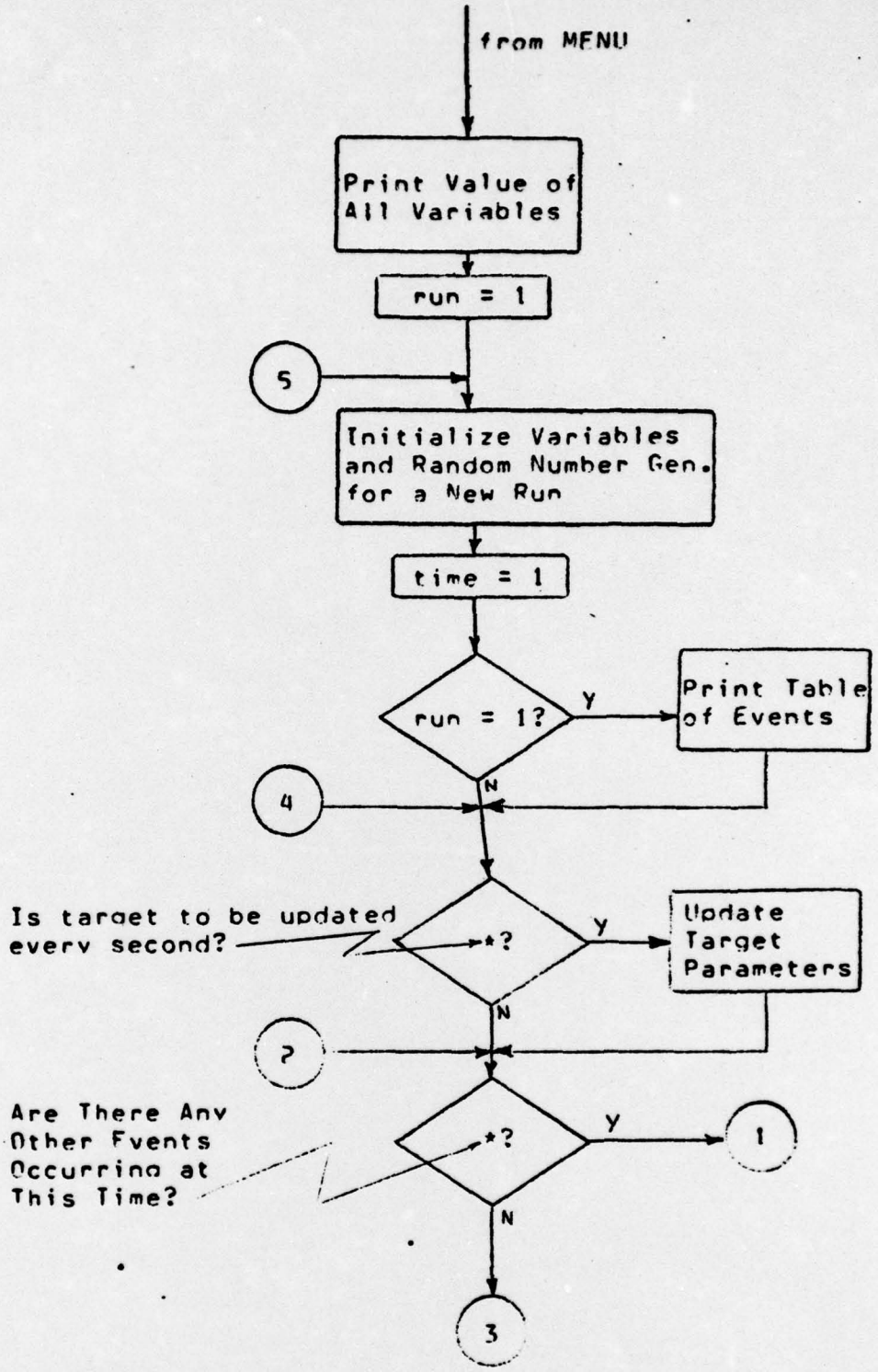

Figure E-5 : Simulation I

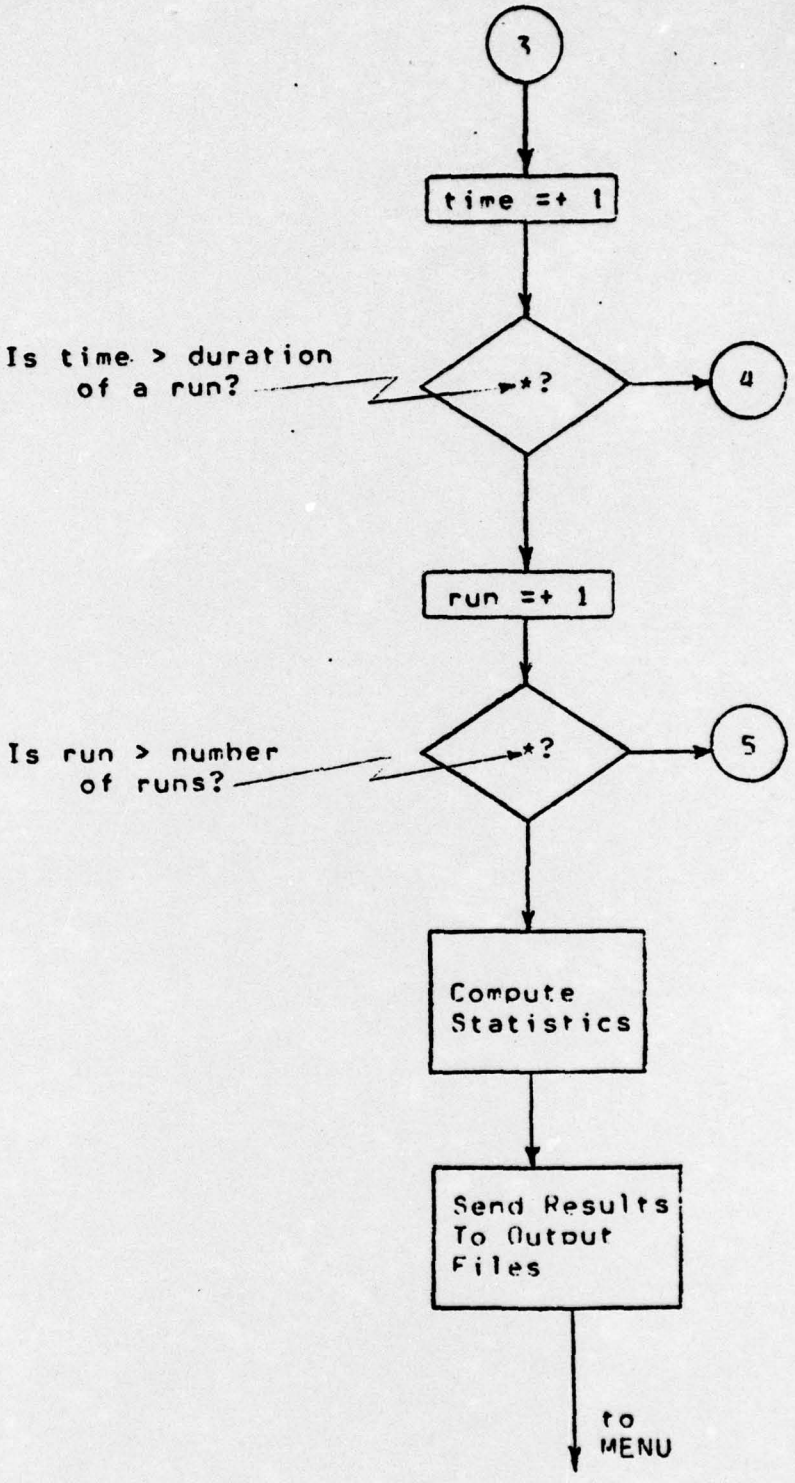

Figure E-6 : Simulation II

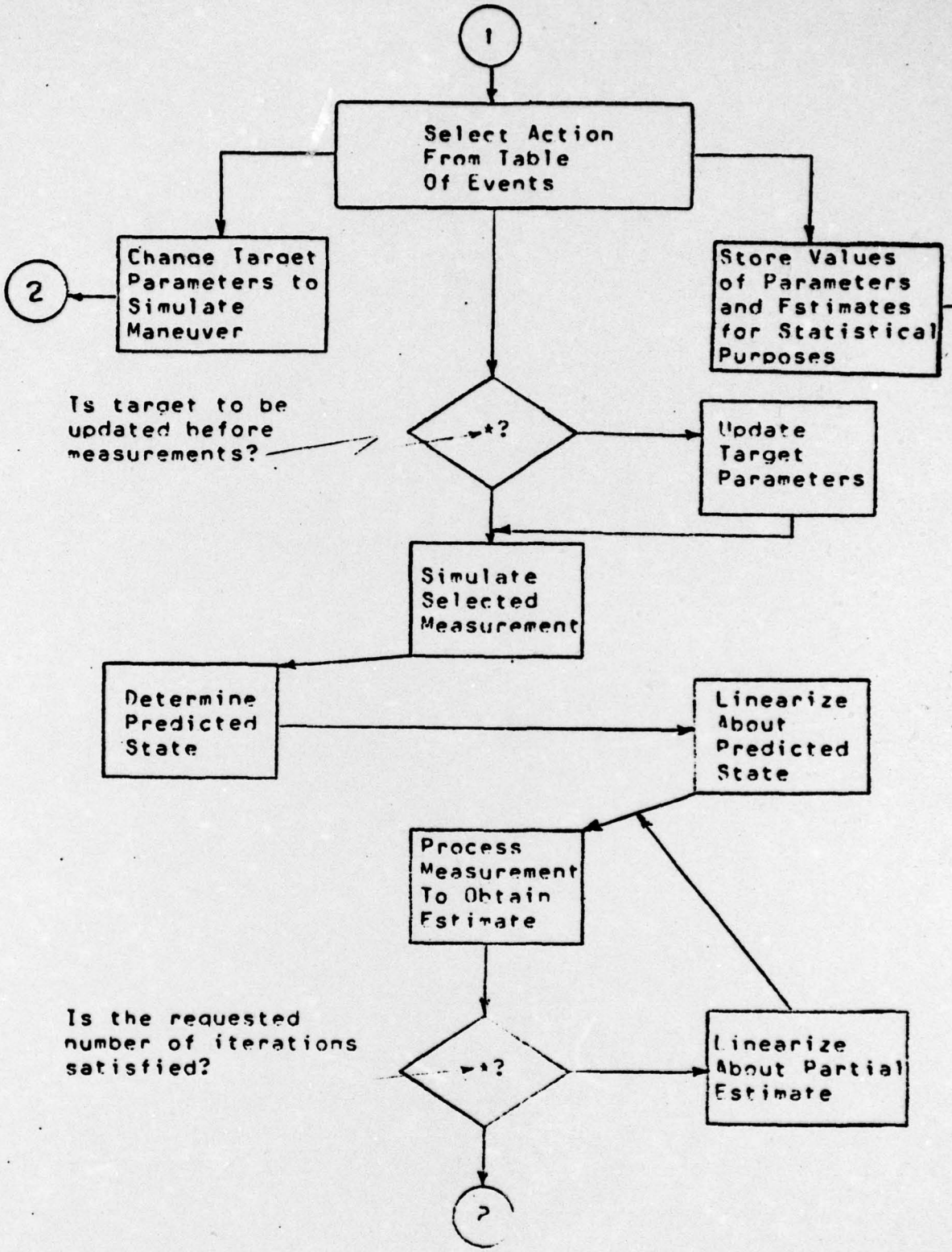

Figure E-7 : Simulation III

TARGET INITIAL PARAMETERS

initial	x - position	: 0.0	km	a
	y - position	: 0.0	km	b
	speed	: 7.0	m/sec	c
	heading	: 305.0	deg	d
	frequency	: 500.8	hertz	e
standard deviation of forcing functions				
	speed/sec	: 0.0	m/sec/sec	f
	heading/sec	: 0.0	deg/sec	g
	frequency/sec	: 0.0	hertz/sec	h

GENERAL DIRECTIONS

number of DIFAR buoys	: 3	buoys	a
number of LOFAR buoys	: 0	buoys	b
number of maneuvers	: 2	man	c
number of runs	: 20	runs	d
duration of runs	: 2000	sec	e
number of key points	: 20	points	f
seed	: 13339		g
average sound velocity	: 1500.0	m/sec	h
range of the buoys	: 8.0	km	i

FILTER INITIAL PARAMETERS

initial	x - position	: -0.5	km	a
	y - position	: 0.0	km	b
	speed	: 6.0	m/sec	c
	heading	: 310.0	deg	d
	frequency	: 500.5	hertz	e
standard deviation of forcing functions				
	speed/sec	: 0.005	m/sec/sec	f
	heading/sec	: 0.050	deg/sec	g
	frequency/sec	: 0.010	hertz/sec	h

Figure E-8 : Listing of problem variables I

INITIAL COVARIANCE MATRIX

	x pos	y pos	speed	heading	freq
x pos	1.0 a	0.3 b	0.0 c	0.0 d	0.0 e
y pos	*	1.0 g	0.0 h	0.0 i	0.0 j
speed	*	*	2.0 m	0.0 n	0.0 o
heading	*	*	*	100.0 s	0.0 t
freq	*	*	*	*	1.0 y

(km, m/sec, degrees and hertz crossmultiplied)

MEASUREMENTS SCHEDULE I

buoy	type	start	period	mean	stdev	
1	B	100	100	0.0	5.0	abcdef
1	F	100	100	0.0	0.04	ghijkl
2	B	500	100	0.0	5.0	mnopqr
2	F	500	100	0.0	0.04	stuvwx

(start and period in seconds)
(mean and std dev in degrees, hertz or seconds)
(period must be zero if measurement is not used)

MEASUREMENTS SCHEDULE II

buoy	type	start	period	mean	stdev	
12	T	500	100	0.0	0.01	abcdef
13	T	500	100	0.0	0.01	ghijkl
23	T	500	100	0.0	0.01	mnopqr
3	B	500	100	0.0	5.0	stuvwx

(start and period in seconds)
(mean and std dev in degrees, hertz or seconds)
(period must be zero if measurement is not used)

Figure E-9 : Listing of problem variables II

TARGET MANEUVERS

1st maneuver :	time =	600	sec	a
	vdot =	0.0	m/sec/min	b
	hdot =	-9.0	deg/min	c
	fdot =	0.0	hertz/min	d

TARGET MANEUVERS

2nd maneuver :	time =	1200	sec	a
	vdot =	0.0	m/sec/min	b
	hdot =	0.0	deg/min	c
	fdot =	0.0	hertz/min	d

BUOYS PARAMETERS

First buoy : type =	DIFAR			a
x - position =	0.0	km		b
y - position =	-3.0	km		c

If DIFAR:

bearing error mean=	0.0	deg	d
std dev =	5.0	deg	e

BUOYS PARAMETERS

2nd buoy : type =	DIFAR			a
x - position =	4.0	km		b
y - position =	-3.0	km		c

If DIFAR:

bearing error mean=	0.0	deg	d
std dev =	5.0	deg	e

Figure E-10 : Listing of problem variables III

SEQUENCE OF EVENTS FROM 601 TO 900 SECONDS

700 sec - bearing measurement by buoy number 1

700 sec - frequency measurement by buoy number 1

700 sec - bearing measurement by buoy number 2

700 sec - frequency measurement by buoy number 2

700 sec - time delay measurement by buoys 1 and 2

700 sec - Monte Carlo point number 7

800 sec - bearing measurement by buoy number 1

800 sec - frequency measurement by buoy number 1

800 sec - bearing measurement by buoy number 2

800 sec - frequency measurement by buoy number 2

800 sec - time delay measurement by buoys 1 and 2

800 sec - Monte Carlo point number 7

900 sec - bearing measurement by buoy number 1

900 sec - frequency measurement by buoy number 1

900 sec - bearing measurement by buoy number 2

900 sec - frequency measurement by buoy number 2

900 sec - time delay measurement by buoys 1 and 2

900 sec - Monte Carlo point number 7

Figure E-11 : Table of events.

PROGRAM CHARACTERISTICS

Press the number corresponding to the option or action desired and c/r.

To continue or return press 0 c/r.

1 - update target every second

2 - update target only before measurements

3 - start printing on line printer

4 - stop printing

5 - put results of next run on output files

6 - modify parameters of the problem

7 - terminate the problem

Figure E-12 : Interruption table.

School, to any interested reader.

LIST OF REFERENCES

1. Naval Air Development Center Report 74255-50, Doppler Tracking of a Maneuvering Target Using an Extended Kalman Filter with a Temporary Fading Memory, by R. Rigolizzo, D. Birnbaum and M. Pembroke, 1975.

2. Mitschang, G. W., An Application of Nonlinear Filtering Theory to Passive Target Location and Tracking Ph.D. Thesis, Naval Postgraduate School, 1974.

3. International Business Machines Report PCI-5M84, Passive Location Studies, by H. A. Myers and B. Diamant, 30 March 1976.

4. Interstate Electronics Corp., Technical Note s/n, Digital Narrowband Frequency Tracking, by G. Ricker, C. Lau and J. Williams, 1971.

5. Jazwinski, A. H., Stochastic Processes and Filtering Theory, Academic Press, 1970.

6. Frank J. Seiler Res. Lab. Report TR-72-004, An Engineers Guide to Building Nonlinear Filters, 1972.

7. Sorenson, H. W. and Stubberub, A. R., "Non-linear Filtering by Approximation of the a-posteriori Density", Int. J. Control, v. 8, n. 1, p.33-51, 1968.

8. Alspach, D. L. and Sorenson, H. W., "Nonlinear Bayesian Estimation Using Gaussian Sum Approximations", IEEE TAC, v. AC17, n. 4, p. 439-447, 1972.

9. Sorenson, H. W., Advances in Control Systems, vol. 3, Chapter 5, Academic Press, 1966.

10. Rosen, J. B., "The Gradient Projection Method for Nonlinear Programming, Part 1 : Linear Constraints", J. Soc. Indust. Appl. Math., v. 8, n. 1, p.189-190, March 1960.

11. Denham, W. F. and Pines, S., "Sequential Estimation when Measurement Function Nonlinearity is Comparable to Measurement Error", AIAA Journal, v. 4, n. 6, p. 1071-1076, June 1966.

12. Kirk, D. E. and Titus, H. A., Evaluation of Linear Estimators for Nonlinear Systems, paper presented at Asilomar Conference on Circuits, Systems and Computters, 9th, Pacific Grove, California, 4 Nov 1975.

13. Sage, A. P. and Melsa, J. L., Estimation Theory with Applications to Communications and Control, pg 25, McGraw-Hill, 1974.

INITIAL DISTRIBUTION LIST

		No. Copies
1.	Defense Documentation Center Cameron Station Alexandria, Virginia 22314	2
2.	Library, Code 0212 Naval Postgraduate School Monterey, California 93940	2
3.	Department Chairman, Code 62 Department of Electrical Engineering Naval Postgraduate School Monterey, California 93940	1
4.	Professor D. E. Kirk, Code 62Ki Department of Electrical Engineering Naval Postgraduate School Monterey, California 93940	1
5.	LCDR Marcilio B. da Cunha Rua Uruguai 527 apt 403 Tijuca - Rio de Janeiro RJ - 20000 Brasil	3
6.	Diretoria de Comunicacoes e Eletronica Ministerio da Marinha Ilha das Cobras - Rio de Janeiro RJ - 20000 Brasil	1
7.	Instituto de Pesquisas da Marinha Rua Ipiru s/n Ilha do Governador - Rio de Janeiro RJ - 20000 Brasil	1

8. Asst Professor V. M. Powers, Code 52Pw — 1
Computer Science Department
Naval Postgraduate School
Monterey, California 93940

9. Professor H. A. Titus, Code 62Ts — 17
Department of Electrical Engineering
Naval Postgraduate School
Monterey, California 93940

10. Capt. R. H. Shumaker — 1
SMC box 2872
Naval Postgraduate School
Monterey, California 93940